To the Graduate Council:

I am submitting herewith a thesis written by Anne Ruth Gogola enititled "Depositional and Diagenetic History of the Lower Silurian 'Basal Transgressive Sandstone' in the Southern Appalachians." I have examined the final copy of this thesis for form and content and recommend that it be accepted in partial fulfillment of the requirements for the degree of Master of Science, with a major in Geology.

Steven G. Driese

Steven G. Driese, Major Professor

We have read this thesis
and recommend its acceptance:

Kula C. Misra

Kenneth R. Walker

Accepted for the Council:

C W Minkel

Vice Provost
and Dean of the Graduate School

STATEMENT OF PERMISSION TO USE

In presenting this thesis in partial fulfillment to the requirements for a Master's degree at The University of Tennessee, Knoxville, I agree that the Library shall make it available to borrowers under rules of the Library. Brief quotations from this thesis are allowable without special permission, provided that accurate acknowledgment of the source is made.

Permission for extensive quotation from or reproduction of this thesis may be granted by my major professor, or in his absence, by the Head of Interlibrary Services when, in the opinion of either, the proposed use of the material is for scholarly purposes. Any copying or use of the material in this thesis for financial gain shall not be allowed without my written permission.

Signature Anne R. Bogle

Date April 19, 1990

DEPOSITIONAL AND DIAGENETIC HISTORY OF THE LOWER SILURIAN 'BASAL TRANSGRESSIVE SANDSTONE' IN THE SOUTHERN APPALACHIANS

A Thesis

Presented for the

Master of Science

Degree

The University of Tennessee, Knoxville

Anne Ruth Gogola

May 1990

ACKNOWLEDGMENTS

Numerous individuals contributed to the completion of this study. I'd like to thank my committee, Dr. Steven Driese, Dr. Kenneth Walker, and Dr. Kula Misra for helping me define the project, providing the input which helped me complete this work in a timely manner, and reading the final product. My advisor, Steven Driese was particularly helpful by providing advice since the onset of this project, accompanying me in the field when I began this work, and by supporting me for one semester with his grant from the Petroleum Research Fund. I'd also like to thank Dr. Walker for the use of his petrographic microscopes and point-counting stage.

I'd also like to thank my fellow graduate students here in the Department of Geological Sciences who taught me as much about geology through casual discussion as I learned in my coursework. Specifically, I'd like to mention the members of the Sand Bar: Chris Bolton, Joachim Dorsch, Michael Neton, and Dan Walker. Most importantly, I must express my appreciation to Lincoln Foreman and Dan Walker for the use of their Macintosh computers, their support, advice, and, more than anything, their friendship.

Special thanks goes to Dr. Arthur Boucot, Dr. Kenneth McKinney, and Dr. William Berry for providing identifications for various fossil specimens.

Partial support for this research was provided by the Discretionary Fund of the Department of Geological Sciences and a grant from the Southeastern Section of the Geological Society of America.

Finally, I'd like to thank my parents and my sister for encouraging me to attend graduate school and their confidence in me when I did not have it in myself.

ABSTRACT

The boundary between Upper Ordovician (Ashgillian) tidal-flat redbeds and Lower Silurian (Llandoverian) marine shelf clastic strata in the southern Appalachians is marked by a distinct 0.6-3 m thick, very fine- to medium-grained, quartzose to sublitharenitic, transgressive sandstone body that can be traced across the Copper Creek, Wallen Valley, Whiteoak Mountain, Pine Mountain, and Sequatchie thrust sheets. It is interpreted to have been deposited in a beach face to inner shelf setting. This 'Basal Transgressive Sandstone (BTS) can be divided into three distinct facies variants. The wave-rippled to horizontally cross-stratified variant (WL) only occurs along the Copper Creek thrust sheet in eastern Tennessee, and it represents deposition in a beach face to upper shoreface setting. The cross-bedded sandstone variant (CBS) occurs along the Whiteoak Mountain thrust sheet and is interpreted as representing channel sequences that filled in existing tidal channels as the sea slowly transgressed over tidal flat deposits of the Upper Ordovician Juniata and Sequatchie formations. The fine-grained bioturbated variant (FGB) occurs along the Pine Mountain, Wallen Valley, Whiteoak Mountain, and Sequatchie thrust sheets. This variant is considered to represent the lower shoreface to inner shelf setting where deposition was slow and continuous to discontinuous, depending upon the degree of bioturbation displayed.

The physical features observed within the BTS are strongly suggestive of the occurrence of an unconformity at the Ordovician-Silurian boundary. The sandstone overlies Upper Ordovician *Lingula* -bearing tidal-flat deposits that were laid down during a relative sea-level lowstand. Evidence for prolonged subaerial exposure occurs in the form of paleosol horizons which occur directly beneath the BTS at the easternmost exposures (Copper Creek thrust), the most proximal setting of the BTS. Phosphatic pebble lags occur there and in all the more distal deposits, and are interpreted to represent ravinement

surfaces which formed through the process of erosional shoreface retreat during a relative sea-level rise. The BTS is always overlain by a distal terrigenous shelf sequence consisting of thin tempestites interbedded with gray-green shale, further indicating a relative sea-level rise. Within the westernmost exposures, a distinctive color change from red to gray occurs almost directly beneath the BTS. All of these features point to the existence of an unconformity. There is question, however, as to the duration of time for which there are no preserved strata between the BTS and the underlying Ashgillian redbeds. Biostratigraphic evidence for an unconformity is lacking due to the paucity of body fossils in the Lower Silurian-age strata and the lack of any chronstratigraphic indicators of narrow range among the species collected. Therefore, this unconformity represents a hiatus of unknown duration.

Point-count data indicate that the most proximal deposits of the BTS, i.e. the WL variant, underwent a paragenetic sequence of deposition, mechanical compaction through burial, chemical compaction through intergranular pressure solution, and quartz cementation. Very minor dolomitization occurred late in the burial history. Rocks of the CBS and FGB variants probably consisted of a large amount of framework carbonate grains that were later completely replaced by ferroan dolomite and ankerite. This interpretation arises from the fact that, in thin-section, the detrital grains appear to be "floating" in ferroan carbonate material such that grain-to grain contacts are extremely rare among framework quartz and rock fragments, with the exception of some of the phosphatic pebble lags. Coarse, sand-sized quartz grains have rare overgrowths within these lags. These precursor carbonate cements have subsequently been replaced, through burial diagenesis, by ferroan dolomite and ankerite. Some precursor ferroan calcite still remains within the phosphatic pebble lags and has been partially replaced by ferroan dolomite and ankerite. Finally, dedolomite has been observed in thin-sections of samples collected from the most weathered outcrop exposures. The occurrence of this phase is apparently a weathering phenomenon.

TABLE OF CONTENTS

CHAPTER PAGE

LIST OF FIGURES

FIGURE PAGE

FIGURE PAGE

LIST OF TABLES

TABLE PAGE

LIST OF PLATES

CHAPTER 1

INTRODUCTION

Recent studies of modern coastal environments have yielded a new understanding of the dynamics of relative sea-level changes. Analyses of ongoing depositional processes along coastal areas such as the U.S. Atlantic coastline provide useful analogs for studies of the ancient rock record. This study attempts to analyze the depositional history of a transgressive sandstone body that was deposited during a relative sea-level rise during the Early Silurian. This sandstone body was briefly described by Driese and others (in press) in their analysis of the Lower Silurian-age Clinch Sandstone, a progradational clastic wedge that occurs in the southern Appalachian basin. The transgressive sandstone body examined in this study constitutes the lower boundary of this 100 -250 m thick sequence.

The concept of sequence stratigraphy has become increasingly more in vogue in the fields of stratigraphy and sedimentology. This has been especially true for geophysical interpretations of passive-margin sequences (see, for example, Posametier and Vail, 1988; Mitchum and others, 1977). Only more recently have workers attempted to apply these principles to more tectonically-influenced depositional basins (see, for example, Jordan and Flemings, 1989; Galloway, 1989). Application of these principles to a transgressive sandstone body in outcrop provides a unique opportunity to test the utility of these principles in the examination of ancient deformed rocks on the outcrop scale.

PURPOSE

The primary purpose of this study is to examine, in detail, the Lower Silurian-age 'Basal Transgressive Sandstone' (BTS), a condensed sequence of shoreface to inner shelf clastics, in order to determine the environments in which it was deposited and the nature and significance of the basal contact with the underlying Upper Ordovician (Ashgillian) redbeds. Secondly, it will be shown that some of the physical features within the BTS formed by the process of erosional shoreface retreat, which is a common process occurring along the U.S. Atlantic coast today (e.g., Swift 1968; 1971; Nummedal and Swift, 1987). A third component of this study is to describe the petrology of the BTS, with special emphasis on the diagenetic features of this sandstone body, by using petrographic techniques.

METHODS

Nine outcrop exposures of Upper Ordovician- to Lower Silurian-age strata (Fig. 1.1, 1.2) were examined and measured, and samples were taken at 10-20 cm intervals for polished slab and thin-section preparation. The stratigraphic intervals measured ranged from 1.5m to 9.6m thick. Polished slabs were examined in order to delineate any sedimentary structures and identify any trace fossils not identified in the field. Thin-sections were examined for texture and composition with a petrographic microscope. The thin-sections were then point-counted using a Swift point-counting stage and Phasecount, a computer-assisted point-counting program written by J. Lincoln Foreman and others (1989). All phases, including cements, were counted in order to aid in diagenetic interpretations. The counts consisted of 1000 to 1500 points

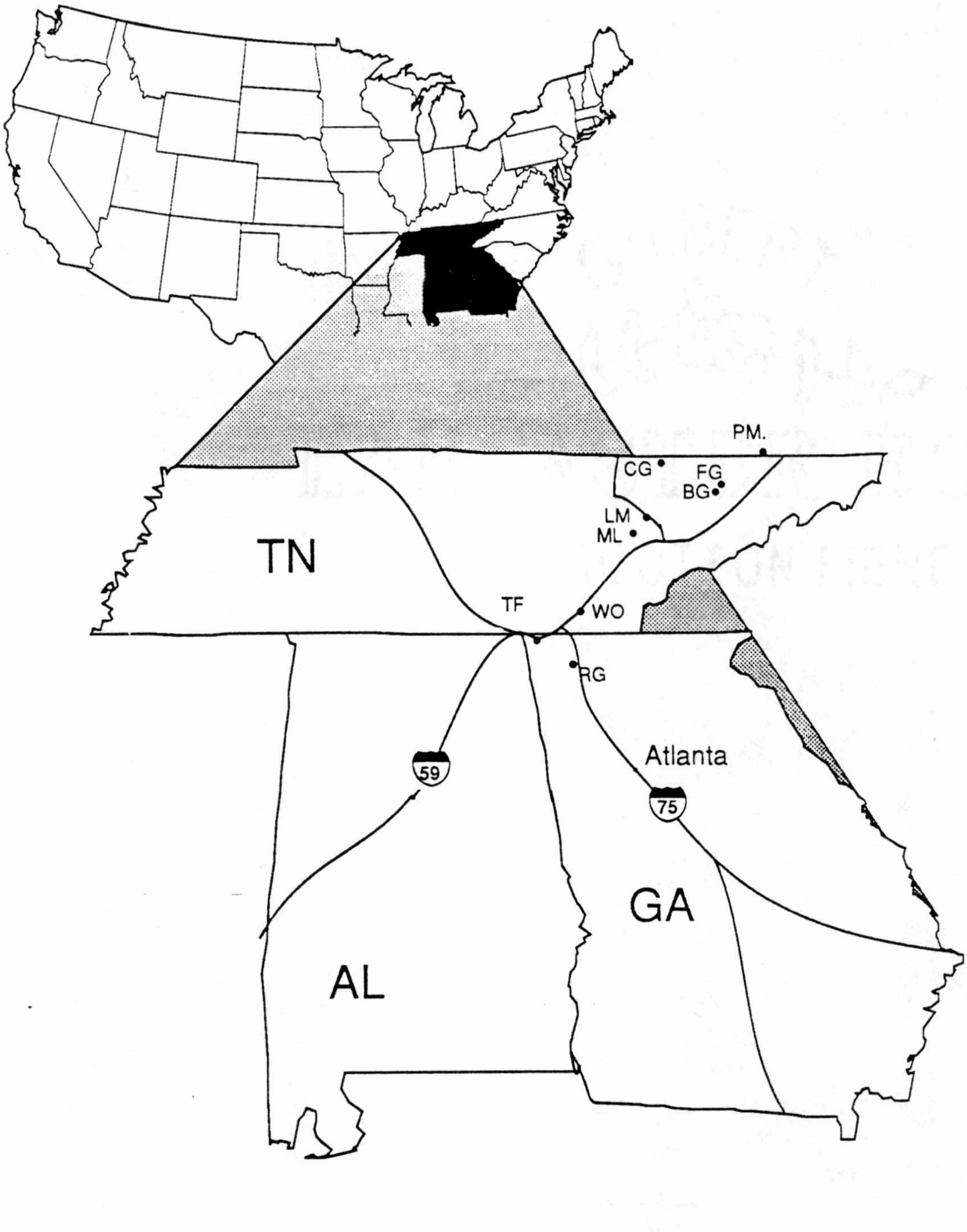

Figure 1.1. Location map for outcrop localities. The localities are PM: Powell Mountain, VA; FG: Flat Gap, TN; BG: Beans Gap, TN; CG: Cumberland Gap, TN; LM: Lone Mountain, TN; ML: Melton Lake, TN; WO: Whiteoak Mountain, TN; RG: Ringgold, GA; and TF: Tiftonia, GA.

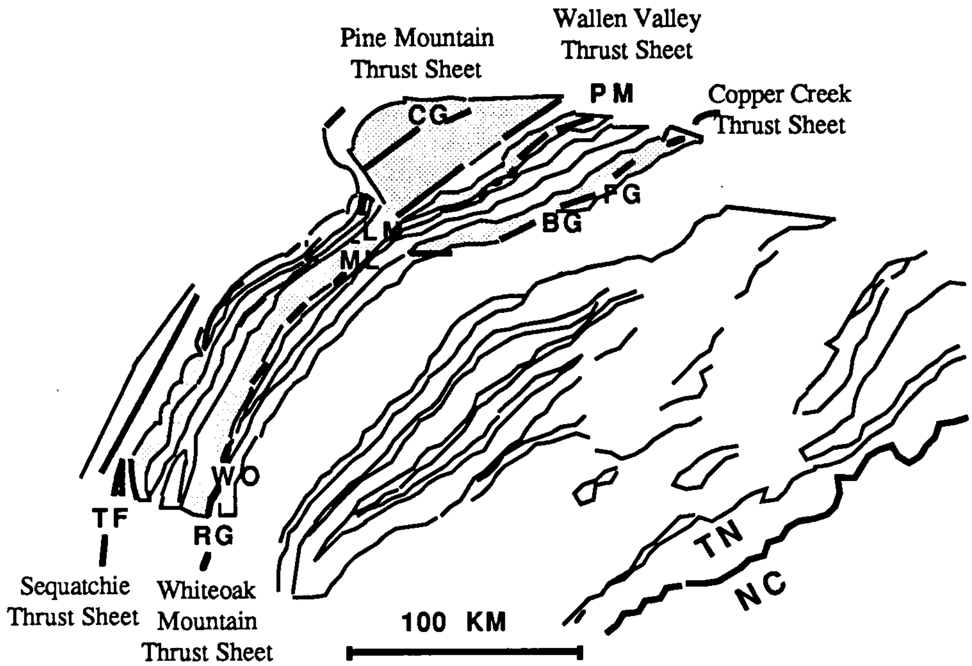

Figure 1.2. Palinspastically restored outcrop map (modified from Roeder and Witherspoon, 1978) showing the locations of outcrops examined in this study. BG: Beans Gap, TN and FG: Flat Gap, TN, occur on the Copper Creek Thrust Sheet; PM: Powell Mountain, VA occurs on the Wallen Valley Thrust Sheet; LM: Lone Mountain, TN; ML: Melton Lake, TN; WO: Whiteoak Mountain, TN; and RG: Ringgold, GA all occur on the Whiteoak Mountain Thrust Sheet; TF: Tiftonia, GA occurs on the Sequatchie Thrust Sheet; and CG: Cumberland Gap, TN occurs on the Pine Mountain Thrust Sheet. Stippled areas indicate those thrust sheets that contain Lower Silurian outcrop exposures.

for each sample in order to achieve a two-sigma confidence interval of 3% (Van der Plas and Tobi, 1965).

A small amount of isotopic data were collected in order to determine if there was any isotopic similarities between samples from within one locality and between localities, and also to determine what benefit, if any, a more extensive pursuit of isotopic data might be (Appendix B). X-ray diffraction data were collected using a Phillips Model X-ray Diffractometer in order to determine the mineralogical composition of the carbonate phases present, and the relative purity of these phases (Appendix C).

TECTONIC SETTING

The Silurian clastic wedge in the southern Appalachians represents the erosion of a northeasterly source that was uplifted during Blountian phase of the Taconic Orogeny during the Middle Ordovician time (Rodgers, 1971; Hatcher, 1987; Hatcher, in press). The Taconic Orogeny resulted from the docking, or collision, of microcontinents along the salients and recesses of the Late Precambrian-Paleozoic continental margin through an eastward-dipping subduction zone. These events signified the initial shrinking or compression of the Iapetos ocean. Final closure of the Iapetos culminated with the collision of the western Avalonian Arc and the Piedmont terrane during the Acadian Orogeny, marking what is now the central Piedmont Suture (Hatcher, 1987).

Initiation of the Blountian orogenic phase caused the formation, in eastern Tennessee, of a deep, northeast-southwest trending foreland basin known as the Sevier basin (Shanmugam and Walker, 1980 ; Walker and others, 1983). Thomas (1977) suggested that the formation of the Sevier basin and the adjacent Taconic highlands was a response to the docking of a microcontinent to the Tennessee recess. The first clastics derived from the Taconic Highlands were deposited as the distal and then proximal turbidites of the Middle Ordovician-age Sevier and Tellico Formations. Coincident with the deposition of the Blount clastic wedge (Rodgers, 1953; Thomas, 1977) along the eastern margin of the Sevier basin was the accumulation of carbonate strata along the western margin of the basin. The Sevier basin eventually became filled through a complex history of carbonate deposition to the west and siliciclastic deposition to the east resulting in a "bipolar" subsidence history (Walker and others, 1983). Deposition of the Upper Ordovician-age Moccasin and Bays formations represents final infilling of the Sevier basin. The sequence of Sevier basin clastics and carbonates combined with the overlying Moccasin and Bays formations to comprise the Blount Group (Rodgers, 1953; Thomas, 1977).

Another microcontinent-continent collision occurred further north in the Pennsylvania promonotory. This was a later event of the Taconic Orogeny which resulted in the formation of the Martinsburg-Shawangunk flysch basin. This basin was filled in by the Martinsburg-Shawangunk clastic wedge, which includes both Ordovician and Silurian rocks (Thomas, 1977). The Martinsburg consists of a succession of turbidites and shale (McBride, 1962), which grade upward into the prograding deltaic redbed deposits of the Juniata Formation (Thompson, 1970b). The Sequatchie Formation, in eastern Tennessee, is considered a very distal equivalent of the Juniata and Queenston redbeds. Thus, the regional extent of the Martinsburg-Shawangunk clastic wedge overlaps onto the capping clastics of the Blount Wedge, which represents the detritus filling the Sevier Basin. The first Silurian rocks are represented by the Shawangunk conglomerate which grades into the Tuscarora sandstone and equivalent Clinch Sandstone.

Thus, deposition of the 'Basal Transgressive Sandstone', the unit of interest in this study, occurred during a time of complex clastic deposition which, in turn, was the result of an even more complex tectonic history.

UPPER ORDOVICIAN-LOWER SILURIAN STRATIGRAPHY

Both the regional and vertical stratigraphic relationships of Upper Ordovician and Lower Silurian strata are shown in Figure 1.3. Upper Ordovician-age strata of interest to this study are the stratigraphically equivalent Juniata and Sequatchie formations. They are considered to be the most laterally extensive redbeds in the Appalachian Basin (Dennison, 1983). The Juniata Formation extends from the central Appalachians southward until it grades into the Sequatchie Formation in northeastern Tennessee. The lateral boundary between the two formations represents a facies change from argillaceous, noncalcareous redbeds (Juniata Formation) to fossiliferous (i.e., marine), red to gray, tidal flat deposits (Sequatchie Formation, Thompson, 1970b; Milici and Wedow, 1977). The Sequatchie Formation continues from northeastern Tennessee west, across the Valley and Ridge, and south into Georgia (Milici and Wedow, 1977; Chowns, 1972). The Lower Silurian strata that were examined are the lowermost Clinch Sandstone (Hagan Shale Member), the lowermost Rockwood Formation, and part of the lowermost Red Mountain Formation. The Clinch Sandstone occurs in northeastern Tennessee and southern Virginia and grades into the Tuscarora Formation further north (Diecchio, 1986; Milici and deWitt, 1988). The Rockwood Formation occurs in central eastern Tennessee and continues west across the Valley and Ridge until it grades into the Brassfield Formation (Miller, 1976). The

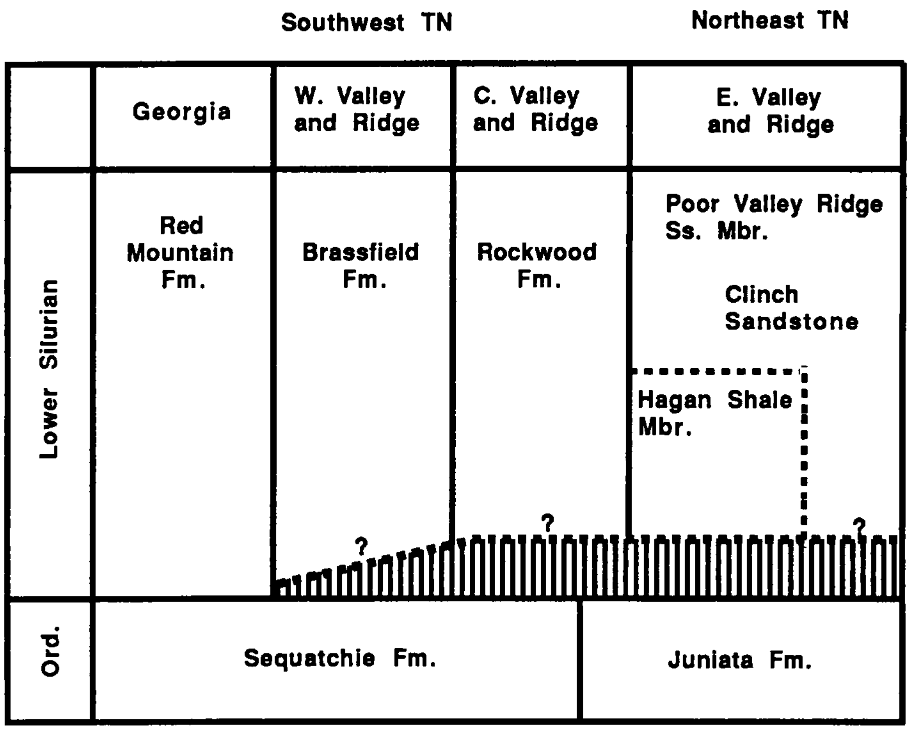

Figure 1.3. Stratigraphic names and relationships for Upper Ordovician and Lower Silurian strata in eastern Tennessee and Georgia. Relationships and nomenclature in northeastern Tennessee are applicable to the Powell Mountain, Virginia locality as well (modified from Dennison, 1983; Milici and Wedow, 1977; Diecchio, 1986; Milici and DeWitt, 1988; and Chowns, 1972).

Rockwood Formation is the equivalent of the Red Mountain Formation in Georgia and Alabama (Chowns, 1972).

LATE ORDOVICIAN DEPOSITIONAL HISTORY

Late Ordovician-age clastic detritus of the southern Appalachians represents the most southerly extent of the Queenston "delta" complex. The clastic sequence is a coarsening-upward progradational wedge which is thought to be the sedimentary record of the Taconic Orogeny (Diecchio, 1986). Exposures in eastern Tennessee and Georgia reveal that the Juniata/Sequatchie (Ashgillian) redbeds were deposited in low-energy, silt- to mud-dominated tidal flat and/or deltaic environments (Driese and others, in press; Driese and Foreman, 1989; Driese and Foreman, in review) during a relative sea-level lowstand near the end of the Ordovician (Ashgillian time) (Dennison, 1976). In southwestern Virginia, however, the Juniata consists of coarse, quartzose, hummocky cross-stratified storm beds interbedded with shale, that are indicative of marine shelf environments (Dorsch, pers. comm. and in prep.). This variation in depositional environments of the Juniata reflects changes in the shape and bathymetry of the Appalachian basin at that time. In other words, it probably became wider and deeper towards the north into what is now the central Appalachians.

LATE ORDOVICIAN-EARLY SILURIAN SEA-LEVEL HISTORY

The Ordovician and Silurian periods marked the ending of what some (Cotter, 1983a; Shanmugam and Moiola, 1982) have speculated to be an overall sea-level highstand due to greater amounts of oceanic rifting during the Early to Middle Ordovician, marking a first-order sea-level stand (Mitchum and others, 1977). Superimposed on this first-order highstand near the end of the Ordovician are the fluctuations in sea-level caused by worldwide glaciation and local tectonism. These perturbations in sea-level are recorded within the strata of the Appalachian Basin.

Sea-level curves of McKerrow (1979), Johnson (1980, 1987), and Fortey and Cocks (1988) indicate a eustatic rise in sea-level at the beginning of the Silurian, which followed a Late Ordovician (Ashgillian) lowstand (Fig. 1.4). Berry and Boucot (1973) attributed the worldwide sea-level lowstand to Late Ordovician-Early Silurian continental glaciation in North Africa. Quinlan and Beaumont (1984) showed that subsidence of the Appalachian foreland basin probably continued on through the Late Ordovician. Thus, a combination of eustatic and tectonic influences resulted in the Late Ordovician relative sea-level lowstand in the southern Appalachians, although the eustatic effect appears to have been the dominant controlling factor in this part of the basin at that time. Further north, in Virginia and West Virginia, there is no physical evidence for a relative sea-level lowstand within the Juniata redbeds, and instead, there is strong evidence for an unconformity produced by tectonism (Dorsch, pers. comm., Bambach, 1987). This suggests that tectonism, differential subsidence, sediment loading, and depositional rate varied along strike of the basin axis.

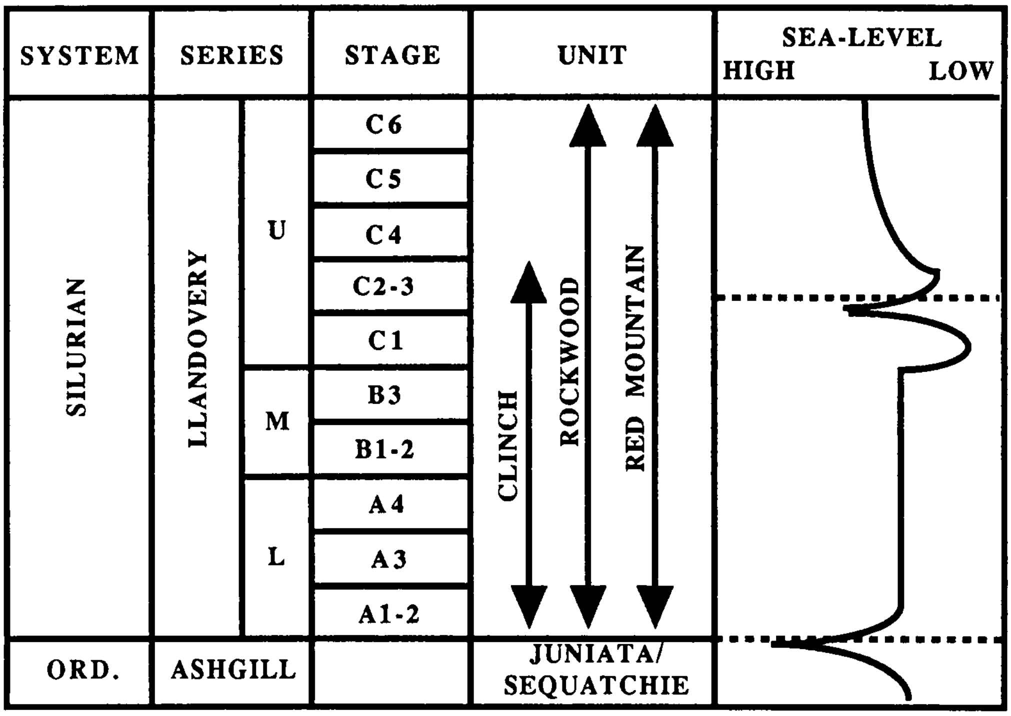

Figure 1.4. Relative sea-level curve for the Upper Ordovician and Lower Silurian. Curve is based on those from Johnson (1980,1987) and McKerrow (1979). Figure is modified from Driese and others (in press).

CHAPTER 2

DEPOSITIONAL ENVIRONMENTS OF THE 'BASAL TRANSGRESSIVE SANDSTONE'

LITHOFACIES

If the study of the BTS was only a small part to a larger study of the entire Lower Silurian clastic sequence, one might only assign a single facies designation to it. It is, however, the primary focus of this study and shows significant variation in sedimentology; therefore it will be divided into three facies variants based on the dominant sedimentary structures observed. These variants and the environmental interpretation for each are listed in Table 2.1.

Table 2.1. Lithofacies variants and environmental interpretation of the 'Basal Transgressive Sandstone'

Lithofacies variant	Environmental Interpretation	Localities where dominant
Wave rippled to horizontally laminated sandstone variant	Beach face to upper shoreface	BG, FG
Fine-grained, bioturbated sandstone variant	Lower to middle shoreface	PM, CG, LM, ML, WO, RG, TF
Cross bedded sandstone variant	Tidal inlet/washover fan	LM, ML, RG

Wave-rippled to horizontally laminated variant (WL)

Description:

The WL variant is a tan-yellow, fine- to very fine-grained sandstone which is thin-bedded to medium-bedded. Climbing wave ripples grade upward into parallel laminations, which may display gentle undulations (Fig. 2.1). Soft-sediment deformation features are present in the form of load structures which are 3- to 5 cm across. The contact with underlying strata at Beans Gap, TN is sharp, and is marked by a 7 cm thick phosphatic pebble lag (Fig. 2.2, Fig. 2.3). The contact with the overlying strata is more gradational.

The BTS at Flat Gap, Tennessee (Fig. 2.4) consists of tan-colored, hematite-stained, fine-grained sandstone beds which are 5-10 centimeters thick. Primary sedimentary structures are not visible in the field because the rock is so intensely weathered. No pebble lags (e.g., ravinement surfaces) occur within this variant at this locality. There is a color change from red semi-fissile to non-fissile shale to 5 centimeters of gray semi-fissile shale directly beneath the BTS at this one locality. The proximity of this section to the Beans Gap section is the reason for placing it in the WL variant.

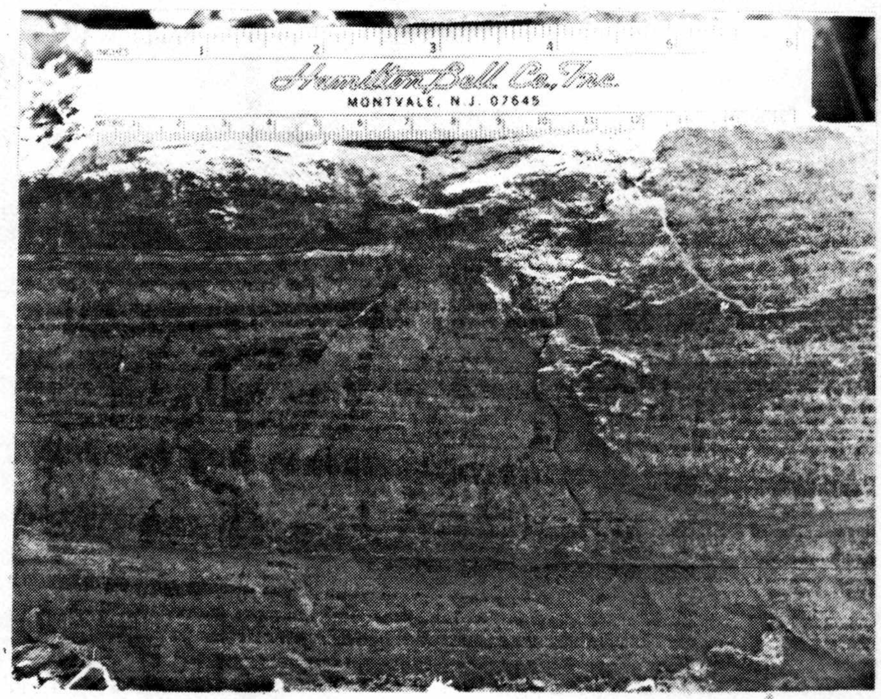

Figure 2.1. Outcrop photograph of the upper part of the BTS at Beans Gap, TN (section BG in Figure 1.2) displaying horizontal laminations (WL variant), which are indicative of beach swash-backswash laminations. Lower scale is in centimeters.

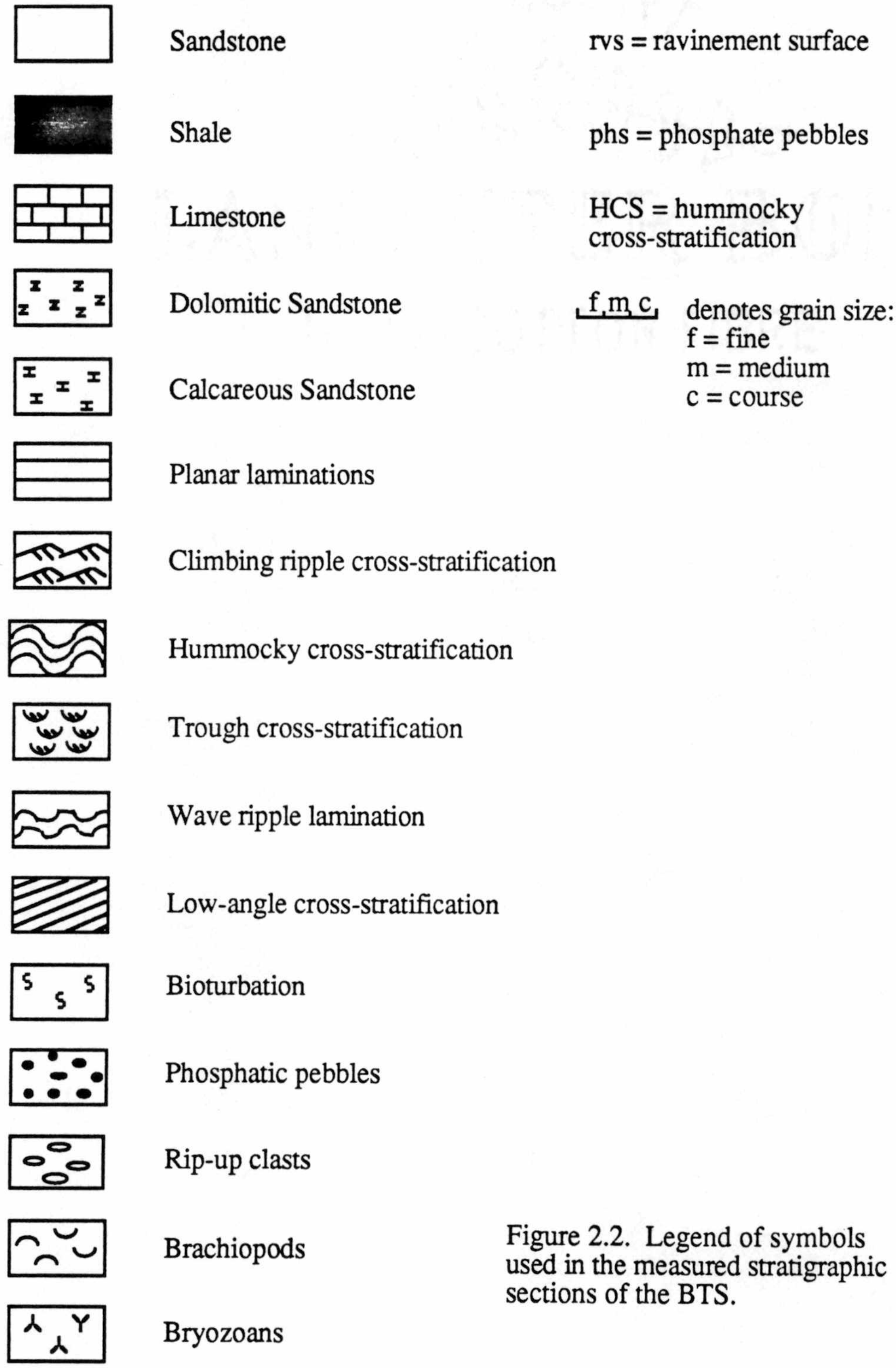

Figure 2.2. Legend of symbols used in the measured stratigraphic sections of the BTS.

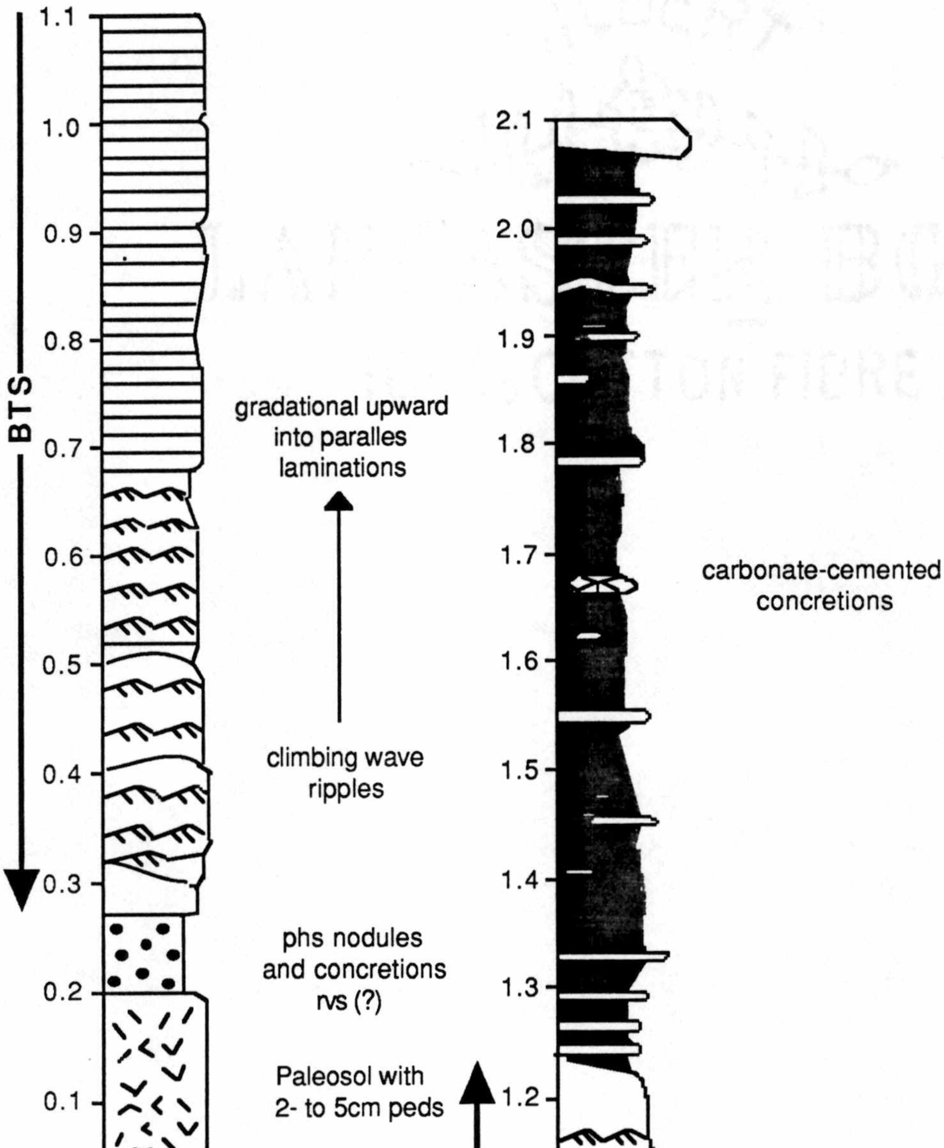

Figure 2.3. Measured stratigraphic section of the BTS at Beans Gap, Tennessee (Locality BG in Figure 1.2). The entire section consists of the WL variant and rests nonconformably upon Upper Ordovician-age paleosol horizons. Section was measured by Steve Driese.

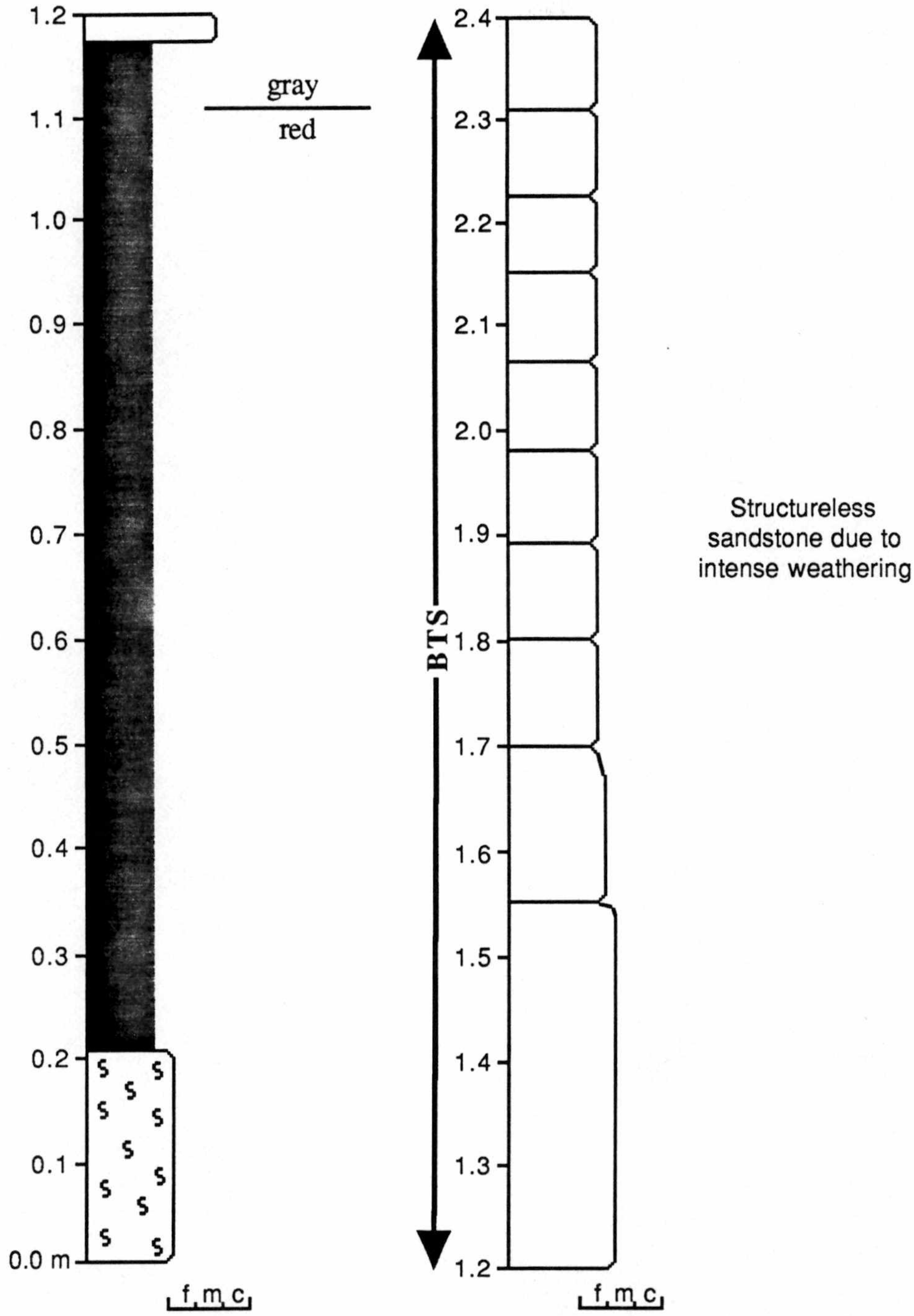

Figure 2.4. Measured stratigraphic section including the BTS at Flat Gap, Tennessee (Locality FG in Figure 1.2). The BTS begins at 1.18 meters and continues up to 3.25 meters (see Appendix A for complete measured section) and it consists entirely of the WL facies variant. Note the distinct color change from red to gray shale directly beneath the BTS.

Interpretation:

The WL variant occurs at only two localities, both of which occur on the Copper Creek thrust sheet (Fig. 1.2) at Bean's Gap and Flat Gap, Tennessee (Figs. 2.3 and 2.4). These are the most proximal deposits of the BTS. The BTS consists entirely of this variant at these two localities. At Beans Gap, TN, the BTS truncates what has been classified by Driese and Foreman (in review) as a Type 3 paleosol: ancient soil horizons which have weak to moderate soil structure development and distinctive color banding that resembles modern Inceptisols (Soil Survey Staff, 1975; Driese and Foreman, in review). The contact with the paleosols is sharp and marked by a phosphatic pebble lag or ravinement surface (see the discussion section at the end of this chapter for development of the ravinement concept; Fig. 2.3). Strata overlying the BTS consist of semi-fissile gray clayshale containing thin lenses of very-fine-grained tan sandstone. These rocks make up part of the Hagan Shale member of the Clinch Sandstone. Schoner (1985a, b) interpreted the Hagan Shale to represent lagoonal and washover fan deposits, whereas Fischer (1987) interpreted the Hagan Shale as representing distal shelf deposits.

The interpretation of the depositional environment for the WL variant is based upon the observed sedimentary structures at Beans Gap, TN (Fig. 2.3). The occurrence of wave ripples indicates at least low velocity (>9 cm/sec) wave orbital motion. The transition from wave ripples to parallel laminations suggests increasing wave orbital velocities such as within a beach swash zone (Reineck and Singh, 1986; Harms and others, 1982). Thus, the sequence of structures in the WL variant is similar to those described by McCubbin (1969; 1982) and Ryer (1977) for Upper Cretaceous shoreline sequences in the Rocky Mountain region. Similarly, Clifton and others (1971) described these same types of structures in their studies of the high-energy, nearshore areas along the coast of southern Oregon. Therefore, the WL variant is interpreted to have been deposited in the beach to upper shoreface environment. One factor, however, makes this interpretation problematic and that is the fact that the wave ripples described previously at Beans Gap, TN are climbing wave ripples. Climbing wave ripples are not reported by the above authors, rather, they report normal asymmetric and symmetric wave ripples for these shallow water environments.

Fine-grained bioturbated variant (FGB)

Description:

The FGB variant consists of gray to brown, dolomitic siltstone to fine-grained sandstone that displays moderate to intense bioturbation. Trace fossils dominantly consist of oval-shaped, 2-10 cm diameter, sharp to diffuse feeding traces (Fig.2.5a). Other trace fossils include branched, dark-colored mottles and vertical to oblique burrows. Vertical burrows tend to be filled with sediment that is different from that of the surrounding rock. One burrow (Fig. 2.5b) was observed to contain distinct spreite suggestive of a feeding trace, however, it was difficult to identify the taxon due to a lack of diagnostic features besides the spreite. The degree of bioturbation varies from rocks that have been completely homogenized to those that have been only partially homogenized and still contain some primary sedimentary structures in the form of horizontal laminations.

Deposits of the FGB variant vary from thin- to thick-bedded, and may encompass the entire BTS. Contacts with the underlying strata may be gradational to sharp. Sharp contacts with the overlying strata are marked by a ravinement surface (Fig. 2.6 a and b) at Powell Mountain and Whiteoak Mountain (Fig. 2.7 and 2.8). At Melton Lake, TN (Fig. 2.9) and Lone Mountain, TN (Fig 2.10), this variant occurs directly

Figure 2.5. (a.) Slab photograph of sample 9.35-WO from Whiteoak Mountain, TN (Locality WO in Figure 1.2) illustrating the FGB variant, in which the rock has been intensely bioturbated. The dominant features are sharp to diffuse, ovoid-shaped burrows which are indicative of feeding structures. (b.) Slab photograph of sample 1.0-RG from Ringgold, GA (Locality RG in Figure 1.2) illustrating both the ovoid-shaped burrows as shown in (a) and curved, vertical burrows. Scales are in centimeters.

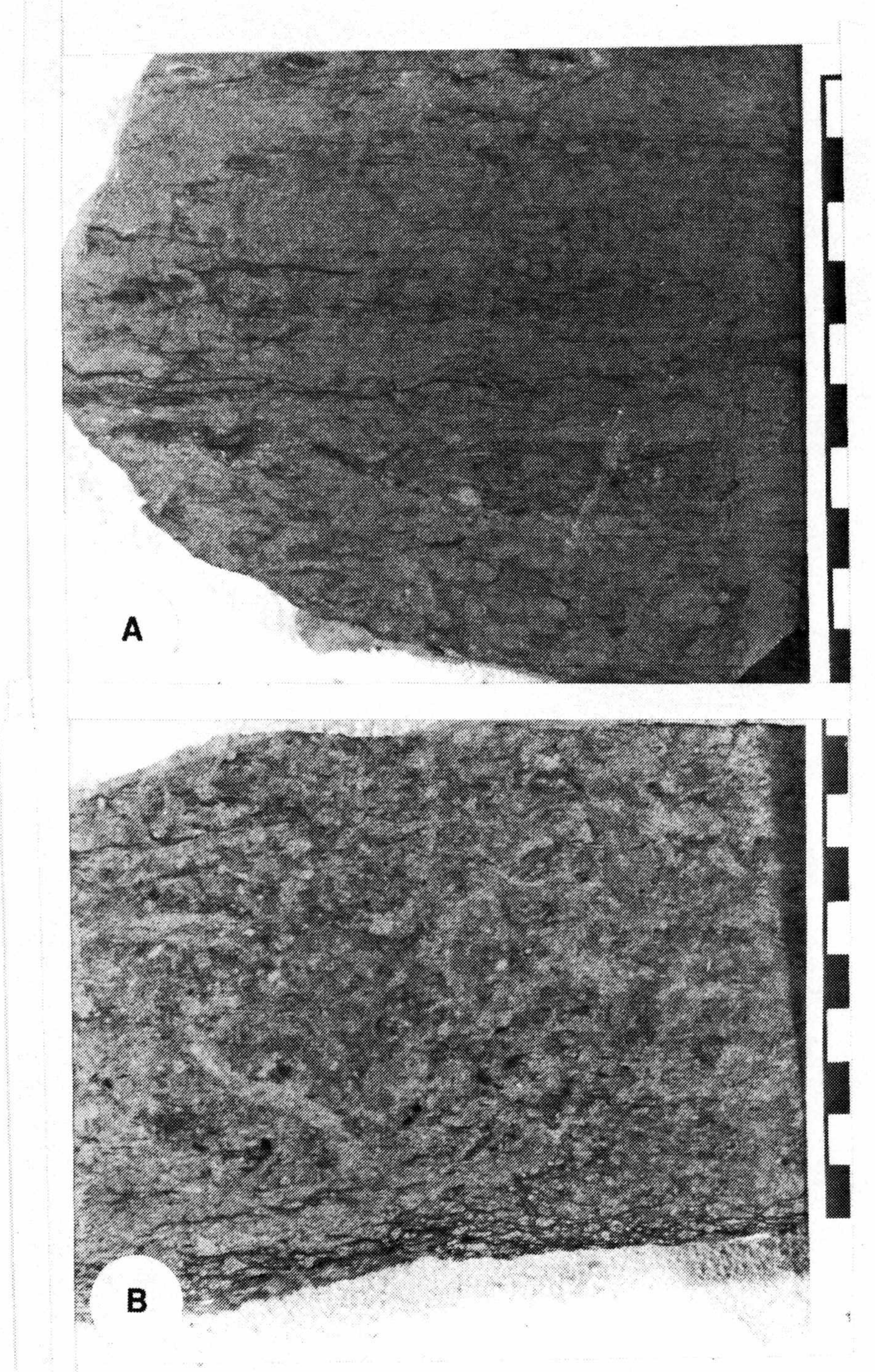
A
B

Figure 2.6. (a.) Whole 1x2 in or 25x45mm (thin-section photograph taken in transmitted light of sample AG-1 collected from the BTS at Powell Mountain, VA showing the sharp contact between the FGB variant and a phosphatic pebble lag. Locality PM in Figure 1.2. (b.) Slab photograph of sample 9.45-WO collected from the top of the BTS at Whiteoak Mountain, TN (Locality WO in Figure 1.2). Again, note the sharp contact between the FGB variant and a phosphatic pebble lag, as well as the contrasting grain sizes. Scale on the right is in centimeters.

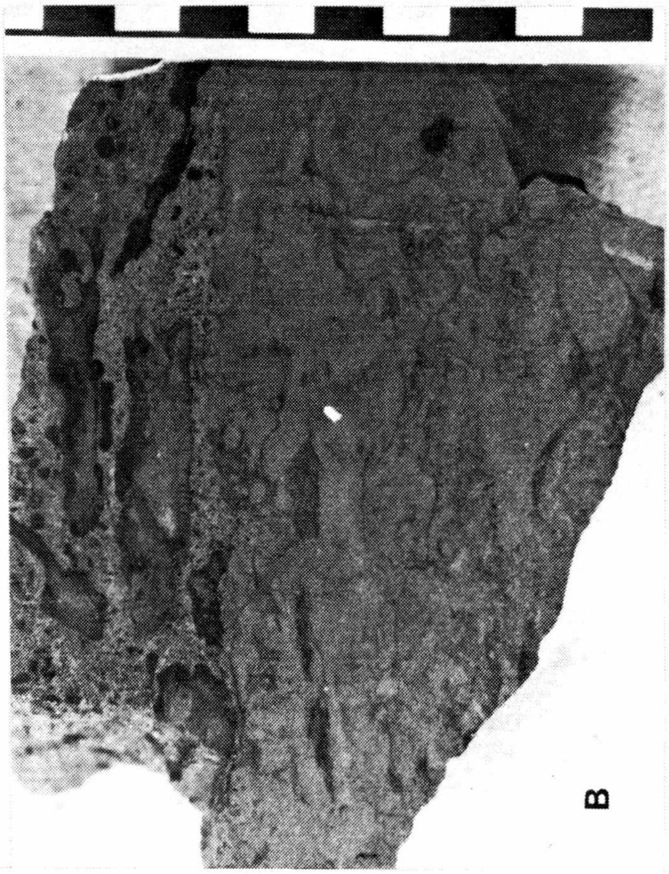
B

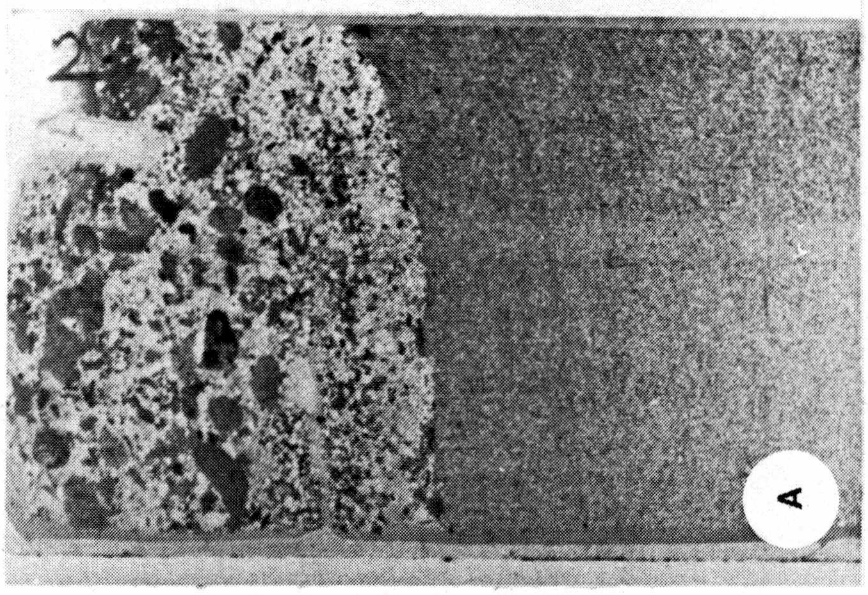
A

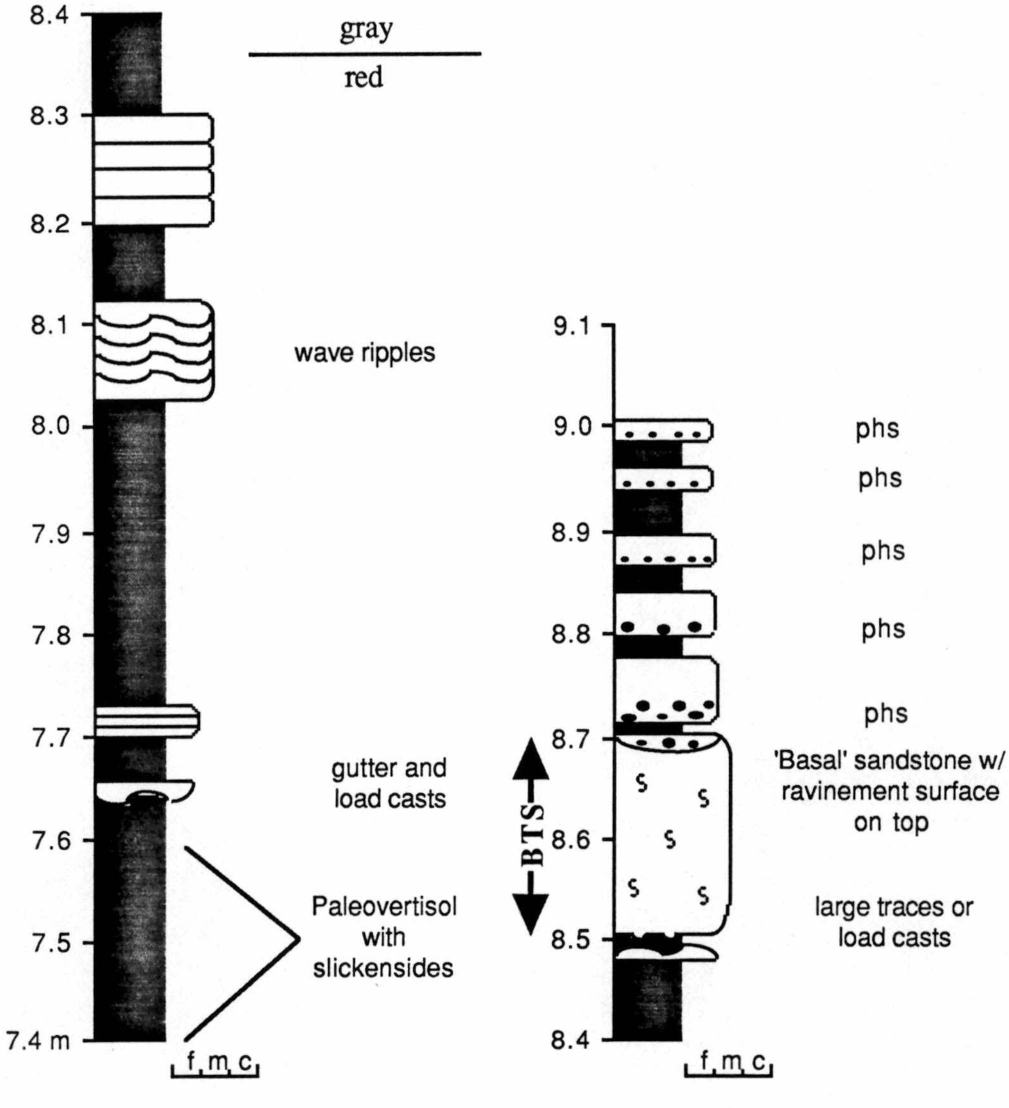

Figure 2.7. Measured stratigraphic section of the BTS at Powell Mountain, Virginia (Locality PM in Figure 1.2). The BTS is only 20 centimeters thick here and is part of the FGB variant. (Section modified from Driese and Foreman, in review).

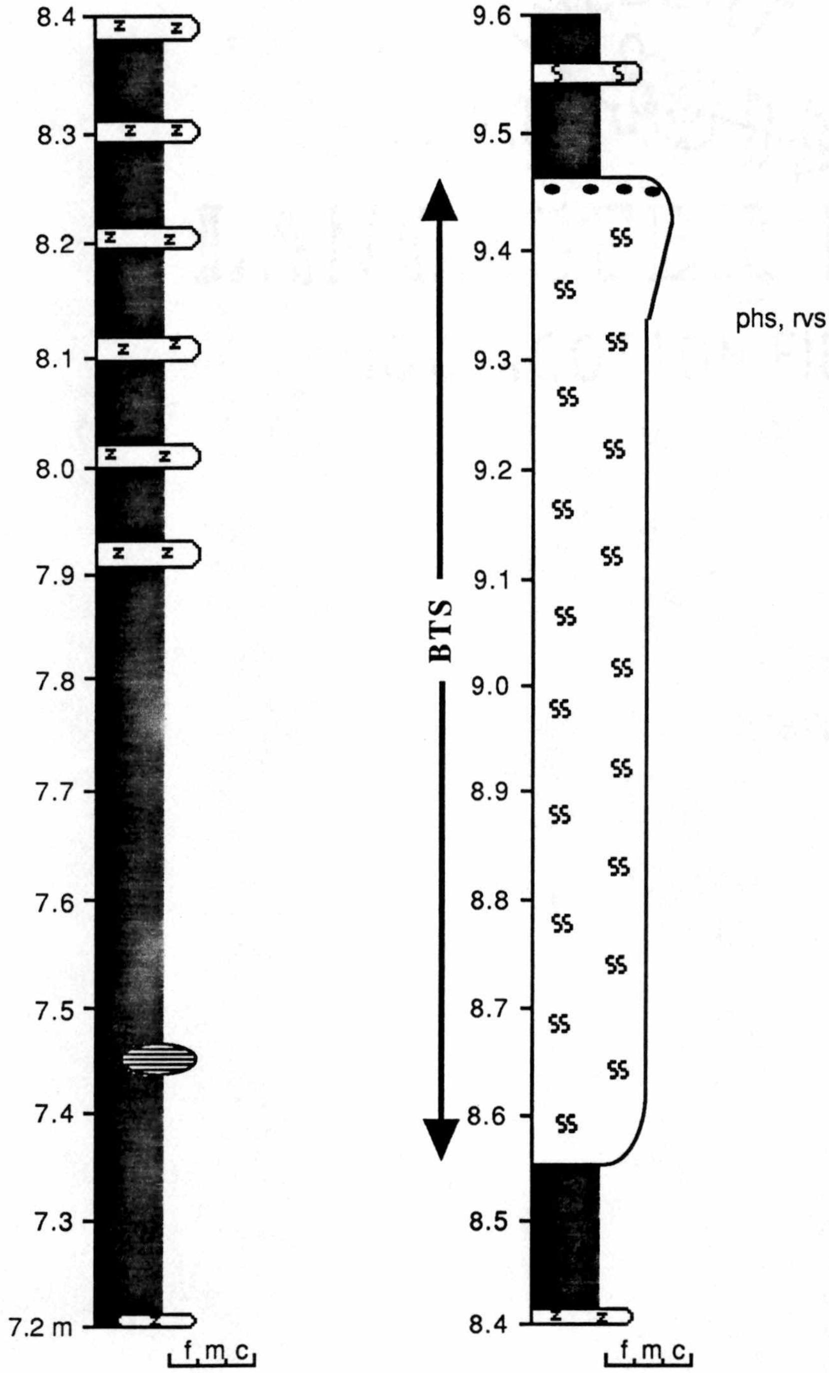

Figure 2.8. Measured stratigraphic section of the BTS at Whiteoak Mountain, Tennessee (Locality WO in Figure 1.2). The BTS is made up entirely of the FGB variant from 8.55 to 9.47 meters. The red-to-gray transition occurs 7.05 meters below the BTS.

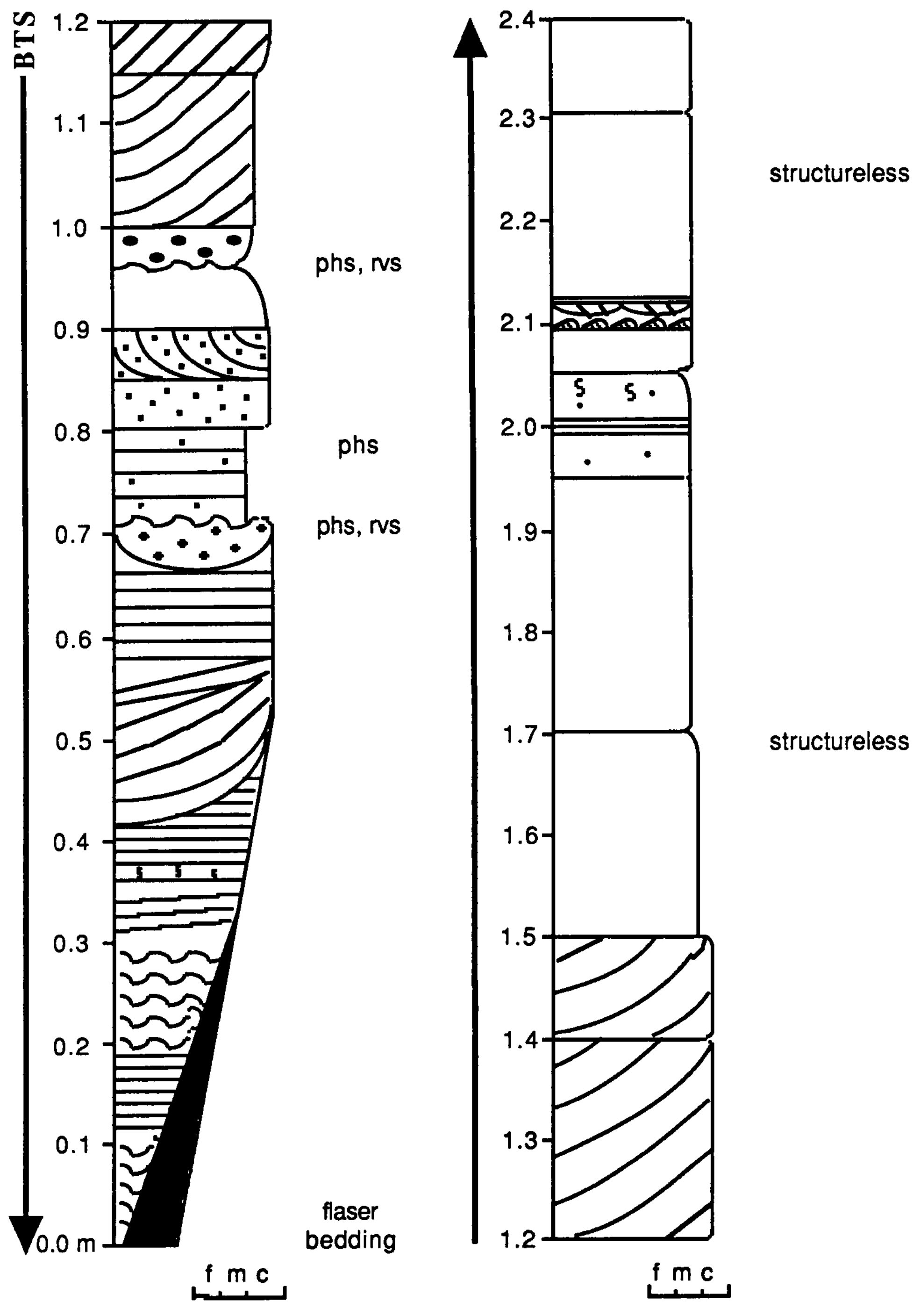

Figure 2.9. Measured stratigraphic section at Melton Lake, Tennessee (Locality ML in Figure 1.2). This section of the BTS consists of the CBS variant from 0.0-1.5 meters and the FGB variant from 1.5-3.0 meters. The red-to-gray color change is covered somewhere below the BTS. See Appendix A for the full section measured.

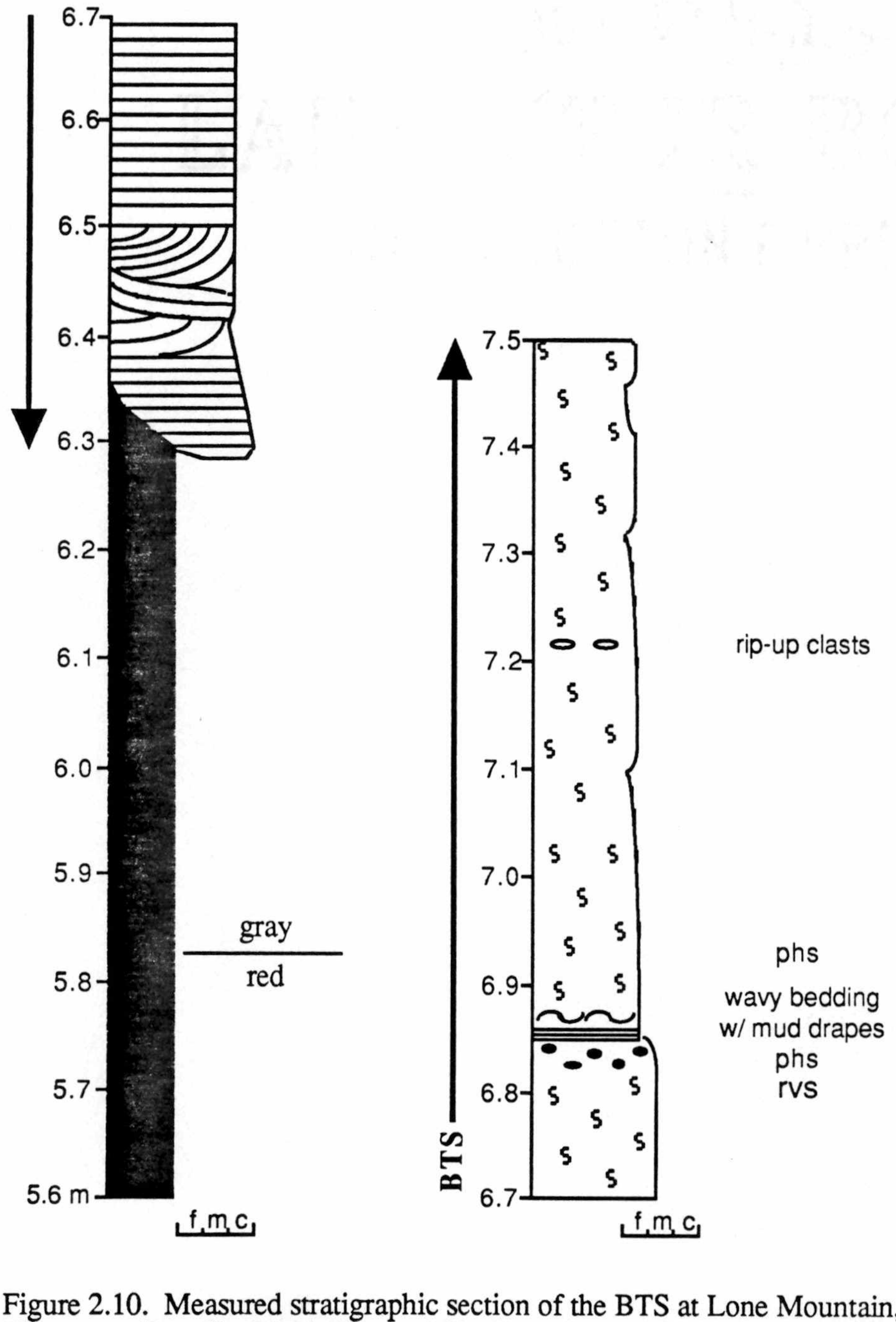

Figure 2.10. Measured stratigraphic section of the BTS at Lone Mountain, Tennessee (Locality LM in Figure 1.2). Note that the BTS consists of the CBS variant (6.3-6.7 meters) and the FGB variant (6.7-7.5 meters).

above a small channel sequence that is part of the cross-bedded sandstone variant (CBS). The contact is marked by a phosphatic pebble lag. Primary physical sedimentary structures structures within this variant are rare to absent, with the exception of the Cumberland Gap, TN section (Fig. 2.11), which contains a bored, phosphatic hardground that is overlain by phosphatic pebbles and red siltstone rip-up clasts (Fig. 2.12 a) Similarly, the BTS at Tiftonia, GA overlies a carbonate packstone that contains a phosphatic hardground which is bored as well (Fig. 2.13). Another exception is the Whiteoak Mountain section, where some samples display primary horizontal laminations that have been partially disrupted by trace fossils (Fig. 2.12 b).

Interpretation:

The intensity of bioturbation in these rocks makes taxonomic identification of individual traces problematic. Therefore, such identifications will not be attempted here. These features, however, do reveal information about the depositional environment of this variant. Sandstone deposits that were intensely bioturbated were deposited under conditions of slow continuous deposition (Howard, 1978), in which organisms could feed for long periods of time within soft, nutrient-rich substrate. Thus, the sediment was completely bioturbated. Sandstone deposits that are moderately bioturbated and therefore occur with remnant horizontal laminations, are interpreted as having been deposited under conditions of slow, but discontinuous deposition, in which periods of nondeposition allowed for increased amounts of

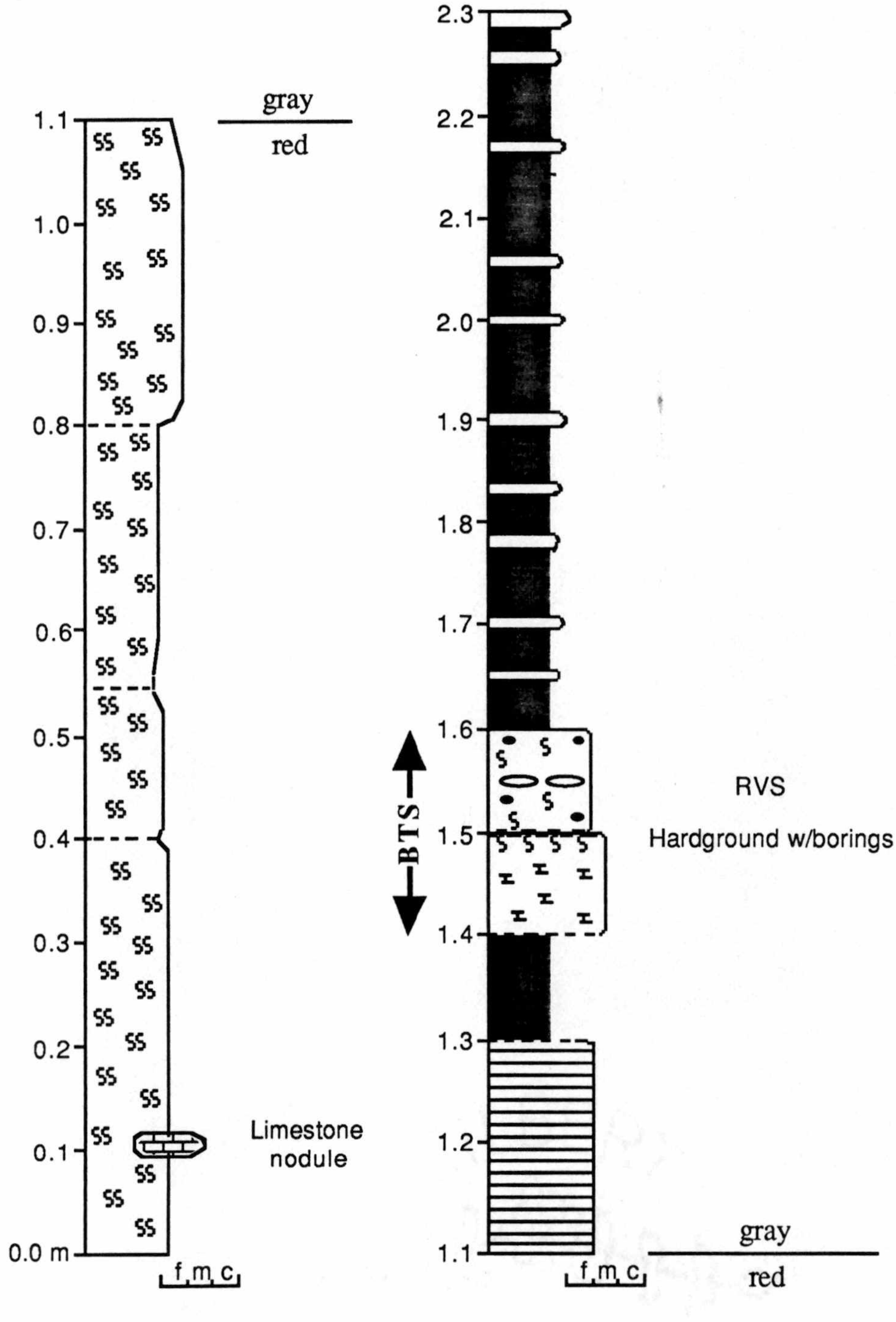

Figure 2.11. Measured stratigraphic section at Cumberland Gap, Tennessee (Locality CG in Figure 1.2). The BTS consists of the FGB variant.

Figure 2.12. (a) Whole thin-section (2x3 in or 51x76 mm) photograph taken in transmitted light of sample 2.95-CG-1 collected from the BTS at Cumberland Gap, TN (Locality CG in Figure 1.2). This sample shows a burrowed horizon (FGB variant) overlain by red-colored rip-up clasts and minor phosphates. (b) Whole thin-section (same scale as in a) photograph of sample 0.75-RGL collected from the BTS at Ringgold, GA (Locality RG in Figure 1.2) illustrating the FGB variant where it has only been moderately bioturbated so that primary horizontal laminations are still visible.

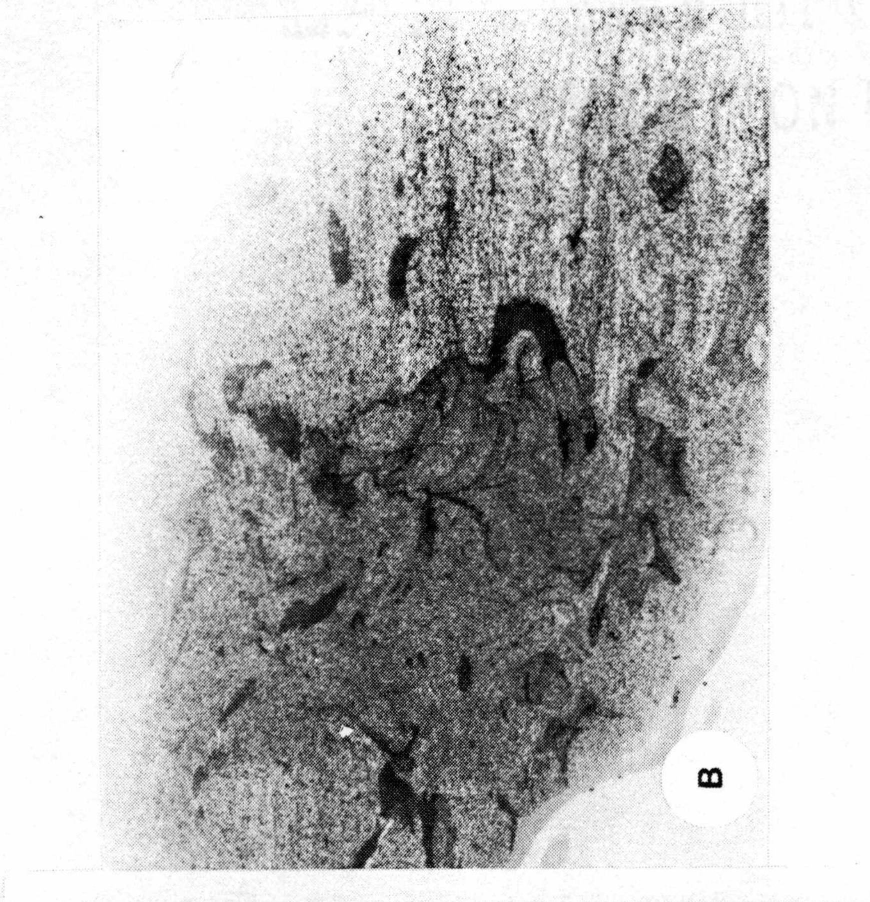
B
A

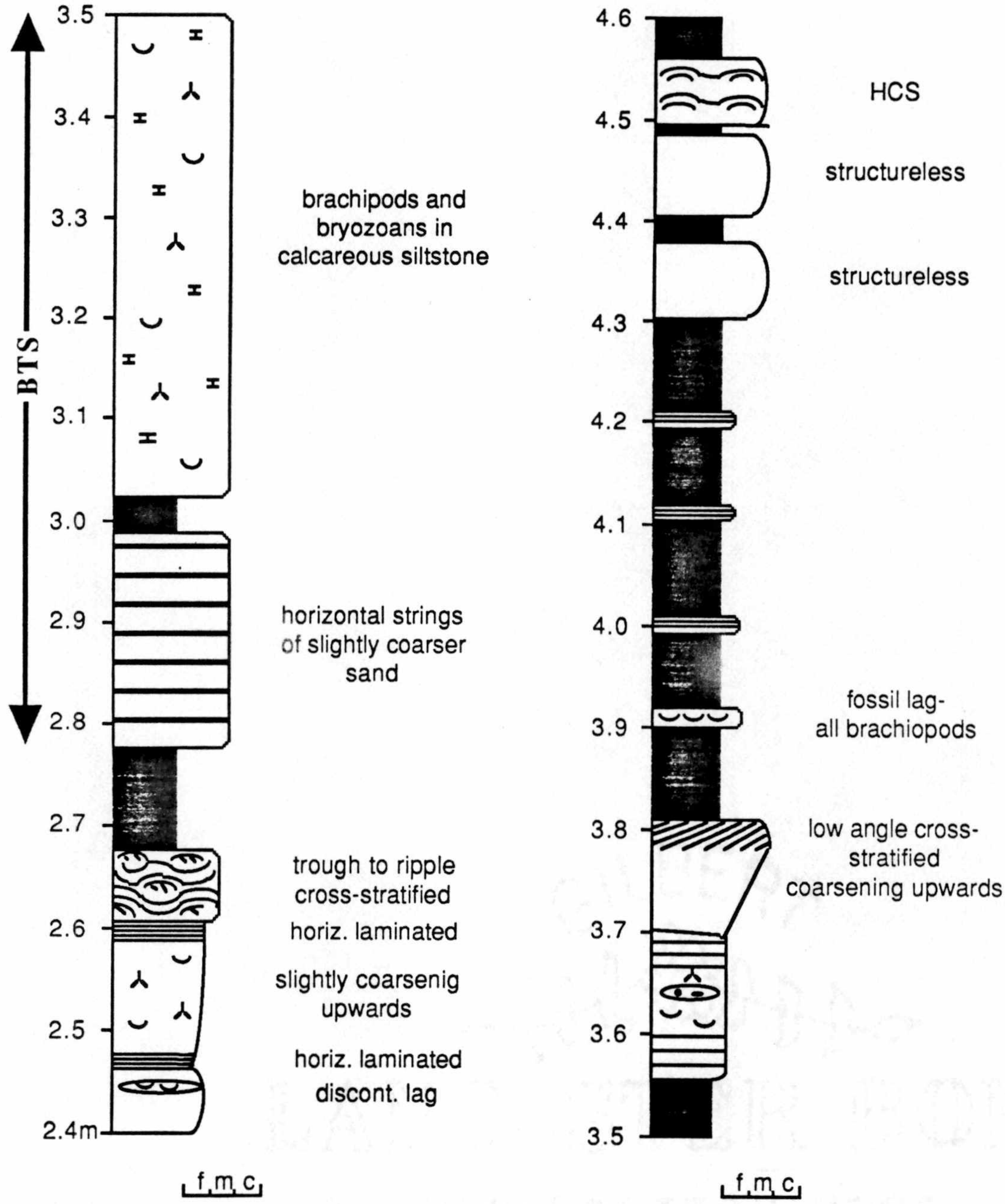

Figure 2.13. Measured stratigraphic section at Tiftonia, Georgia (Locality TF in Figure 1.2). The BTS consists of the FGB variant here. The red-to-gray color change occurs at 1 meter above the base of the measured section and is shown in Appendix A.

biogenic activity. The implication of the above interpretation is that the BTS was deposited under overall low energy conditions.

Dorjes (1971) and Reineck and Singh (1986) have suggested that the transition zone between coastal sediments and shelf sediments (as well as the inner shelf) arecharacterized by intense bioturbation. Most of the traces appear to be horizontal feeding traces (Fig. 2.5) suggestive of the *Cruziana* Ichnofacies, which represents the shelf environment (Seilacher, 1967). Vertical traces, such as that shown in Figure 2.5 b are more indicative of the *Skolithos* and *Glossifungites* variant, which represent the shoreface environments (Seilacher, 1967). Vertical traces indicative of suspension-feeding are rare, however, in the BTS. Therefore the FGB variant is interpreted to represent the lower shoreface to inner shelf environments. The lower shoreface is represented by partially bioturbated sandstone deposits and the transition to inner shelf environments are represented by the intensely bioturbated sandstone deposits.

The FGB variant overlies the fine-grained, siliciclastic redbeds of the Juniata Formation and the mixed carbonate-siliciclastic redbeds of the Sequatchie Formation. These formations display repetitive sequences of rippled to horizontally laminated siltstone beds overlain by mudcracks, and followed by rip-up clasts. Carbonate deposits are interbedded with siltstone in the westerly and southerly outcrop belts. The sequence of sedimentary structures in these underlying deposits is indicative of the periodic drowning and subaerial exposure that occurs during tidally-controlled deposition (Weimer and others, 1982).

The strata overlying the BTS consist of interbedded gray clayshale and hummocky cross-stratified sandstone, indicating the establishment of an inner shelf depositional environment, as will be shown in the ensuing discussion.

Cross-bedded Sandstone Variant (CBS)

Description:

The CBS variant consists of discontinuous, tan-gray, fine-grained to medium-grained, dolomitic sandstone that contains both horizontal laminations and low-angle cross-stratification. Rare ripple laminations with clay drapes may also be present. Small-scale climbing wave ripples were noted in one bed at Ringgold, GA (Fig. 2.14). Wherever the CBS variant occurs, the base is marked by a scour which incises into the underlying strata. These scours typically contain of pebbles of different compositions, including phosphate and rock fragments. Pebble lags also occur at varying positions within this variant as well. Bedding thicknesses vary, but are on the order of 30 to 60 centimeters. The occurrence of this variant is restricted to outcrops along the Whiteoak Mountain thrust belt and it is always overlain by rocks of the FGB variant, thereby making the BTS thickest at these localities. These localities are Lone Mountain, TN (Fig. 2.10), Melton Lake, TN (Fig. 2.9) and Ringgold, GA (Fig. 2.14)

Interpretation:

Facies CBS represents small channel sequences whose vertical suite of sedimentary structures (mostly horizontal laminations and low- to high-angle cross laminations; Fig. 2.15) is typical of tidal channel sequences such as those found in the Aux Vases (Mississippian) channel sandstones in the Rural Hill oil field, Illinois (Weimer and others, 1982), as well as those of the Upper Almond Formation (Cretaceous) in Wyoming (Weimer and others, 1982). Channel sandstone deposits of the Upper

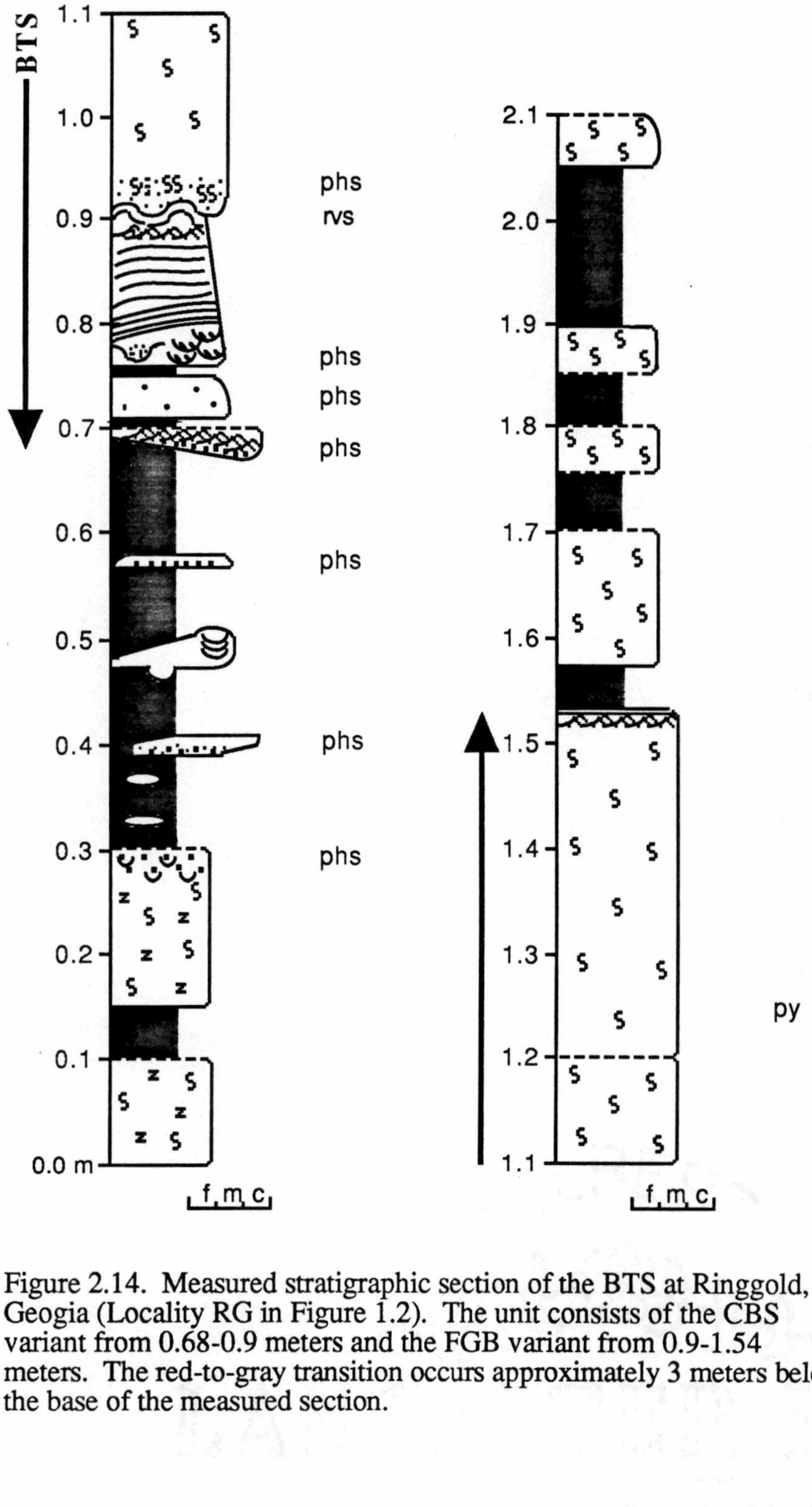

Figure 2.14. Measured stratigraphic section of the BTS at Ringgold, Geogia (Locality RG in Figure 1.2). The unit consists of the CBS variant from 0.68-0.9 meters and the FGB variant from 0.9-1.54 meters. The red-to-gray transition occurs approximately 3 meters below the base of the measured section.

Figure 2.15. Outcrop photograph of the BTS at Lone Mountain, TN (Locality LM in Figure 1.2). Note the thin, discontinuous channel sequences (arrows) that occur at the base of the BTS. Note the author for scale in the center of the photograph just to the left of the tree.

Almond Formation are characterized by a sharp scoured base, one or more shell lags, and an overall fining-upwards trend. High-angle cross-stratification is common, as are clay drapes. These characteristics are nearly identical to those observed at the Melton Lake section (Fig. 2.9). The Upper Almond inlet sequences are overlain by a transgressive shoreface sandstone (Weimer and others, 1982). A good example of transgressive tidal inlets occur in the southern Gulf of St. Lawrence, Canada where 90% of the sediment transport (landward of a barrier system) has been attributed to present-day and former tidal inlets (Reineck and Singh, 1986).

The CBS variant is associated with the FGB variant, which has a lower shoreface to inner shelf signature. This transgressive sandstone body is indicative of deeper water than the transgressive sandstone of the Upper Almond Formation. It is interpreted here that the CBS variant formed from remnant tidal channels that were part of the Upper Ordovician tidal flats. These became filled in with reworked sediments as sea-level gradually rose and eroded the upper parts of the existing tidal flat. This would explain why the BTS channel sequences are not much thicker.

Discussion:

Thicknesses of the BTS vary both across-and along-strike. Across-strike variations reflect both the shelf bathymetry and antecedent topography. Similarly, along-strike variations reflect the antecedent topography as well. Maximum thicknesses occur along the central Rockwood Belt where the Melton Lake exposure is 1 meter thicker than other exposures along the Whiteoak Mountain thrust sheet (Fig.1.2) as well as those exposures along the Copper Creek thrust sheet that are part of the WL variant. The greatest thicknesses occur at Lone Mountain and Melton Lake, where the base of the BTS is marked by thin channel sequences. This is an effect of the antecedent topography. That is, the channel sequences represent the infilling of tidal channels that existed as sea-level first began to rise. An isopach map of the BTS (Fig. 2.16) that does not include the thicknesses added by the channel sequences illustrate the sheet-like form of the BTS.

At all localities, except for Flat Gap (Fig. 2.4), the common feature which aids in the correlation of the BTS across four thrust sheets is the presence of phosphatic pebble lags, which are interpreted to represent ravinement surfaces. These lag deposits are an important clue to the depositional history of the BTS. This feature, combined with the observed vertical trends, represents the most unequivocal evidence for a regional transgression.

During this sea-level rise, the process of shoreface retreat produced a number of distinctive features , all of which can be observed in the Lower Silurian BTS. The fact that the BTS can be traced across five thrust sheets, as well as along-strike, indicates that it represents a thin, but laterally continuous, veneer of sandstone which was deposited during a transgression, identifying it as what Swift (1971) termed a *transgressive sand sheet* or a *surficial sand sheet* (Swift, 1968; Saito and others, 1989; Fig. 2.16).

The fine-grained, quartzose nature of the BTS, and the occurrence of phosphatic pebble lags within the sandstone body, indicate that it is made up of palimpsest (Swift and others, 1971; McManus, 1975; Davis, 1983) sediment, which includes reworked relict sediment derived from the underlying Juniata and Sequatchie formations and minor amounts of new sediment which may have been supplied by the Taconic highlands further north. Phosphatic pebble lags (Fig. 2.17), or ravinement surfaces, within the BTS formed through the process of erosional shoreface retreat during a relative sea-level rise (Bruun, 1962; Swift, 1968; Swift and others, 1971; Nummedal

Figure 2.16. Isopach map of the BTS drawn on a palinspastic base that was modified from Roeder and Witherspoon (1978). The contour interval is 50 cm. Note the continuous sheet-like nature of the sandstone body. Thicknesses for Melton Lake, TN (ML), Lone Mountain, TN (LM), and Ringgold, GA (RG) do not include the thicknesses of the channel sequences because these are small-scale, discontinuous features.

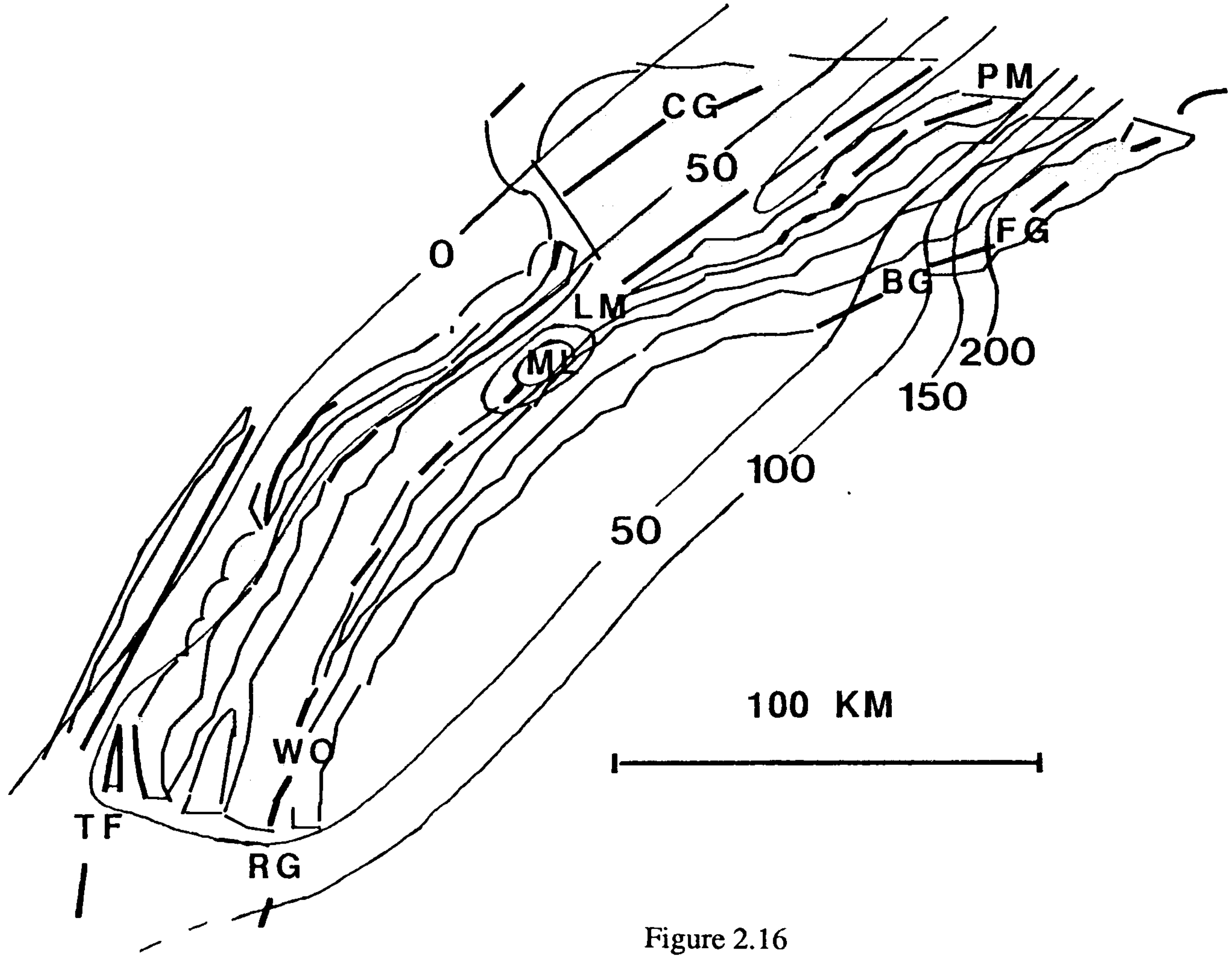

Figure 2.16

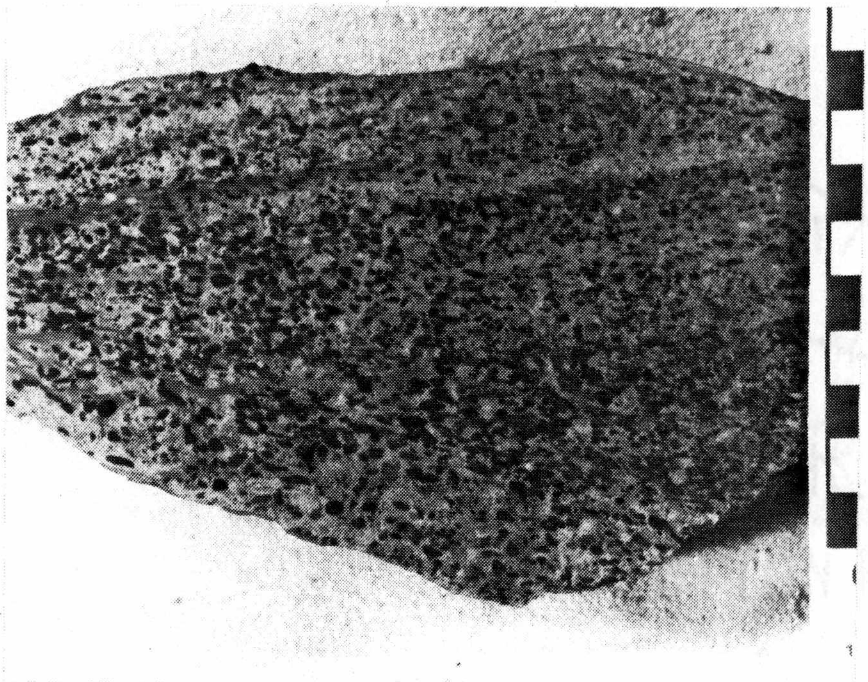

Figure 2.17. Slab photograph of sample 0.75-ML collected from the CBS variant at Melton Lake, TN (Locality ML in Figure 1.2) illustrating a coarse, cross-bedded, phosphatic pebble lag. Scale is in centimeters.

and Swift, 1987). Lag deposits, whether they consist of detrital pebbles or shelly material, are one of the most common features observed within transgressive sand sheets (see, for example, Saito and others, 1989; Kidwell, 1989; Pattison, 1988; Plint, 1988; Nummedal and Swift, 1987; Pilkey and others, 1981; Swift, 1968; Swift and others, 1971).

Ravinement surfaces form by the shoreward aggradation of the marine environments existing marginal to the shoreline (Fig. 2.18). According to Swift (1968), the ravinement process is that by which the shoreface is adjusted in order to provide an optimal surface to absorb wave energy. This adjustment is a vertical adjustment (Bruun, 1962; 1983). Numerous modern analogs exist where active erosional shoreface retreat has been, and is being observed. The best examples exist along the Atlantic Coast of the United States. At localities such as Ocean City, Maryland; Assawoman Island, Virginia; and the Outer Banks of North Carolina, this process is causing the retreat of the shoreface and the extension, shoreward, of the shelf ramp. According to Everts (1987), the new extension of the shelf ramp may bedepositional when new sediment is deposited upon pre-recent deposits as the shoreface retreats, or erosional if the same pre-recent sediment is scoured as the shoreface retreats. Factors affecting the style of shoreface retreat and ramp formation depend upon the shape of the shoreface, the size of the sediment within the shoreface, volume losses due to transport mechanisms (e.g., the presence of longshore currents), and finally, the effects of sea-level rise (e.g., rapid or slow; Everts, 1987). Features within the BTS such as the fine-grained nature of the unit, the pebble lags, and the scours into the underlying strata all indicate that the extension of this ancient ramp was

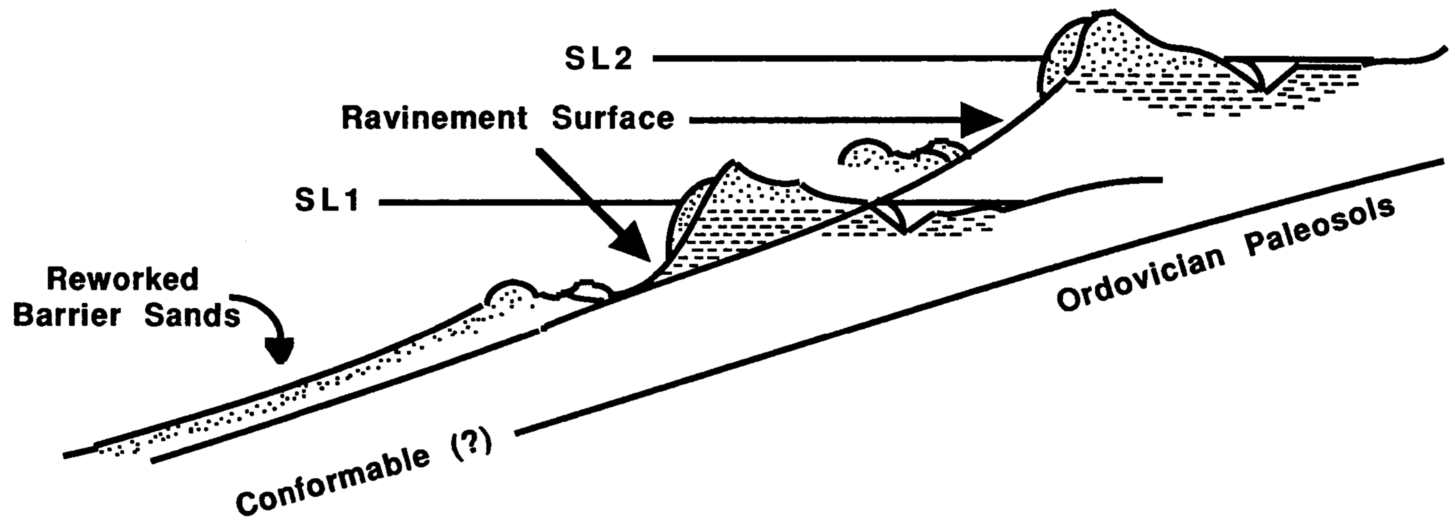

Figure 2.18. Model of the occurrence of erosional shoreface retreat. SL1 represents the initial relative sea-level lowstand during the late Ordovician. SL2 signifies the relative rise in sea-level that occurred at the very end of the Orodovician Period. During the rise, barrier or bar sands are reworked and redistributed as a sheet sand deposits with only coarse lags or ravinement surfaces left in the wake of the former barrier island. The barrier system then aggrades shoreward

erosional.

Ravinement lags are not necessarily restricted to shoreface environments. Saito and others (1989) have documented the occurrence of a ravinement surface made up of shell debris within the distal shelf and shelf slope deposits off the coast of Japan. No direct analogs exist for the BTS because there is no evidence for the existence or formation of a barrier island system during the Early Silurian. Also, the BTS is much finer-grained than the medium- to coarse sands being deposited along the Atlantic coast. This difference can be attributed to the lack of new clastics being supplied to the southern Appalachian basin during the earliest Silurian time. Only minor amounts of "modern" sand was provided and this occurs in the sandstones of the lag deposits. The rest of the strata were formed through the reworking of the very fine-grained underlying redbeds.

Other features which indicate that the BTS is a transgressive sand sheet include the observed vertical sequence of shoreface deposits (BTS) to inner shelf deposits (interbedded gray shale and wave-rippled to hummocky cross-stratified sandstone, Fig. 2.19 a and b). The term 'hummocky cross-stratification' (HCS) was first introduced by Harms (1975). Since that first identification, this sedimentary structure has become commonly recognized in the rock record. HCS is indicative of increased wave energy and occurs within the lower shoreline, at the transition between the shelf and the shoreface (Reineck and Singh, 1986). Interbedded HCS sandstone and shale sequences have been interpreted to have been deposited as a result of alternating storm-deposited sand and slowly-deposited hemipelagic mud. Therefore, water depths for such deposits are between fairweather wave base and storm wave base (Hamblin and Walker, 1979; Dott and Bourgeois, 1982; Walker and others, 1983;

Figure 2.19. (a.) Outcrop photograph taken of the strata which directly overlie the BTS at Melton Lake, TN (Locality ML in Figure 1.2). Features shown are storm beds, including micro-hummocky cross-stratification, interbedded with shales yielding unequivocal evidence for an upward-deepening trend following the deposition of the BTS. Note hammer for scale. (b.) Outcrop photograph of an amalgamated micro-hummock taken at the top of the BTS at Tiftonia, GA (Locality TF in Figure 1.2). The combined flow origin of this structure is illustrated by the combination of internal low-angle cross-stratification of a unidirectional flow origin enclosed in a combined-flow micro-hummock. Pencil is approximately 7 in long.

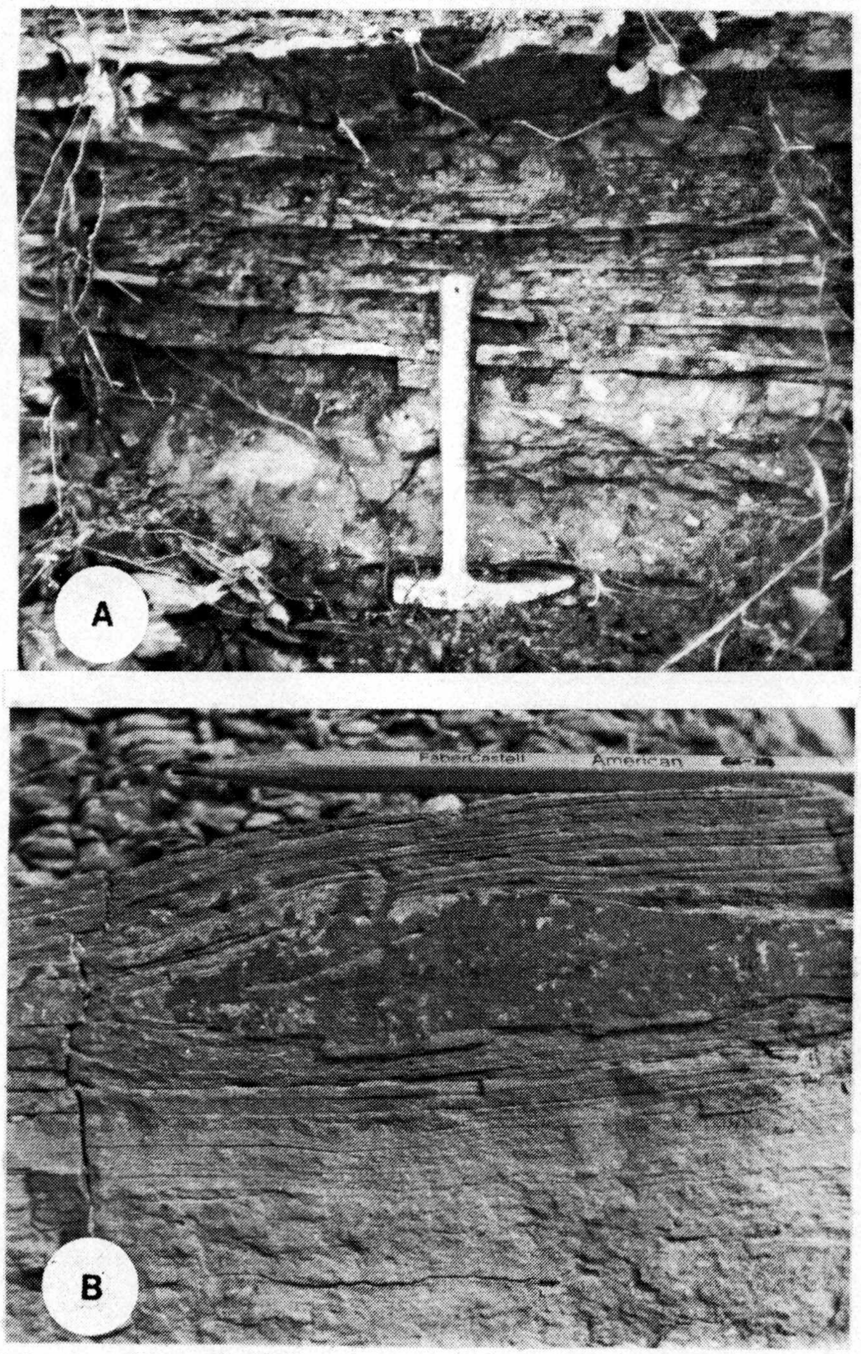
A
B
FaberCastell
American

Duke, 1985). Such a sequence of lithologies and sedimentary structures overlying the BTS are unequivocal evidence of a deepening trend.

Moving down section, the BTS directly overlies and truncates subaerial erosion surfaces, i.e. paleosol horizons. These paleosols are well-developed along the Copper Creek thrust at Bean's Gap, TN and the Wallen Valley thrust at Powell Mountain, VA (Fig. 1.2). Recent work by Driese and Foreman (in review) has delineated three types of paleosols whose differences can be attributed to their relative depositional position within the tidal flat, which is now represented by the upper Juniata Formation in the southern Appalachians. As will be discussed later, the tops of the paleosol horizons represent a hiatus, and perhaps even an unconformity.

Although a complete transgressive sequence is lacking within the BTS, the variants described in the previous chapter can be vertically superimposed with respect to the predictions of Walther's Law to produce an idealized vertical sequence of transgressive deposits. By combining an 'average' thickness for each variant based on the measured stratigraphic sections (Fig. 2.20), the total thickness for the ideal transgressive sequence would be on the order of 3 meters.

The BTS thus represents a sequence-bounding surface which is also a transgressive surface. This surface marks the boundary between the Middle to Upper Ordovician carbonate to siliciclastic sequence which represents the infilling of the Sevier basin (Walker and others, 1983), and the Lower Silurian (Llandoverian) clastic wedge. The term 'sequence boundary' is used here according to the definition given by Galloway (1989) which states, " The defining genetic stratigraphic sequence boundary is a sedimentary veneer or surface that records the depositional hiatus that occurs over much of the transgressed shelf and adjacent slope during maximum marine flooding". Similarly, Jordan and Flemings (1989) have shown, using a

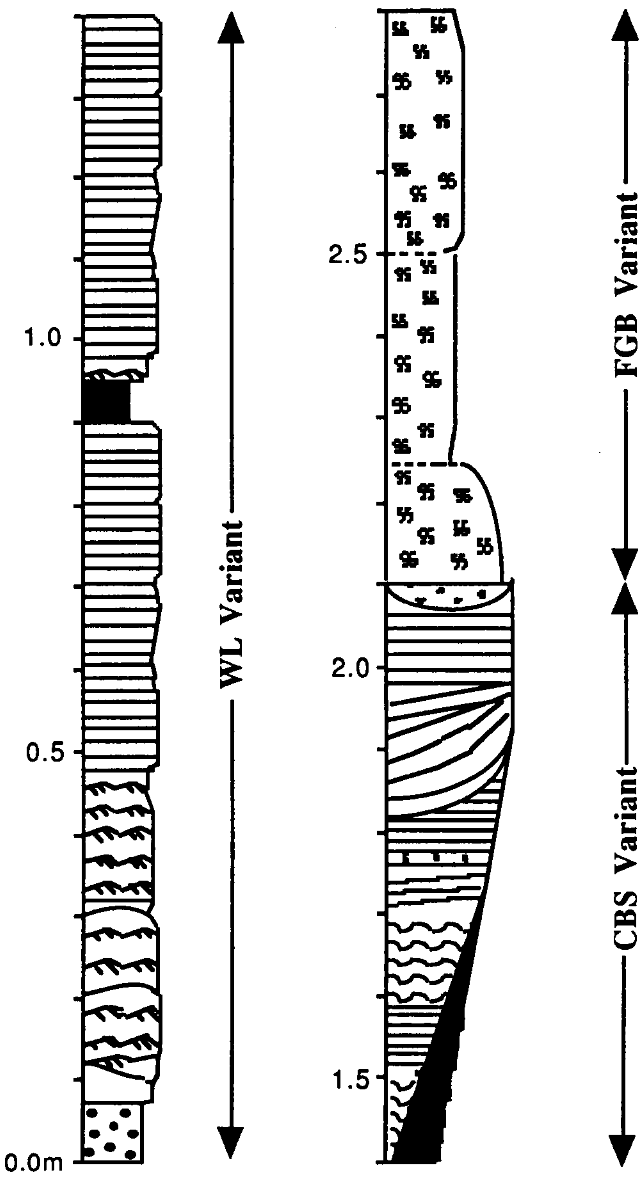

Figure 2.20. Idealized transgressive sequence based on lateral relationships between the facies variants within the BTS. Note that these facies variants do not all occur together at any on locality, however, each facies variant can be observed in outcrop moving from the eastern thrust sheets to the western thrust sheets.

forward-driven numerical model for clastic deposition in a foreland basin, that sea-level variation in a foreland basin will produce a stratigraphic sequence much different from that of passive margins due to differences in subsidence/sediment supply geometries. Their model predicts that foreland basin sequences will be bounded by marine flooding surfaces and condensed sections as opposed to widespread erosional (subaerial) unconformities, such as those found in passive-margin sequences. Passive-margin sequences, as described by the Exxon Group (see, for example, Mitchum and others, 1977; Vail, 1987), are bounded by surfaces which represent sea-level lowstand (extensive subaerial unconformities) and are centered on marine-flooding events. Galloway's (1989) genetic stratigraphic sequence paradigm and Jordan and Fleming's (1989) foreland basin sequence model are much more applicable to outcrop studies of exhumed foreland basins because they take into account the fact that the stratigraphic architecture is controlled by a combination of sediment supply, basin subsidence (and tectonism), and eustatic sea-level change. Thus, the application of these stratigraphic sequence models are not strictly limited to passive margins.

The following is a description of the sequential development of the Lower Silurian shoreline (Fig. 2.21 a and b). During Ashgill time a prograding mud-to silt-dominated (due to low sediment supply) tidal flat existed that locally experienced significant periods of subaerial exposure conducive to soil formation, perhaps associated with a eustatic lowstand (Driese and Foreman, in review). A relative sea-level rise, due to Gondwana deglaciation and local tectonism, commenced at the end of this time period. During the initial rise in sea-level, tidal flat shoals and longshore bars aggraded toward the shoreline as a result of wave action (Gohren, 1975). Deposition of the BTS occurred through processes which were originally suggested by Swift and others

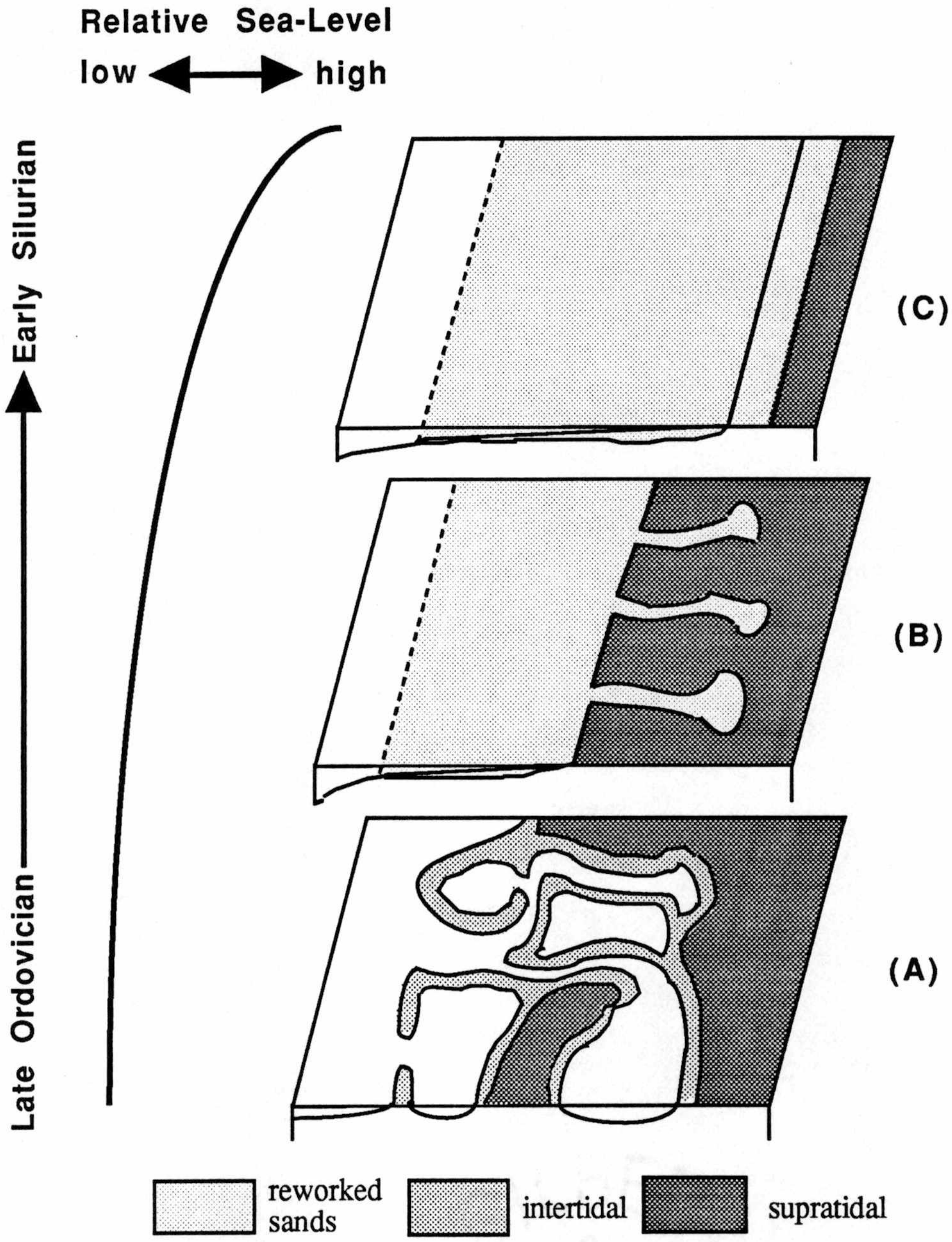

Figure 2.21. Figures illustrating the progression of paleoenvironments and a closeup of the facies variant relationships during the Lower Silurian Period. (a) progression of paleoenvironments, from bottom to top, during a relative sea-level rise. (A) represents Juniata/Sequatchie tidal flat environments (modified from Driese and Foreman, in review); (B) represents an intermediate time of sea-level rise during which tidal flat sands were being reworked by erosional shoreface retreat during the initiation of a sea-level rise. (B) was not preserved except for very local preservation of lower parts of tidal channel sequences; (C) represents a similar system to (B) during the sea-level highstand accompanied by maximum retreat of the shoreline. Note how the channels of the tidal flat system became filled in with reworked sediments as a result of the transgression.

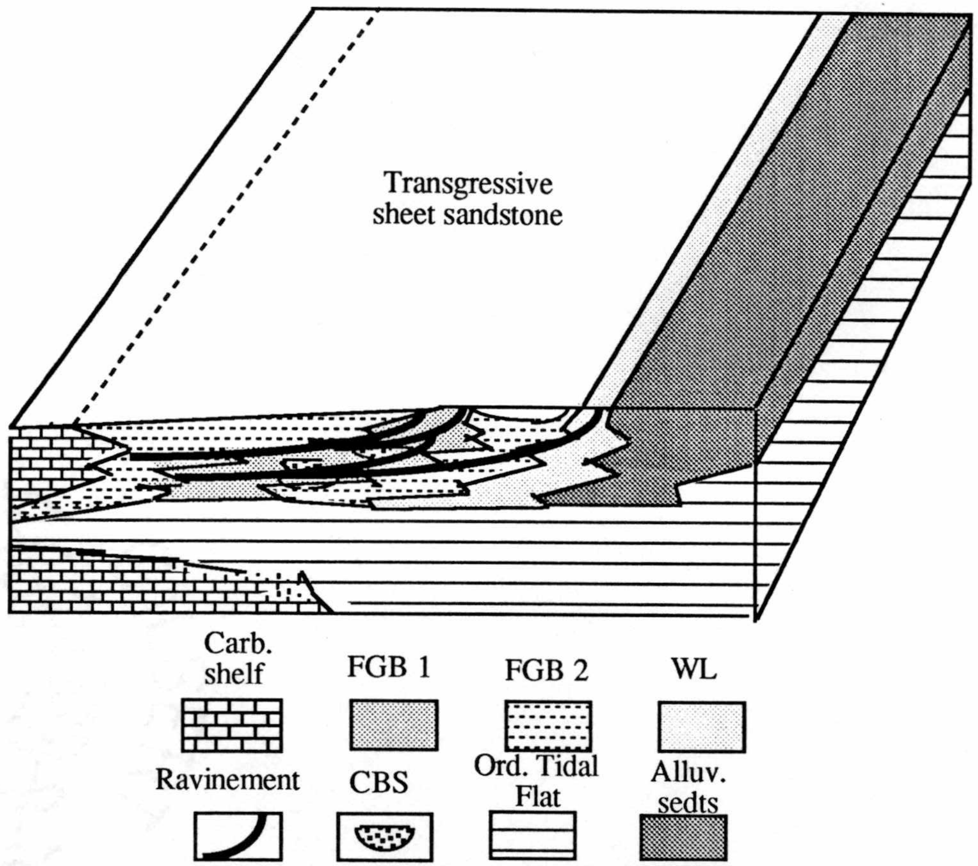

(b) Three dimensional portrayal of the sedimentary facies variant relationships during the relative sea-level highstand during the Lower Silurian Period. Note the aggradation of sediments both horizontally and vertically. FGB 1 and 2 are inferred partially and fully bioturbated sands, respectively. Lower Silurian alluvial sediments are inferred to have existed, however, they have since been thrust over and stripped away by erosion. Note high degree of vertical exaggeration. No horizontal scale implied.

(1971). As the coast retreated, a transgressive sand layer formed from the reworking of existing silt and sand deposits of the uppermost Juniata/Sequatchie tidal flats. Upper shoreface and beach sand moved coastward as a result of washovers at the same time that the middle and lower shoreface silt and sand was redistributed seaward by erosional shoreface retreat. Only pebble lags, or ravinement surfaces, were left behind, which indicates that the uppermost meter or more of the tidal flat was removed by the reworking process. Remnants of existing tidal channels were filled in by some of the reworked sediment resulting in the formation of the CBS variant. Sea-level continued its slow, erosive rise so that what was once a shallow-water, intertidal to supratidal environment was partially removed and redeposited in a lower shoreface to inner shelf setting. This setting was characterized by slow, discontinuous to continuous deposition of the relict sediments, and extensive reworking by organisms feeding within the substrate. Therefore, the record of Early Silurian sea-level rise occurs in a condensed sequence, which is the BTS.

BIOSTRATIGRAPHY

The BTS may actually represent the Ordovician-Silurian boundary; however, more definitive faunal data are required to prove this hypothesis. This presents a problem because body fossils are commonly absent within the BTS. Also, there is a significant overlap among the more common fossil species of Upper Ordovician- and Lower Silurian-age fauna. Present faunal data indicate that the paleosol horizons developed from *Lingula* - bearing tidal-flat deposits (Driese and Foreman, in review). Further west (Whiteoak Mountain thrust, Pine Mountain Thrust, Sequatchie Thrust) the BTS overlies fossiliferous limestone beds, which contain a typical Ashgillian brachiopod fauna; the shelf strata which overlie the BTS, in contrast, contain a Lower Llandovery (A 1-2) brachiopod fauna (Gogola and Driese, 1989).

Analyses of graptolite zonation have been the standard method of correlation for Ordovician and Silurian age rocks (Cocks, 1985; Churkin and others, 1977; Fortey and Cocks, 1978) One graptolite was collected from the lower Rockwood Formation. It was not ideally preserved but has been tentatively identified as a *Climacograptus pseudonormalis* which is a member of the C. normalis group (W. Berry, pers. comm.) and is not included in published Ordovician-Silurian graptolite zones (see. for example, Churkin and others, 1977; McKerrow, 1979). These taxa range from the latest Ordovician to the Early Silurian which, unfortunately, makes this specimen inadequate for placing the Ordovician-Silurian boundary. Other methods of correlation for Silurian- and Ordovician-age rocks include conodonts and brachiopod fauna (Cocks and Copper, 1981) and, some brachiopods were collected from within and above the BTS.

Brachiopod specimens collected from the Rose Hill Shale in Hagan, VA, which is about 90 meters up-section from the BTS, (BTS not exposed here)have been identified as *Eocoelia* , which might be close to *E. intermedia.* These are roughly mid-Late Llandovery in age (A. Boucot, pers. comm.). Some poorly preserved shells and fragments of *Leptaena*, plectambonitid, possible atrypacean, orthid type were also collected from just above the BTS at Tiftonia, GA (Locality TG in Figure 1.2) and these could be of almost any age within the later Ordovician-Silurian range (A. Boucot, pers. comm.).

Samples collected from the packstone/grainstone that occurs just beneath the BTS at Tiftonia, GA (Figure A.9, Appendix A) consists of a huge diversity of bryozoans which were identified by Ken McKinney at Appalachian State University. Since there are no faunal studies of later Ordovician and Silurian assemblages in the southern Appalachians, the identification of the bryozoans in the samples mentioned above is limited to generic names only (K. McKinney, pers. comm.). The assemblage from Tiftonia, GA includes *Batostomella, Constellaria, Gortanipora, Mesotrypa, Batostoma, Nicholsonella, Fenestella,* which are reportedly rare in Ordovician-age rocks, *Dekayella, Helopora,* and various unidentified bifoliates. Finally, specimens of *Hallopora* and *Rhombotrypa quadrata* were also identified. R. quadrata is known only from the Richmondian (middle to late Ashgillian), and true Hallopora is considered to be latest Ordovician to early Devonian (K. McKinney, pers. comm.). Therefore, the carbonate rocks that lie directly beneath the BTS at Tiftonia, GA are unquestionably Upper Ordovician in age.

One sample containing a bryozoan was collected directly from the BTS at Tiftonia, GA. This fossil specimen is reportedly an undescribed species of *Hallopora* and is almost certainly of Silurian-age, and it is probably pre-Niagaran Silurian since it is not the widely known *H. elegantula* from the Niagaran (K. McKinney, pers. comm.). Thus, the BTS apparently represents the Ordovician-Silurian boundary, at least at Tiftonia, GA.

CHAPTER 3

PHYSICAL EVIDENCE FOR AN UNCONFORMITY

According to Krumbein and Sloss (1963) and Davis (1983), disconformities are the most common type of unconformity preserved in the stratigraphic record. Features to look for when identifying a disconformity include: 1) the presence of a basal conglomerate that contains clasts which are of the same lithology as the underlying unit, 2) evidence for weathering, such as fossil soil horizons, or, if they have been eroded away, a red discoloration, 3) truncation of underlying beds, 4) the presence of borings, which imply that the surface had been lithified and then eroded, and 5) relief produced by erosion of a previously lithified surface. Four of the features listed above have been observed within the BTS, or at its contact with the underlying redbeds.

The basal conglomerate occurs in the form of the phosphatic pebble lags (Figs. 2.5 a and b, Fig.2.16), which have been interpreted to represent ravinement surfaces. These have been observed in various positions within the BTS. The occurrence of phosphates has been reported in the Juniata/Sequatchie redbed sequence (Driese and Foreman, in review) and also occur as economic deposits within Ordovician strata exposed on the Nashville Dome in central Tennessee (Smith and Whitlatch, 1940). The Ordovican Period represents a major episode of phosphogenesis (Cook and McElhinny, 1979; Sheldon, 1980). Therefore, the phosphatic pebble lags are interpreted here to have been largely derived from the reworking of the underlying Ordovician (Ashgillian) redbeds.

Evidence for subaerial exposure occurs at the Bean's Gap (Fig. 2.2), and Powell Mountain (Fig. 2.6), and, possibly, Flat Gap (Fig. 2.3). Paleosol horizons are especially well-developed at the first two localities, and each paleosol horizon probably represents approximately 10,000-15,000 years of exposure (Driese and Foreman, 1989; Driese and Foreman, in review). According to Driese and Foreman (in review), the physical features by which paleosols are recognized include angular blocky peds, platy peds, small-scale and low-angle inclined pedogenic slickensides (*sensu* Gray and Nickelsen, 1989), large-scale pedogenic slickensides that may locally form pseudo-anticlines, clastic dikes, horizons of carbonate nodules, and color mottling. Pedogenic slickenside surfaces and the faces of angular and blocky peds may be coated with birefringent clays and manganese oxides.

Where paleosol horizons are absent, a distinct color change from red to gray occurs within the shale strata underlying the BTS. In a few cases, this color change occurs right at the contact with the BTS (see complete measured sections, Appendix A).

Truncation of the underlying beds occurs at the localities where the paleosol horizons occur, with an angular discordance (of about 1-2 degrees) between the BTS and the paleosol horizons.

The presence of borings were noted at the Cumberland Gap, TN and Tiftonia, GA sections (Fig. 3.1 a and b). The bored intervals appear to be phosphatic hardgrounds, which are indicative of a nondepositional, if not an erosional surface.

As stated earlier, the Early Silurian transgressive surface represents a sequence boundary in the sense of Galloway (1989) and Jordan and Flemings (1989). The corresponding unconformity is regional in that evidence for its existence occurs over the entire area of this study. The complicated tectonic history of the Taconic Orogeny is responsible for creating the variable Ordovician-Silurian depositional environments

Figure 3.1. Carbonate packstone/wackestone that occurs directly subjacent to the BTS at Tiftonia, GA illustrating the occurrence of a phosphatic hardground that is associated with abundant amounts of glauconite. Scales are in centimeters. Note the small borings at the top of (b). (a) Outcrop photograph. (b) Slab photograph

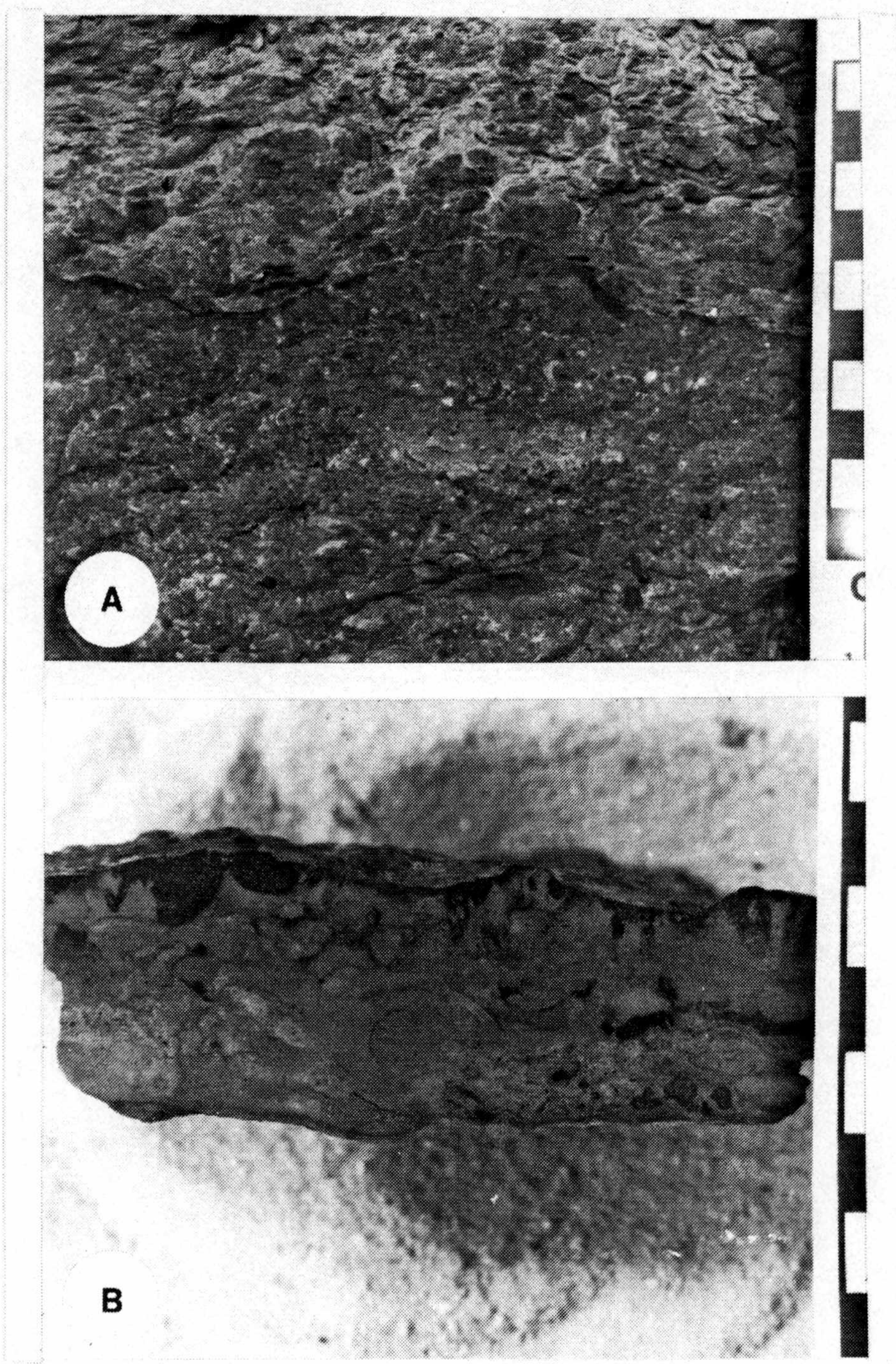
A
B

along the length of the Appalachian Basin. That, combined with post-Taconic orogenic events prevents one from tracing the unconformity any further than the extent of the study area. A similar type of disconformity has been proposed to exist in the lower part of the Tuscarora Formation (Clinch Sandstone equivalent) in western Virginia and adjacent West Virginia (Bambach, 1987). It is apparently marked by a conglomeratic lag deposit and an angular discordance with the underlying strata. Strata underlying the unconformity display variable thicknesses whereas the overlying strata are uniform in thickness (Figures 3.2 and 3.3). Bambach (1987) placed this unconformity between two informal stratigraphic units that he defines as the "lower and upper Tuscarora". This "lower Tuscarora" unit, however, contains interbedded, hummocky cross-stratified white sandstone beds and redbeds and probably represents a facies change in the upper Juniata Formation, and therefore should be regarded as the Juniata Formation (Dorsch, pers. comm.). This angular discordance may represent the most distal manifestation of the angular unconformity that occurs between the Juniata and Tuscarora formations in the central Appalachians. In New York and eastern Pennsylvania, there is an angular unconformity known as the Taconic unconformity between the Martinsburg Formation and the Tuscarora Sandstone (Shawangunk Conglomerate). The origin of this unconformity has been attributed to tectonic uplift during the Taconic Orogeny followed by deposition (Diecchio, 1986; Rodgers, 1971). Outcrops of these rocks occur along thrust sheets that are more proximal to the Blue Ridge Front. Unfortunately, these rocks are not preserved in Tennessee, North Carolina, and Georgia. If these rocks were preserved in these states, one might expect to see the Taconic unconformity here as well. It could then be correlated with the hiatus/unconformity over which the BTS lies.

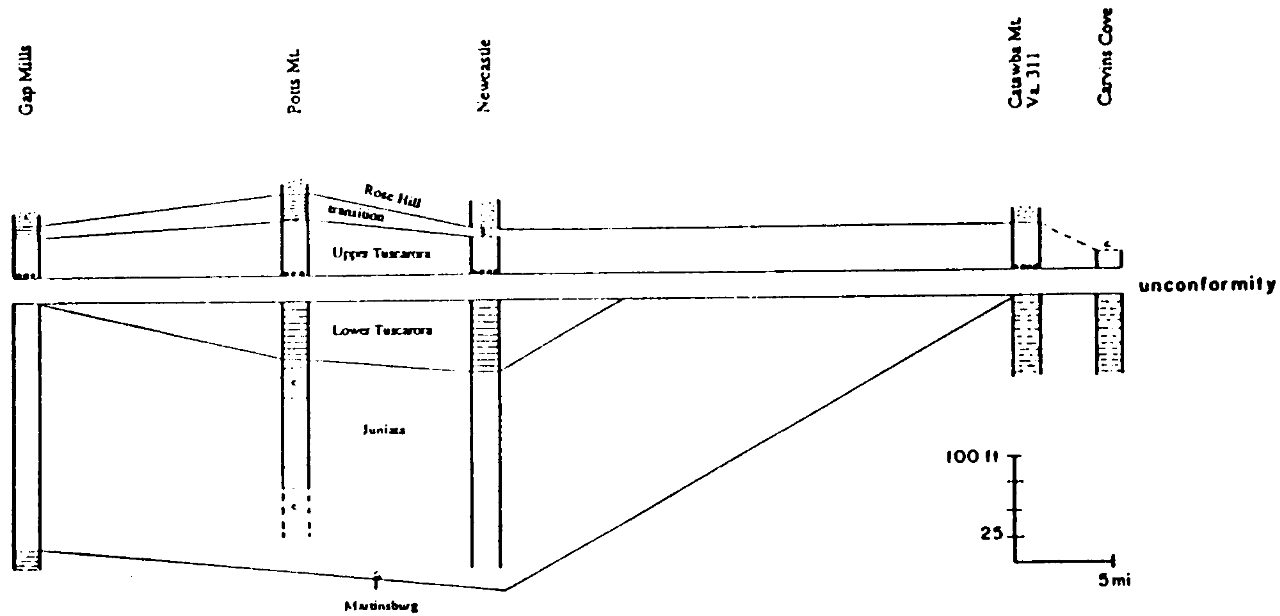

Figure 3.2. Southeast-northwest cross section from, Carvin's Cove Reservoir to Gap Mills, West Virginia illustrating what Bambach (1987) has interpreted to be a paraconformity between what he entitles the lower and upper Tuscarora. Note the great variation in thicknesses of the units below the unconformity versus the uniformity of thickness in the Tuscarora Formation. This difference indicates that the unconformity was the result of deformation and erosion of the units below the unconformity before deposition of the overlying Tuscarora. Cross section is from Bambach (1987).

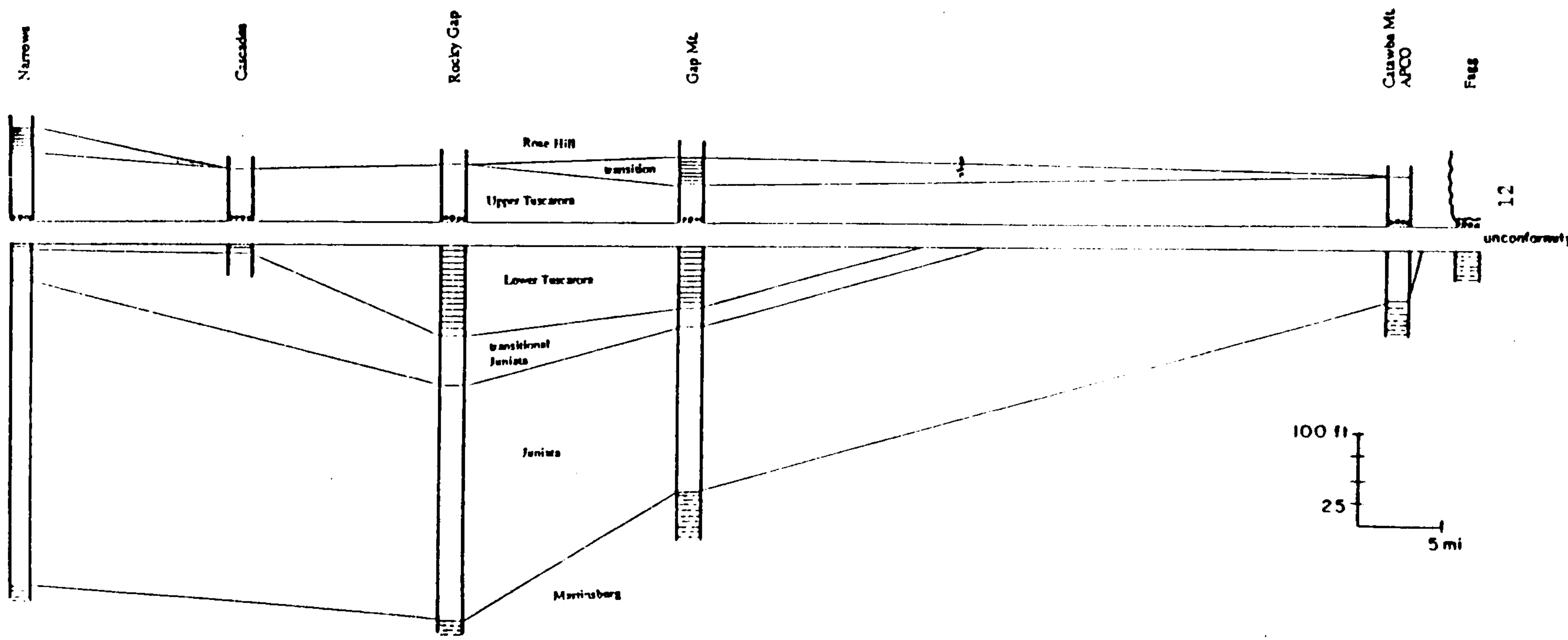

Figure 3.3. Southwest-northeast cross section from Fagg, VA to Narrows, VA that illustrates Bambach's interpretation of the Ordovician-Silurian unconformity which he believes occurs within the Tuscarora Formation as opposed to the contact between the Tuscarora and Juniata Formations. Again, note the variation in strata thickness below the unconformity versus that above it. Cross section from Bambach (1987).

Although the physical features described all indicate the presence of an unconformity, there is one major problem in proving the existence of this unconformity. There are no constraints to indicate the amount of time for which there are no strata, even at the Tiftonia, GA section where bryozoan specimens indicate that the BTS occurs at the Ordovician-Silurian boundary. The lack of diagnostic body fossils in the other BTS localities make it impossible to assign a date to the deposition of the BTS to compare with fossils within the underlying strata. According to Vail (1977), a true unconformity has to include at least one million years of time for which strata are missing. This more recent definition of an unconformity was created to aid in the delineation of unconformities on seismic sections. The best time evaluation that can be made for the missing strata below the BTS can only be done with the paleosol horizons. These horizons provide an approximate measure of the duration of subaerial exposure. This has been estimated to be on the order of fifteen to twenty-five thousand years- hardly an unconformity according to Vail's (1977) definition. The physical features described above do indicate the presence of a disconformity in the traditional sense of Krumbein and Sloss (1963). They state, " Relationships between lithosomes separated by a surface of nondeposition or erosion are unconformable, and the separating surface is an unconformity." No specific amount of time has to be represented by missing strata such that even a hiatus of tens of thousands of years can be considered an unconformity. Therefore, the physical features described previously are representative of a disconformity.

For the localities confined to the area of this study, placement of the unconformity is concurrent with the features previously described as indicators of an unconformity. At Beans Gap and Powell Mountain (Plate 1), the tops of the paleosol horizons represent the unconformity, because they clearly represent subaerial erosion surfaces.

Placement of the unconformity (Plate 1) at the more central localities along the Whiteoak Mountain Thrust sheet (Melton Lake, TN and Lone Mountain, TN, Figure 1.2) corresponds to the tops of the channel sequences which are marked by a phosphatic pebble lag or ravinement surface. The point at which the shales that occur beneath the BTS change from maroon to gray up-section is interpreted to represent the unconformity at Flat Gap, TN and Whiteoak Mountain, TN (Plates 1 and 2) . Finally, the bored hardgrounds of Cumberland Gap, TN and Tiftonia, GA, which probably represent periods of nondeposition, are the westernmost exposures of the Ordovician-Silurian unconformity (Plates 1 and 2), with the exception of those sedimentary rocks occurring along parts of the eastern flank of the Nashville Dome, where Lower Silurian strata are entirely missing. Therefore, this disconformity continues westward and northward into an angular unconformity.

CHAPTER 4

PETROLOGY OF THE BTS

Traditional QFL ternary plots of point-count data indicate that the BTS is a quartz arenite (Fig. 4.1) whose provenance, following the classification of Dickinson (1985), falls into the field of craton interior (e.g. continental interior or passive-margin). This setting is clearly not the tectonic setting in which the BTS was deposited because the Appalachian basin is a foreland basin. Therefore, factors other than tectonic setting controlled the framework composition of the BTS. One major factor that controls framework composition is grain size. According to Dickinson (1985), the best point-counting statistics for provenance studies are achieved by point-counting medium-grained to coarse-grained sandstone lithologies. Fine-grained sediment is indicative of greater transport distances from the source rock. As sand grains are transported far from their original source, igneous and metamorphic rock fragments will be broken down into individual mineralogical components, and the even more labile constituents, such as volcanic rock fragments, will be totally destroyed. Wilson and Pittman (1977) showed that workers could easily misinterpret the provenance of sandstone by ignoring subtle diagenetic features, especially authigenic clays. No evidence, such as grain outlines of labile fragments or partially dissolved grains, was found within the BTS samples to indicate that such processes occurred. Furthermore, although feldspar grains are extremely rare within the BTS samples, plagioclase grains, when present, appeared fresh and unaltered.

Framework grains within the BTS dominantly fall into the silt- to fine-grained sand-size realm. Matrix material is commonly a significant component within the

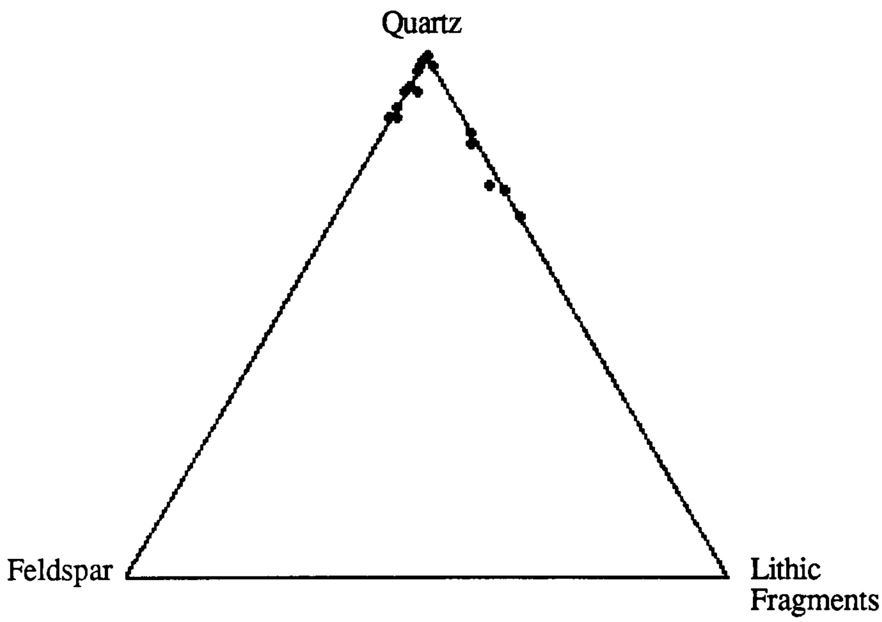

Figure 4.1. Ternary QFL plot of BTS point-count data. Note that most samples fall within the field of quartz arenite. This diagram is not truly representative of the BTS samples because these three components commonly make up less than 50% of the rock.

BTS, and was thus point-counted as detrital clay even though that "matrix" probably contained some silt. The grain size limit for matrix was chosen as 30 microns, which would be a value of 5.0 or more on the phi scale or anything finer than medium silt according to the Wentworth size class. According to Dott (1964), this arbitrary size cut-off is preferable because 30 microns corresponds exactly to 5.0 on the phi scale and because standard thin-sections are 30 microns thick so any attempt at identifying a grain of that size or smaller would be questionable. Figure 4.2 illustrates the volume percent of matrix (labeled detrital clays/matrix) occurring in each sample.

Utilizing the sandstone classification system of Dickinson (1985) was not practical for some of the BTS samples for reasons mentioned above. Perhaps a more useful scheme to be applied here is that of Dott (1964). Those samples from the BTS that contain greater than ten percent matrix could be classified as quartz wacke, as opposed to a quartz arenite, thus implying that the BTS is more texturally immature at some localities than at others. Quartz wacke is clearly more descriptive of the BTS at these localities than the name quartz arenite. In order to truly describe these rocks, however, the rock name must be modified to include that component which commonly makes up more that 50% of the rock and may make up to 75% of the rock. Thus, the BTS could be designated as a ferroan dolomitic quartz wacke or a ferroan dolomitic quartz arenite due to the preponderance of ferroan dolomite. (Fig. 4.3). These are the most useful descriptive names for these rock. Classification schemes for mixed carbonate and siliciclastic rocks have been proposed by Mount (1985) and Zuffa (1980). These systems of classification, however, are not applicable to the BTS samples because the carbonate components included in the classification schemes are detrital and not authigenic, as in the BTS. There is no way of knowing if primary carbonate grains once made up a volumetrically significant percentage of the BTS.

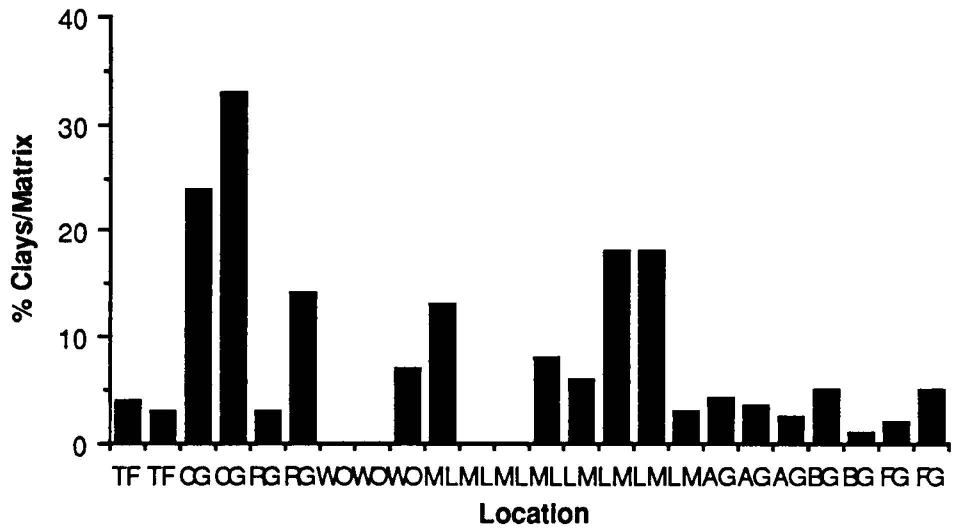

Figure 4.2. Plot of the percentage of detrital clay/matrix occurring within each sample from each locality. Note that there are a number of samples with greater than 10 percent detrital clays which would then justify the reclassification of those samples as quartz wackes after Dott (1964). Percentages are based on point-count data. Location abbreviations are as follows; FG: Flat Gap, TN; BG: Beans Gap, TN; AG: Powell Mountain, VA; LM: Lone Mountain, TN; ML: Melton Lake, TN; WO: Whiteoak Mountain, TN; RG: Ringgold, GA; CG: Cumberland Gap, TN; TF: Tiftonia, GA.

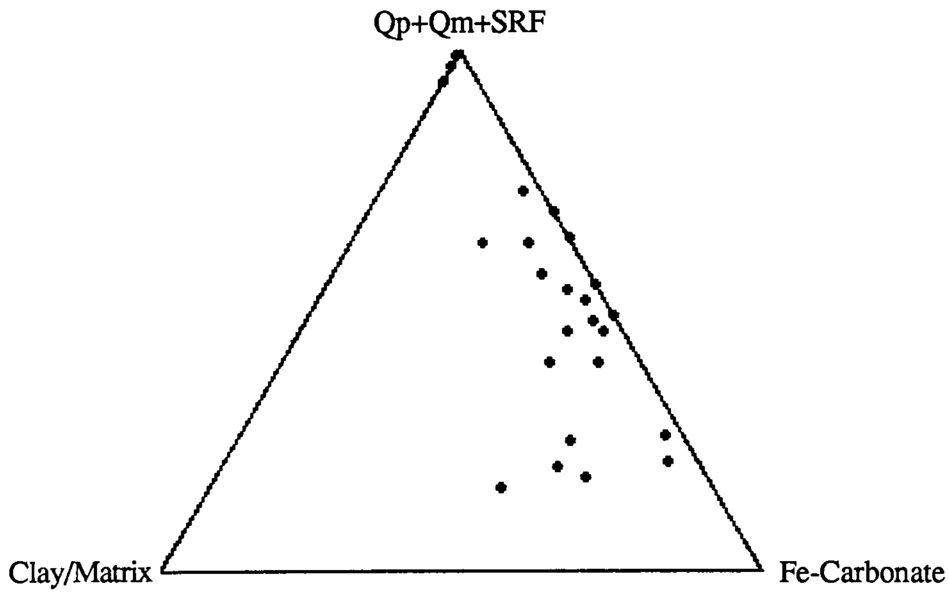

Figure 4.3. Ternary plot of clay/matrix, sedimentary rock fragments (SRF), monocrystalline and polycrystalline quartz (Qm+Qp), and ferroan carbonates. These components comprise greater than 90% of the constituents that were point-counted for this study. Note that some samples contain 50%-75% ferroan carbonate material (dolomite and ankerite). The total number of samples point-counted is 24. A total of 1000-1500 points were counted for each 2x3 thin section and approximately 740 points were counted for each 1x2 thin section.

It has been shown in previous chapters that the physical features which occur in the BTS indicate that the process of erosional shoreface retreat, caused by a relative sea-level rise, resulted in the deposition of the BTS. It was therefore interpreted that the BTS is composed of relict sediment, thus masking the true provenance of the BTS. Diagenesis partially influenced the siliciclastic framework compositions through the partial replacement of quartz grains by ferroan dolomite, thus decreasing the net volume percent of quartz. Authigenic clay and feldspar are rare to absent which, were they present, would indicate that progressive diagenesis had altered the original framework composition through the destruction of labile grains. It will remain unknown whether or not a volume of precursor carbonate that was similar to the existing intergranular volume (minus cement porosity, *sensu* Houseknecht, 1987) ever existed.

Some interesting trends do occur with respect to the regional distribution of framework types based on point-count data. The percentage of monocrystalline quartz within the eastern, central, and western thrust sheets all display the same trend. The amount of quartz present always tends to increase toward the south (Fig. 4.4). This is apparently a reflection of the hydrodynamic regime during the time of relative sea-level rise. Longshore currents must have served to carry sediments from the north to the south as they were being reworked. Driese and others (in press) suggested that the Early Silurian shelf system contained a dominant component of geostrophic (i.e., along-shelf) flow from north to south. The paleoceanographic phenomena such as prevailing wind patterns and storm patterns may have already been in place during this relative sea-level rise and therefore may also be invoked to explain the pattern of increasing abundances of monocrystalline quartz toward the south.

Detrital clay (or matrix) becomes continually more abundant within the more distal (i.e. westerly) deposits of the BTS (Fig. 4.2). This would be expected to occur as the

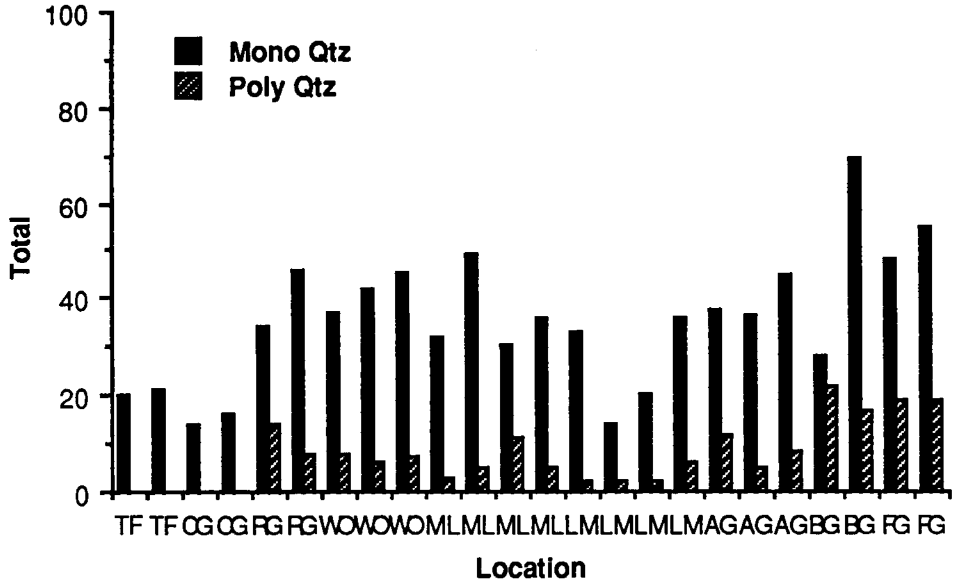

Figure 4.4 . Bar graph showing the average percentage as well as the geographic distribution of monocrystalline and polycrystalline quartz. The eastern thrust sheet (Copper Creek thrust) localities are FG: Flat Gap, TN; and BG: Beans Gap, TN. The central thrust sheet localities (Whiteoak Mountain and Wallen Valley thrusts) are AG: Powell Mountain, VA; LM: Lone Mountain, TN; ML: Melton Lake, TN; WO: Whiteoak Mountain, TN; and RG: Ringgold, GA. The western thrust sheet localities (Pine Mountain and Sequatchie thrusts) are CG: Cumberland Gap, TN and TF: Tiftonia, GA. Note the obvious decrease in total polycrystalline quartz as well as monocrystalline quartz from east to west (right to left in the diagram).

average monocrystalline quartz content diminishes toward the west. It is interpreted here that the overall pattern reflects changing depositional processes.

Sedimentary phosphates occur in quantities greater than ten percent within the pebble lags, which have been interpreted as representing ravinement surfaces. These phosphate grains occur as aggregates of clay-sized phosphate material. Silt grains are commonly enclosed within the phosphate pebbles. The phosphate grains are dark brown, in both plane light and cross-polarized light . In a few instances, phosphatic material partially replaces allochems which were originally composed of calcite (Fig. 4.5).

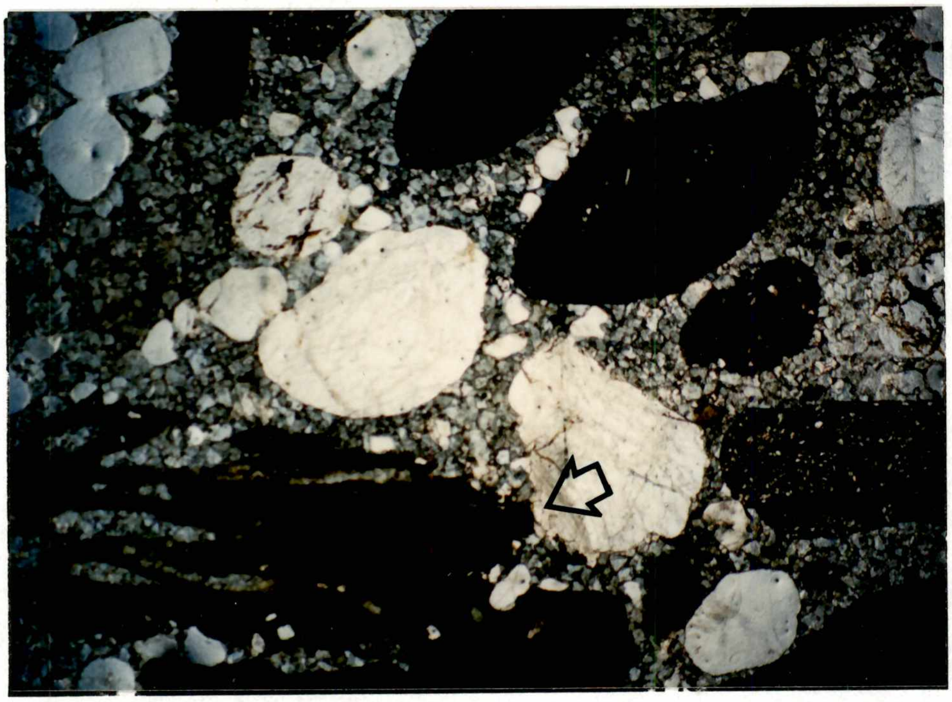

Figure 4.5. Thin-section photomicrograph under cross-polarized light of sample 0.75-ML (Locality ML in Figure 1.2) illustrating the appearance of phosphate grains in thin-section. Note the bryozoan (arrow) that has been replaced with phosphatic material. Also notice the abundance of ferroan dolomite/ankerite replacing the matrix. Field of view is 6 mm in the long dimension.

CHAPTER 5

CEMENTS AND THEIR PETROGRAPHIC FEATURES

Three different diagenetic carbonate phases are present within the BTS. These are ferroan dolomite, ferroan calcite, and ankerite. Petrographically, ferroan dolomite appears to be by far the most common diagenetic phase as well as the most abundant phase present in many of the samples (Fig. 5.1 a and b). Dolomite crystals are subhedral to euhedral, or idiotopic (*sensu* Gregg and Sibley, 1984) rhombohedrons, which occur as a replacement phase and fill pore spaces as well. This pore-filling phase may be replacive as well because it has been observed to have partially replaced detrital quartz (Fig. 5.2) Zoning is evident in the coarse, idiotopic dolomite if the sample is slightly weathered (Fig. 5.3). Ankerite occurs in the same manner as dolomite, and is impossible to distinguish from dolomite petrographically. Broad XRD peaks for the dolomite group indicate a gradational mineralogical relationship between dolomite and ankerite. In fact, measurement of peak symmetry and the determination of peak centroids (see Appendix C for procedure and results) have revealed that ankerite is truly the dominant ferroan carbonate phase and dolomite is more of a minor phase.

By comparing XRD results with the observed petrographic character of the ferroan carbonate it is interpreted here that ankerite makes up the core of the zoned rhombohedral carbonate crystals and ferroan dolomite represents the rims of these phases. Petrographically, the cores of the rhombohedrons display heavy iron-oxide stains, whereas the rims tend to be more clear (Fig. 5.3).

Figure 5.1. Thin-section photomicrographs of the FGB variant in sample AG-1 from Powell Mountain, VA (Locality PM in Figure 1.2). Ferroan dolomite/ankerite has partially replaced quartz (arrows). Field of view is 2.3 mm in the long dimension. (a) Plane polarized light. (b) Cross-polarized light.

Figure 5.1 a.

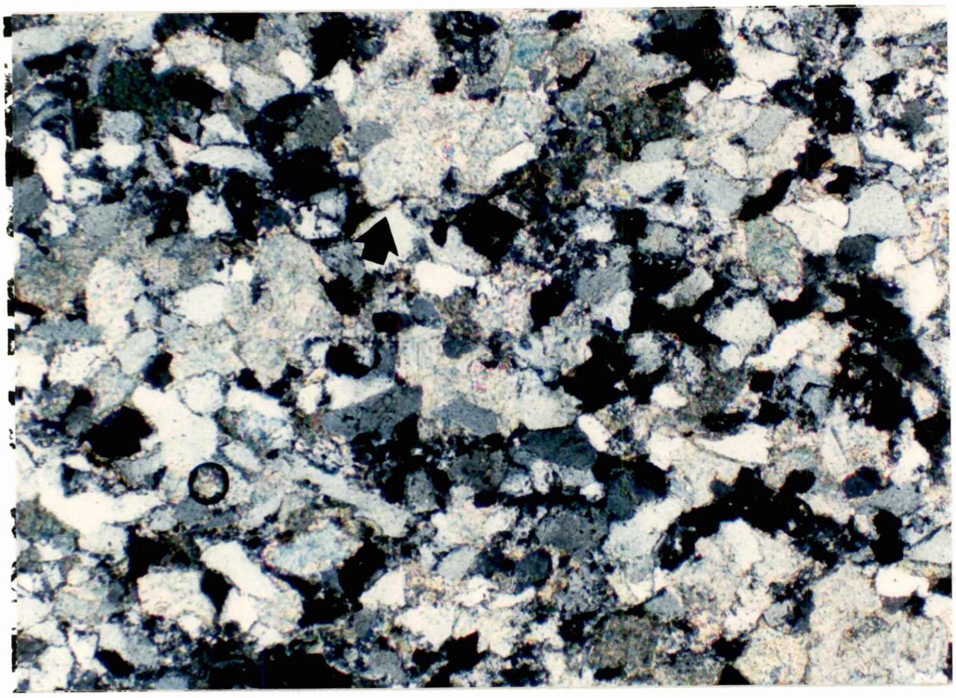

Figure 5.1 b.

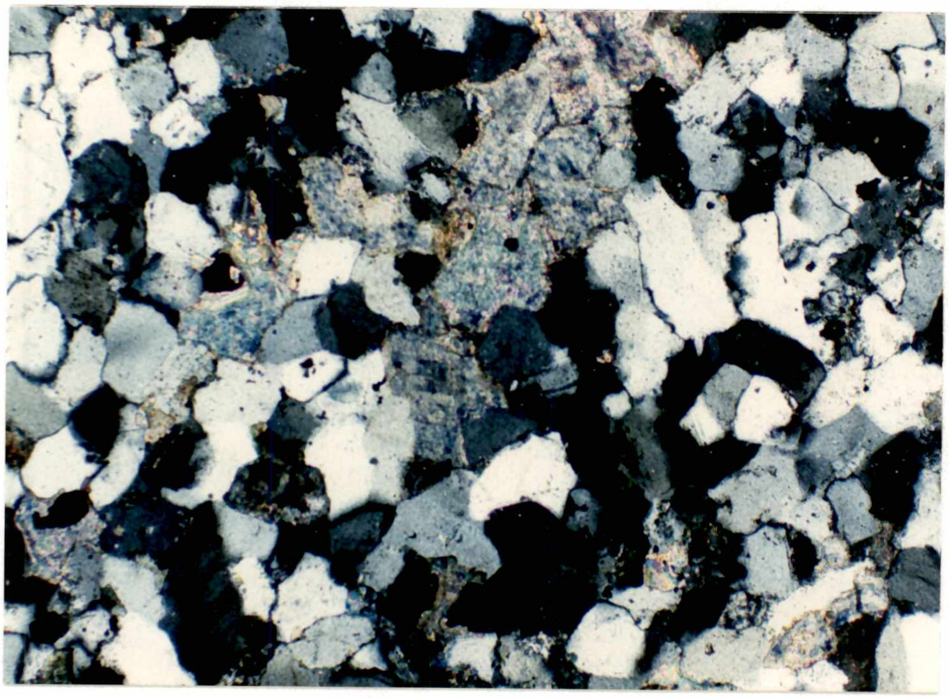

Figure 5.2. Thin-section photomicrograph of sample 1.5-ML-1 (Locality ML in Figure 1.2) of the CBS variant taken under cross-polarized light. Note the presence of sutured grain boundaries and concave-convex boundaries which indicate intergranular pressure solution. Quartz overgrowths are present as well. These features predate the formation of ferroan dolomite/ankerite. Field of view is 1.2 mm in the long dimension.

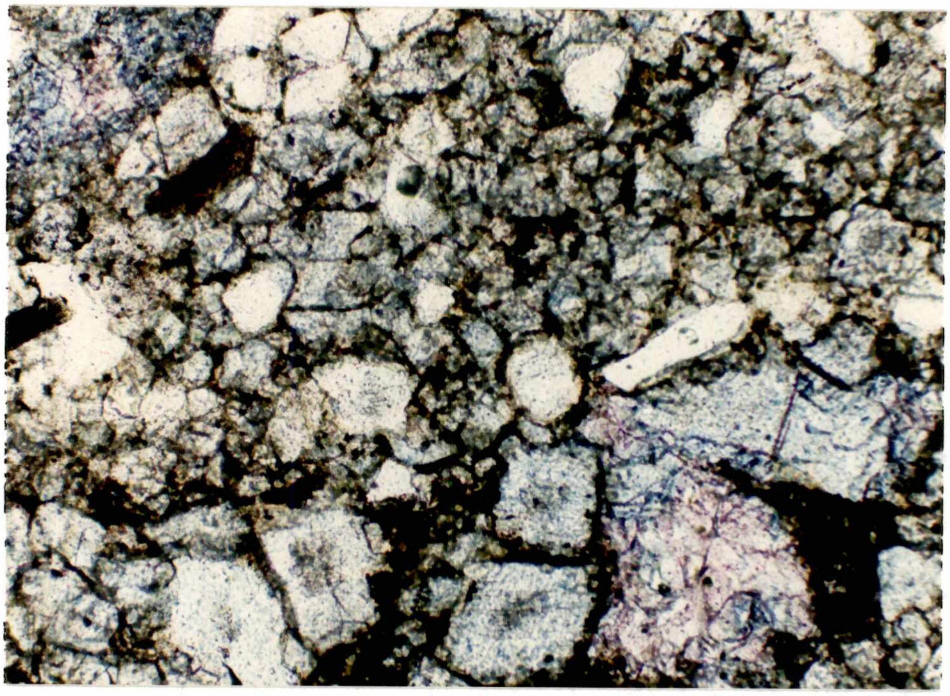

Figure 5.3. Thin-section photomicrograph in plane light showing coarse, blocky ferroan calcite replaced by euhedral zoned ferroan dolomite/ankerite. The cores of the rhombohedrons are very dark and cloudy, which suggests that there is a higher concentration of iron in the cores as opposed to the rims. Note how the dolomite is much coarser near the large pore filled with ferroan calcite, as compared to other parts of the sample. Field of view is 2.3 mm in the long dimension.

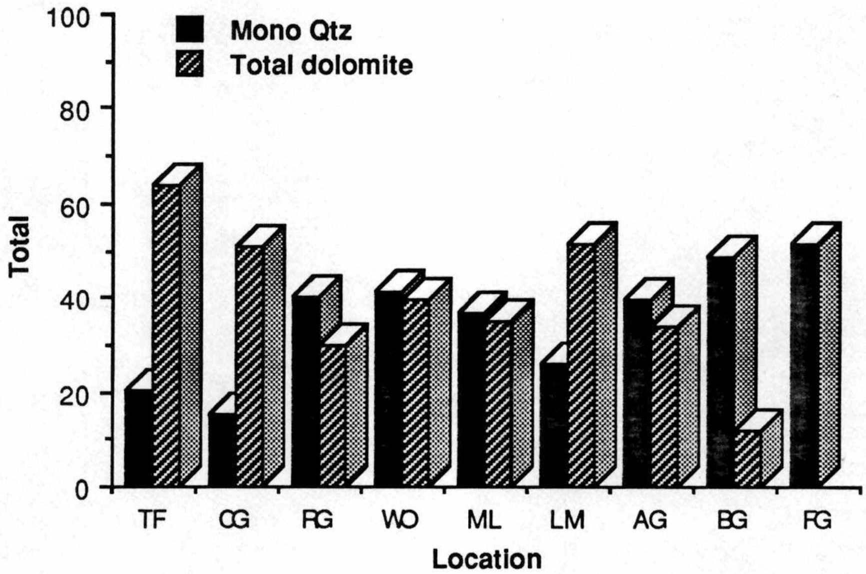

Figure 5.4. Bar graph illustrating that ferroan dolomite is, on average, one of the the most abundant phases present at each locality and commonly may only be exceeded by monocrystalline quartz. The only localities where it is not abundant are those that occur along the eastern most thrust sheet at Beans Gap (BG) and Flat Gap (FG). Note the increase in abundance towards the west.(AG: Powell Mountain; LM: Lone Mountain; ML: Melton Lake; WO: Whiteoak Mountain; RG: Ringgold; CG: Cumberland Gap; TF: Tiftonia).

Framework grains commonly appear to be "floating" within the ankerite, indicating that much of the relict sediment that was deposited as the BTS consisted of reworked carbonate grains. During burial, framework carbonate grains were then replaced by dolomite and ankerite. The ankerite may have formed through the neomorphism of previously existing nonstoichiometric dolomite, or by the replacement of calcite by ankerite (Gregg and Sibley, 1984). Unfortunately,when using textural criteria alone, it is impossible to distinguish between ankerite that formed as a result of neomorphism versus that which formed as a replacement phase.

Dedolomite occurs in the extremely weathered samples from Cumberland Gap and Beans Gap (Fig. 5.5). Thin sections from Cumberland Gap reveal fine, subhedral to euhedral rhombohedrons of calcite which nonselectively replace both framework grains and matrix, however, calcite is much less abundant at this locality as compared to the abundance of ferroan dolomite/ankerite at other localities.. At Beans Gap, no calcite exists in the dedolomite, and only iron oxide residues with a rhombohedral shape remain. The abundance of iron-oxide and the morphology of the calcite crystals indicate that the rhombohedrons were once ferroan dolomite or ankerite. Intense weathering by oxygen-rich meteoric waters caused the oxidation of iron present in the ferroan dolomite/ankerite. The original dolomite and ankerite was then dissolved and calcite precipitated in place of the dolomite and ankerite. Frank (1981) suggested that higher concentrations of iron in ferroan dolomite makes them all the more susceptible to dedolomitization. Similarly, Holail and others (1988) have suggested that an event of regional exposure caused the formation of dedolomite within the El Heiz Formation (Upper Cenomanian) of the Bahariya Oasis, Egypt.

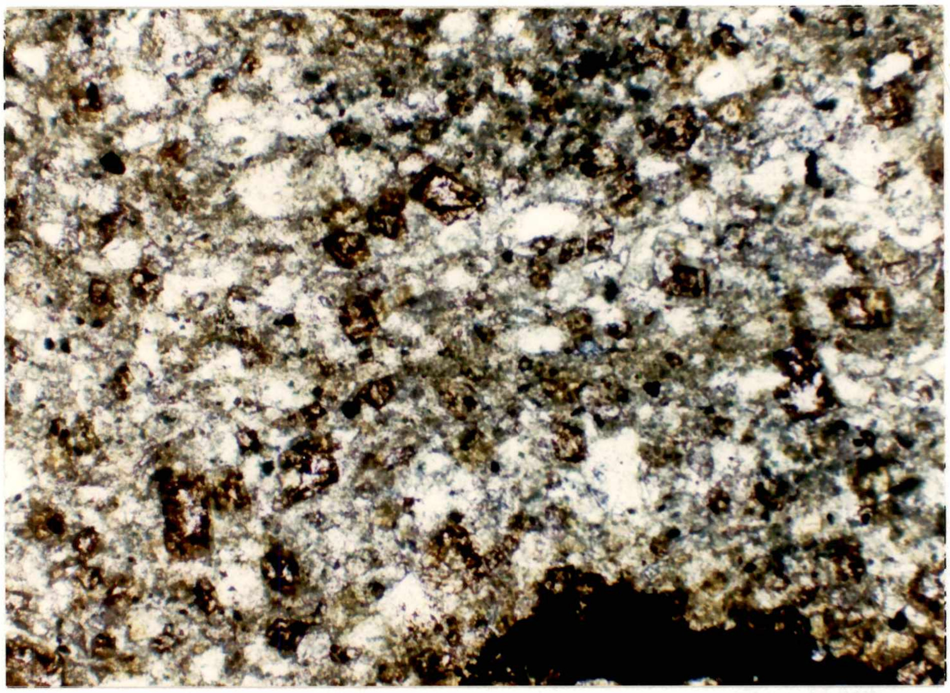

Figure 5.5. Thin-section photomicrograph of sample 3.15-CG-3 from Cumberland Gap, TN (Locality CG in Figure 1.2) illustrating the occurrence of dedolomite. Here one can see discrete pink rhombohedrons that were once dolomite and have been weathered to calcite. Field of view is 6 mm in the long dimension.

The occurrence of ferroan calcite is restricted to the coarse-grained phosphatic pebble lags, in which the calcite forms a coarse, blocky spar cement. Some of the ferroan calcite cements are partially replaced with euhedral ferroan ankerite (Fig. 5.3).

Isotopic data was obtained for the ferroan dolomite phases that occur in samples from Melton Lake, TN and Powell Mountain, VA (Localities ML and PM, respectively, in Figure 1.2). It was determined that the lithologies examined in this study are presently unsuitable for stable isotopic studies of the carbonate mineral phases with current sampling techniques.

There is a paucity of silica cement within the BTS, in contrast to the overlying Clinch sandstone clastic wedge (Schoner, 1985a, b). Point-count and visual-estimate data suggest, however, that there is a direct relationship between the amount of quartz cement and the amount of detrital clay within each sample (Fig. 5.6). Where there is an abundant amount of clay (>~6%), there is little or no quartz cement. Conversely, when quartz cement is present in amounts greater than 5%, there is very little detrital clay. Pressure solution features are common within samples that contain notable amounts of quartz cement. These include sutured and concave-convex grain boundaries (Molenaar, 1986; Houseknecht, 1984). The simplest explanation for the paucity of silica cements involves two aspects. First, etrital quartz commonly occurs in the silt- to fine-sand sizes. James and others (1986) have shown that in the Nugget Sandstone (Jurassic) of south-central Wyoming, silica overgrowths on monocrystalline quartz are seven times more common for the medium- to coarse-grained fraction versus the fine-grained fraction. Petrographic observations of the BTS reveal that silica cement is restricted to the occurrence of the WL variant and, occasionally, the CBS variant (Fig. 5.7) and is commonly in the presence

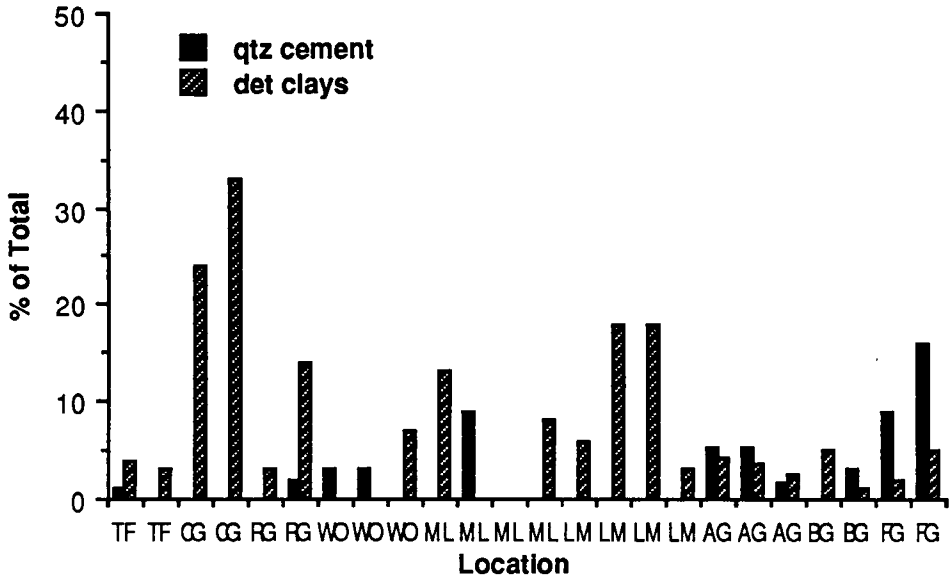

Figure 5.6. Comparative bar graph showing the percentage of quartz cement (solid bars) versus clay/matrix (patterned bars). Localities are FG: Flat Gap, TN; BG: Beans Gap, TN; AG: Powell Mountain, VA; LM: Lone Mountain, TN; ML: Melton Lake, TN; WO: Whiteoak Mountain, TN; RG: Ringgold, GA; CG: Cumberland Gap, TN; and TF: Tiftonia, GA.

Figure 5.7. Thin-section photomicrograph, under cross-polarized light, of sample FG-1 from Flat Gap, TN (Locality FG in Figure 1.2) illustrating pressure-solution features such as concave/convex grain boundaries (arrow) and quartz overgrowths. Such features are common to the FGB variant and in the associated pebble lags. Field of view is 2.3 mm in the long dimension.

of medium- to coarse-grained framework quartz. Second, infiltration of the matrix by clay minerals or clay-sized particles such as iron-oxide served to coat grains and fill available pore spaces, so that silica cementation was inhibited (Molenaar, 1986).

ORIGIN OF DIAGENETIC PHASES

Petrographic examination of the underlying Upper Ordovician-age carbonate strata has revealed the occurrence of the same diagenetic carbonate phases as in the BTS. Subhedral to euhedral ferroan dolomite (ankerite) is the dominant diagenetic phase present. These phases probably formed by the replacement of relict carbonate framework grains. Marine and meteoric cements are nearly absent or have been replaced by ankerite. Calcareous allochem grains tend to be partially replaced by ferroan dolomite (ankerite?) as well. Such commonalities between the BTS and underlying strata imply that both underwent a similar diagenetic history.

A source of Fe^{2+}, Mg^{2+}, Ca^{2+}, and possibly, Si^{4+} is required to explain the occurrence of the diagenetic phases discussed in the previous section. One reaction that would generate these ions is the conversion of smectite to illite (Lahann, 1980; Boles and Franks, 1979; Eberl and Hower, 1976; Petrovic, 1976; Towe, 1962). Examination of the Juniata paleosols by X-ray fluorescence and X-ray diffraction has revealed that the predominant clay mineral phase present is illite (Driese and Foreman, in review). The illite probably formed as a product of smectite diagenesis. This process begins at burial temperatures of approximately 50 degrees Celsius (Perry and Hower, 1970; Lahann, 1980). It is significant to note that this is the same as the critical roughening temperature (CRT) for ankerite as suggested by Gregg and Sibley (1984). Ions generated from the smectite-to-illite conversion will migrate upwards through the process of diffusion

(Petrovic, 1976).

According to Lahann (1980), extensive silica cementation will occur at the lower temperature end of illitization (i.e., 50 degrees Celsius). As the temperature of illitization increases, the "characteristic distance of diffusion" (Petrovic, 1976), or CDD, will decrease thus decreasing the amount of distance the ions generated through illitization will travel.

It is proposed here that smectite diagenesis provided some of the silica for the silica cements observed in the BTS. Most of the silica, however, was probably the product of pressure solution. X-ray fluorescence and X-ray diffraction data from Driese and Foreman (in review) of the paleosol horizons which underlie the BTS at Beans Gap and Powell Mountain have revealed that the dominant clay mineral phase present is a well-ordered illite. This indicates that these siltstone and shale deposits probably underwent a smectite-to-illite conversion during diagenesis. Only a small amount of silica precipitated before burial temperatures increased to the point that the CDD for Si^{4+} decreased and was insufficient to reach the BTS. Illitization of the underlying, once smectite-rich, shale and siltstone deposits also provided the Mg^{2+}, Ca^{2+}, and Fe^{2+} required for the precipitation or neomorphism of carbonate phases. Illitization of smectite phases rich in iron and magnesium tends to occur more slowly. Therefore, the release of large amounts of these ions would require a much higher temperature regime where, as suggested by Boles and Franks (1979), iron and magnesium will be taken up by burial ankerite (or ferroan dolomite) cements.

PARAGENESIS

The paragenetic sequence of events was determined by observing cross-cutting relationships among diagenetic phases with the petrographic microscope (Fig. 5.8). The first cement phase to have precipitated is inferred to have been calcite, based on the fact

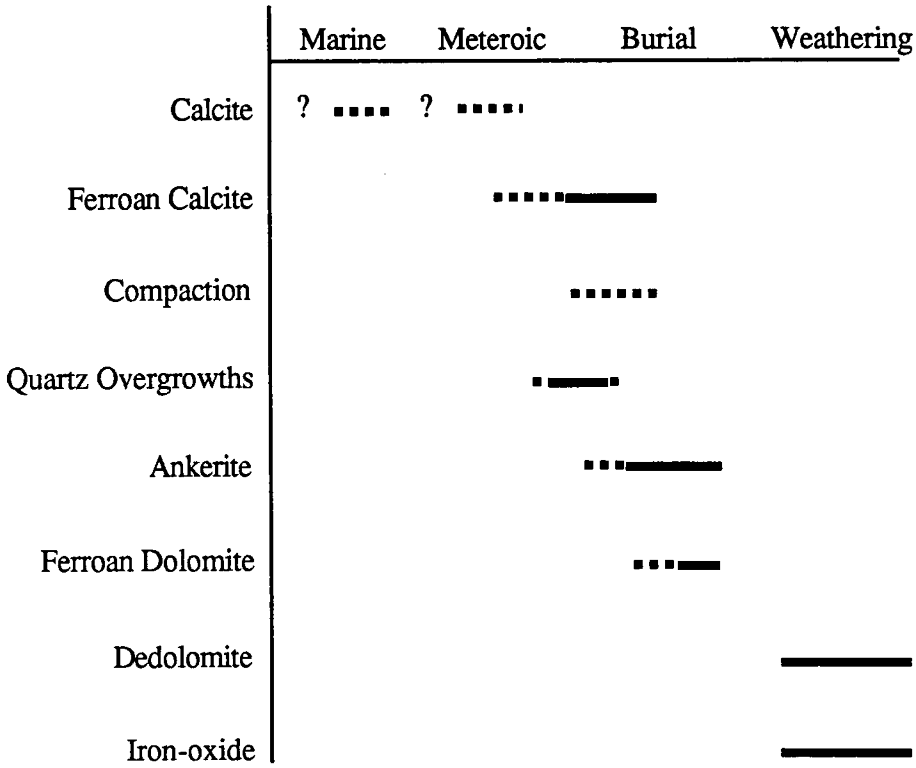

Figure 5.8. Paragenetic sequence of cement and replacement phase formation. Question marks for calcite indicate that this phase is inferred to have existed, however, it was never observed due to extensive replacement by ankerite and dolomite.

that framework grains are floating in ferroan dolomite and ankerite. Had there been no original framework carbonate grains present, those samples with abundant carbonate phases would have undergone extensive compaction, resulting in abundant grain-to-grain contacts and smaller volumes of replacement carbonate phases. Ferroan calcite precipitated as a primary cement within coarser-grained samples which had large pore volumes still intact. This probably occurred within the meteoric realm as depositional iron became reduced and subsequently available to incorporate into cement phases.

Samples of the WL variant did not experience any carbonate cementation, perhaps due to a lack of original framework carbonate grains, and therefore mechanical and chemical compaction was an important controlling factor in the burial history. Initially, mechanical compaction served to reduce pore volume and reorient grains. Chemical compaction through intergranular pressure solution commenced as more and more grains came into contact with each other. Consequently, these samples underwent little to no replacement by ferroan carbonate phases in the burial environment.

As deep burial commenced, ferroan carbonate phases (ferroan dolomite and ankerite) began replacing precursor calcite and ferroan calcite. As proposed earlier, a possible mechanism for the initiation of this phenomenon might have been the release of magnesium and large (?) quantities of iron, as a result of the smectite-to-illite transformation within the underlying shale deposits. This mechanism could also have provided silica for earlier quartz cementation in the samples from the WL variant, however, intergranular pressure solution may have provided sufficient quantities of silica for the quartz cements.

CHAPTER 6

CONCLUSIONS

The Lower Silurian 'Basal Transgressive Sandstone' (BTS) was deposited as the result of a relative rise in sea-level at the end of the Ordovician Period. The principle cause of the sea-level rise was the deglaciation of Gondwana and/or subsidence caused by the mechanical and chemical compaction of the subjacent stratigraphic sequence. Tectonism caused by the Taconic Orogeny in the central Appalachians may have contributed to this sea-level rise as well. The significance of this rise in the southern Appalachians is that the deposition of the BTS defines a sequence boundary between the Juniata and Sequatchie Upper Ordovician redbeds and the Lower Silurian clastic wedge. Along with the BTS sequence boundary, a disconformity of unknown length occurred between Late Ordovician and Early Silurian time.

The Ordovician-Silurian unconformity is indicated by several physical features which have been observed in outcrop. These features include: 1.) the occurrence of paleosol horizons directly beneath the BTS at the most proximal localities (Copper Creek thrust); 2.) the occurrence of phosphatic pebble lags, a common feature within the BTS, which is interpreted to correspond to a basal conglomerate, a type of feature that commonly marks paraconformities; 3.) a distinctive color change from red to gray, which occurs in the shale deposits directly beneath the BTS at the more distal localities, -this color change is more gradational at some of the more proximal localities, however, it is still notable, and the occurrence of 4.) phosphatic hardgrounds at some of the more distal localities, which suggests a period of nondeposition and/or erosion. Thus, at the most proximal localities the unconformity is placed at the top of the paleosol horizons. Within the central

Rockwood Belts, the unconformity corresponds to the lowermost ravinement surface (phosphatic pebble lag). At the most distal exposure in the north (Cumberland Gap, TN), the unconformity is placed at the base of the BTS, where there is a color change in the shale deposits directly beneath the BTS. Finally, the unconformity is placed at the occurrence of a phosphatic hardground just below the BTS at the most distal exposure in the south (Tiftonia, GA).

During the relative sea-level rise, Upper Ordovician tidal-flat deposits became reworked through the process of erosional shoreface retreat. The depositional history of the BTS can be described by dividing it up according to variant designations. The WL variant was deposited in a beach face to upper shoreface environment dominated by clastic detritus. These rocks consist of fine-grained quartz arenite displaying wave ripples, horizontal laminations, and rare bioturbation. The middle to lower shoreface environment is represented by the CBS variant, which consists of thin channel sequences that were deposited in the remnant tidal channels of the Ordovician tidal flat system. Physical features include low-angle cross-stratification, horizontal laminations, and climbing ripples. Grain sizes range from fine to medium sand,with lenticular and discontinuous, coarse, phosphatic pebble lags. The FGB variant consists of very fine-grained, matrix-rich sandstone, which has been extensively bioturbated and is interpreted to represent the middle shoreface to inner shelf environments. The degree of bioturbation within this variant is indicative of slow, continuous deposition for rocks that are intensely bioturbated, and slow, discontinuous deposition for those lithologies that are moderately bioturbated. This variant may occur associated with the CBS variant, or by itself in the most distal localities. Coarse, phosphatic pebble lags also occur with this variant. The phosphatic pebble lags are interpreted to be ravinement surfaces formed through the process of erosional shoreface retreat caused by the relative rise in sea-level. This interpretation is based upon comparison with modern analogs from the U.S. Atlantic coast. The entire BTS consists of relict sediment reworked from the underlying Ordovician redbeds and an additional coarse component possibly supplied from the Taconic highlands in what is now the central Appalachians.

The diagenesis and overall petrology of the BTS reflects the changing environments it was deposited in. The most proximal deposits, those of the WL variant, contain the most abundant amounts of detrital quartz and little to no carbonate matrix or allochem grains. These rocks underwent a diagenetic history of mechanical compaction, chemical compaction by intergranular pressure solution between quartz grains, and cementation by quartz. Silica necessary for the formation of quartz overgrowths was probably derived from the silica dissolved by pressure solution. Some silica may have been freed through the smectite to illite transformation of the underlying shale deposits.

The diagenesis of samples from the CBS and FGB variant is more complicated interpret because early features have been overprinted by late replacement features. The paragenetic sequence proposed for these rocks is summarized in what follows. Framework carbonate grains made up part of the original relict sediments deposited through the process of erosional shoreface retreat. The evidence for this is sparse, however, because framework grains are "floating" in replacement ferroan dolomite and ankerite, a precursor carbonate must have once existed. Ferroan calcite precipitated during late (?) meteoric diagenesis. Some minor chemical compaction through intergranular pressure solution occurred within the coarse phosphatic pebble lags at this time, which may have provided the dissolved silica for the minor amounts of quartz cement observed in these samples.

Subhedral to euhedral ferroan dolomite and ankerite began replacing precursor carbonate phases as well as parts of framework grains, during burial diagenesis. This event served to occlude any remaining porosity, as well as to delete any record of marine and/or meteoric carbonate cement precipitation. A proposed source of iron and magnesium for the replacement phases is the conversion of smectite to illite. Other mechanisms of dolomitization are ruled out on the basis of the lack of necessary environments that are commonly invoked for these models. Early, direct precipitation of dolomite requires evaporitic environments where the magnesium-to-calcium ratio and dissolved carbonate are elevated. Sulfate reduction dolomitization mechanisms might be indicated by the presence of pyrite as a common phase, however, this has not been observed within the BTS. Finally, one might invoke a mixing zone model, however, this would not explain the concentrations of iron which are so high that ankerite is actually more common than ferroan dolomite, unless these phases actually replaced a precursor disordered mixing-zone dolomite. The smectite-to-illite transformation mechanism is the most favorable model to invoke here for the formation of burial ankerite and ferroan dolomite because ankerite, which is most abundant in these rocks, is the phase predicted to form (Boles and Franks, 1979) and illite has been identified in the underlying clayshale paleosol deposits once composed of dominantly smectite (Driese and Foreman, in review). Thus, it is the simplest explanation for the observed phenomena. In order to obtain a more unequivocal explanation, further work is necessary and would require some detailed geochemical analyses which are beyond the scope and purpose of this study.

LIST OF REFERENCES

LIST OF REFERENCES

Bambach, R.K., 1987, The Ordovician-Silurian unconformity in western Virginia and adjacent West Virginia: Appalachian Basin Industrial Associates, v.13, p.2-14.

Berry, W. B. N., and Boucot, A. J., 1973, Glacio-eustatic control of Late Ordovician-Early Silurian platform sedimentation and faunal changes: Geological Society of America Bulletin, v. 84, p. 275-284.

Boles, J. R., and Franks, S. G., 1979, Clay diagenesis in Wilcox sandstones of Southwest Texas: Implications of smectite diagenesis on sandstone cementation: Journal of Sedimentary Petrology, v. 49, p. 55-70.

Bruun, P., 1962, Sea level rise as a cause of shore erosion: Jour. Waterways and Harbors, Div., Am. Soc. Proc., v. 88, p. 117-130.

Bruun, P., 1983, Review of conditions for uses of the Bruun Rule of erosion: Coastal Engineering, v. 7, p. 77-89.

Chowns, T.M., 1972, Depositional environments in the Upper Ordovician of northwest Georgia and southeast Tennessee *in* Chowns, T.M., ed., Sedimentary Environments in the Paleozoic Rocks of Northwest Georgia: Georgia Geological Society Guidebook 11, p. 1-12.

Churkin, M., Jr., Carter, C., Johnson, B.R., 1977, Subdivision of Ordovician and Silurian time scale using accumulation rates of graptolitic shale: Geology, v. 5, p. 452-456.

Clifton, H.E., Hunter, R.E., and Phillips, R.L., 1971, Depositional structures and processes in the non-barred high-energy nearshore: Journal of Sedimentary Petrology, v. 41, p. 651-670.

Cocks, L.R.M., 1985, The Ordovician-Silurian boundary: Episodes, v. 8, p. 98-100.

Cocks, L.R.M., and Copper, P., 1981, The Ordovician-Silurian boundary at the eastern end of Anticosti Island: Canadian Journal of Earth Sciences, v. 18, p. 1029-1034.

Colquhoun, D.J., 1969, Coastal plain terraces in the Carolinas and Georgia: U. S. A. Quaternary Geology and Climatology, Publication 1701, p. 150-162.

Cook, P. J., and McElhinny, M. W., 1979, A reevaluation of the spatial and temporal distribution of sedimentary phosphate deposits in the light of plate tectonics: Economic Geology, v. 74, no. 2, p. 315-330.

Cotter, E., 1983a, Silurian depositional history *in* Nickelsen, R.P., and Cotter, E., eds., Silurian depositional history and Alleghenian deformation in the Pennsylvanian Valley and Ridge: 48th Annual Field Conference of Pennsylvania Geologists, Guidebook, p. 3-28.

Cotter, E., 1983b, Shelf, paralic, and fluvial environments and eustatic sea-level fluctuations in the origin of the Tuscarora Formation (Lower Silurian) of central Pennsylvania: Journal of Sedimentary Petrology, v. 53, p. 25-49

Davis, R. A., 1983, Depositional Systems: a genetic approach to sedimentary geology: Prentice-Hall, Inc., Englewood Cliffs, New Jersey, 669p.

Dennison, J.M., and Head, J.W., 1975, Sea level variations interpreted from the Appalachian basin Silurian and Devonian: American Journal of Science, v. 275, p. 1089-1120.

Dennison, J.M., 1983, Sedimentary tectonics of the Appalachian basin: Notes for a short course: Dallas Geological Society, 129p.

Dickinson, W.R., 1985, Interpreting provenance relations from detrital modes of sandstones: *in* Zuffa, G.G., ed., Provenance of arenites, Dordrecht-Boston-Lancaster: D. Reidel Pub. Co., p. 333-361

Diecchio, R. J., 1986, Upper Ordovician and Silurian stratigraphy of the Virginia and West Virginia Valley and Ridge: sedimentary and structural effects of the Taconic Orogeny: Guidebook for field trip no. 7, Society of Economic Paleontologists and Mineralogists Third Annual Midyear Meeting, p. 217-252.

Dott, R.H., 1964, Wacke, graywacke, and matrix- what approach to immature sandstone classification?: Journal of Sedimentary Petrology, v. 34, p. 625-632.

Dott, R.H., and Bourgeois, J., 1982, Hummocky stratification: significance of its variable bedding sequences: Geological Society of America Bulletin, v. 93, p. 663-680.

Driese, S.G., and Foreman, J.L., 1989, Eustatic and sedimentological controls on the development of paleosols: examples from Upper Ordovician strata, southern Appalachians: Geological Society of America Abstracts with Programs, v. 21, no. 6, p. 128.

Driese, S.G., Fischer, M.W., Easthouse, K.A., and Marks, G.T., 1990, Model for genesis of shelf sandstone sequences, southern Appalachians: paleoenvironmental reconstruction of an Early Silurian shelf system *in* Swift, D.J.P., Oertel, G.F., and Tillman, R.W., eds., Shelf Sand and Sandstone Bodies: Geometry, Facies, and Distribution: International Association of Sedimentologists Special Publication No. 12, p.

Duke, W.L., 1985, Hummocky cross-stratification, hurricanes and winter storms: Sedimentology, v. 32, p. 167-194.

Eberl, D., and Hower, j., 1976, Kinetics of illite formation: Geological Society of America Bulletin, v. 87, p. 1326-1330.

Everts, C.H., 1987, Continental shelf evolution in response to a rise in sea level *in* Nummedal, D., Pilkey, O.H., and Howard, J.D., eds., Sea-Level Fluctuation and Coastal Evolution : Society of Economic Paleontologists and Mineralogists Special Publication No. 41, p. 49-58

Fischer, M. W., 1987, Sedimentology of the Lower Silurian Clinch Sandstone along Clinch Mountain, northeastern Tennessee: Univ. of Tennessee, unpub. M.S. Thesis, 156p.

Foreman, J.L., Steinhauff, D.M., Labotka, T., Walker, K.R., 1989, Phasecount: Computer-assisted point count program for thin-section spatial analysis: Southeastern Section of the Geological Society of America 38th Annual Meeting, p. 38.

Foreman, J.L., 1986, Composition and distribution of carbonate phases in the Lower Devonian Ridgeley Sandstone (Oriskany Group), southwest Pennsylvania: Bowling Green State University, unpub. M.S. Thesis, 118p.

Fortey, R.A., and Cocks, L.R.M., 1988, Arenig to Llandovery faunal distributions in the Caledonides *in* Harris, A.L., and Fettes, D.J., eds., The Caledonian-Appalachian Orogen: Geological Society Special Publication No. 38, p. 233-246.

Frank, J.R., 1981, Dedolomitization in the Taum Sauk Limestone (Upper Cambrian), southeast Missouri: Journal of Sedimentary Petrology, v. 51, p. 7-18.

Galloway, W. E., 1989, Genetic stratigraphic sequences in basin analysis I: Architecture and genesis of flooding-surface bounded depositional units: American Association of Petroleum Geologists Bulletin, v. 73, no. 2, p. 125-142.

Gogola, A. R., and Driese, S. G., 1989, Physical evidence for a sequence-bounding unconformity: the Ordovician-Silurian boundary in the southern Appalachians: Geological Society of America Abstracts with Programs, v. 21, no. 6., p.79.

Gohren, H., 1975, Dynamics and morphology of sand banks in the surf zone of outer tidal flats: Proc. 14th International Conference on Coastal Engineering, p. 871-883.

Gray, M.B., and Nickelsen, R.P., 1989, Pedogenic slickensides, indicators of strain and deformation processes in redbed sequences of the Appalachian foreland: Geology, v. 17, p. 72-75.

Gregg, J.M., and Sibley, D.F., 1984, Epigenetic dolomitization and the origin of xenotopic dolomite texture: Journal of Sedimentary Petrology, v. 54, p. 908-931.

Hamblin, A.P., and Walker, R.G., 1979, Storm-dominated shallow marine deposits: the Fernie-Kootenay (Jurassic) transition, southern Rocky Mountains: Canadian Journal of Earth Sciences, v. 16, p. 1673-1690.

Harms, J.C., Southard, J.B., and Walker, R.G., 1982, Structures and sequences in clastic rocks: Society of Economic Paleontologists and Mineralogists Short Course No. 9, 249p.

Hatcher, R. D., Jr., in press, Tectonic synthesis of the U.S. Appalachians: Ch. 14 *in* The Appalachian-Ouachita Orogen in the United States, Geological Society of America Decade of North American Geology, v. F-2

Hatcher, R. D., Jr., 1987, Tectonics of the southern and central Appalachian internides: Annual Reviews in Earth and Planetary Sciences, v. 15, p. 337-362.

Holail, H., Lohmann, K.C., and Sanderson, I., 1988, Dolomitization and dedolomitization of Upper Cretaceous carbonates: Bahariya Oasis, Egypt *in* Shukla, V., and Baker, P.A., eds., Sedimentology and Geochemistry of Dolostones: Society of Economic Paleontologists and Mineralogists Special Publication No. 43, p. 191-208.

Houseknecht, D.W., 1984, Influence of grain size and temperature on intergranular pressure solution, quartz cementation, and porosity in a quartzose sandstone: Journal of Sedimentary Petrology, v. 54, p. 348-361.

Houseknecht, D.W., 1987, Assessing the relative importance of compaction processes and cementation to reduction of porosity in sandstones: American Association of Petroleum Geologists Bulletin, v. 71, p. 633-642.

Howard, J.D., 1975, Sedimentology and trace fossils in Basan, P.B., ed., Trace Fossil Concepts: Society of Economic Paleontologists and Mineralogists Short Course No. 5, p. 13-45.

Krumbein, W.C., and Sloss, L.L., 1963, Stratigraphy and Sedimentation, 2nd Edition: W.H. Freeman and Company, San Francisco, 660p.

James, W.C., Wilmar, Glenn C., and Davidson, Bruce G., 1986, Role of quartz type and grain size in silica diagenesis, Nugget Sandstone, south-central Wyoming: Journal of Sedimentary Petrology, v. 56, p. 657-662.

Johnson, M. E., 1980, Paleoecological structure in Early Silurian platform seas of the North American midcontinent: Palaeogeography, Palaeoclimatology, Palaeoecology, v. 30, p. 191-216.

Johnson, M.E., 1987, Extent and bathymetry of North American platform seas in the early Silurian: Paleoceanography, v. 2, p. 185-211.

Jordan, T.E., and Flemings, P.B., 1989, Dependence of stratigraphic sequence architecture on basin type: Geological Society of America Abstracts with Programs, v. 21, no. 6, p. 35.

Kidwell, S.M., 1989, Stratigraphic condensation of marine transgressive records: origin of major shell deposits in the Miocene of Maryland: Journal of Geology, v. 97, p. 1-24.

Lahann, R.W., 1980, Smectite diagenesis and sandstone cement: the effect of reaction temperature: Journal of Sedimentary Petrology, v. 50, p. 755-760.

McCarthy, I.A.J., 1987, Transgressive variant in the South Munster Basin, Ireland: Sedimentology, v. 34, p. 389-422.

McBride, E.F., 1962, Flysch and associated beds of the Martinsburg Formation (Ordovician), central Appalachians: Journal of Sedimentary Petrology, v. 32., p. 39-91.

McCubbin, D.G., 1969, Cretaceous strike-valley sandstone reservoirs, northwestern New Mexico: American Association of Petroleum Geologists Bulletin, v. 53, p. 2114-2140.

McCubbin, D.G., 1982, Barrier island and strand-plain variant *in* Scholle, P.A., and Spearing, D., eds., Sandstone Depositional Environments: American Association of Petroleum Geologists Memoir #31, p. 247-279.

McKerrow, W. S., 1979, Ordovician and Silurian changes in sea level: Geological Society of London Quarterly Journal, v. 136, p. 137-145.

McManus, D.A., 1975, Modern versus relict sediment on the continental shelf: Geological Society of America Bulletin, v. 86, p. 1154-1160.

Milici, R.C., and Wedow, H., Jr., 1977, Upper Ordovician and Silurian stratigraphy in Sequatchie Valley and parts of the adjacent Valley and Ridge, Tennessee: United States Geological Survey Professional Paper 996, p.1-37.

Milici, R.C., and deWitt, W., Jr., 1988, The Appalachian Basin *in* Sloss, ed., Sedimentary Cover-North American Craton; U.S.: Boulder, Colorado, Geological Society of America, The Geology of North America, v. D-2, p. 427-469.

Miller, R.L., 1976, Silurian nomenclature and correlations in southwest Virginia and northeast Tennessee: U.S. Geological Survey Bulletin 1405-H, p.1-25.

Mitchum, R.M., Jr., Vail, P. R., and Thompson, S., III, 1977, Seismic stratigraphy and global changes of sea level, part 2: the depositional sequence as a basic unit for stratigraphic analysis, *in* C. E. Payton, ed., Seismic stratigraphy- applications to hydrocarbon exploration: American Association of Petroleum Geologists Memoir 26, p. 53-62.

Molenaar, N., 1986, The interrelation between clay infiltration, quartz cementation, and compaction in lower Givetian terrestrial sandstones, northern Ardennes, Belgium: Journal of Sedimentary Petrology, v. 56, p. 359-369.

Mount, J.F., 1985, Mixed siliciclastic and carbonate sediments: a proposed 1st-order textural and compositional classification: Sedimentology, v. 32, p. 435-442.

Nummedal, D., and Swift, D. J. P., 1987, Transgressive stratigraphy at sequence-bounding unconformities: some principles derived from Holocene and Cretaceous examples *in* Nummedal, D, Pilkey, O.H., and Howard, J.D., eds, Sea-Level Fluctuations and Coastal Evolution: Society of Economic Paleontologists and Mineralogists Special Publication No. 41, p. 241-260.

Pattison, S.A.J., 1988, Transgressive, incised shoreface deposits of the Burnstick Member (Cardium "B" Sandstone) at Caroline, Crossfield, Garrington, and Lochend; Cretaceous western interior seaway, Alberta, Canada *in* James, D.P., and Leckie, D.A., eds., Sequences, Stratigraphy, Sedimentology: Surface and Subsurface: Canadian Society of Petroleum Geologists, Memoir 15, p. 155-166.

Perry, E. A., and Hower, J., 1970, Burial diagenesis in Gulf Coast pelitic sediments: Clays Clay Minerals, v. 18, p. 165-177.

Petrovic, R., 1976, Rate control in feldspar dissolution- II. The protective effect of precipitates: Geochimica Cosmochima Acta, v. 40, p. 1509-1522.

Pilkey, O.H., Blackwelder, B.W., Knebel, H.J., and Ayers, M.W., 1981, The Georgia embayment continental shelf: stratigraphy of a submergence: Geological Society of America Bulletin, v. 92, p. 52-63.

Plint, A.G., 1988, Sharp-based shoreface sequences and "offshore bars" in the Cardium Formation of Alberta: their relationship to relative changes in sea level *in* Wilgus, C.K., Hastings, B.S., St. C. Kendall, C.G., Posamentier, H.W., Ross, C.A., and Van Wagoner, J.C., eds., Sea-Level Changes: An Integrated Approach: Society of Economic Paleontologists and Mineralogists Special Publication No. 42, p. 357-370.

Posamentier, H.W., and Vail, P.R., 1988, Eustatic controls on clastic deposition II-sequence and systems tract models *in* Wilgus, C.K., Hastings, B.S., St. C. Kendall, C.G., Posamentier, H.W., Ross, C.A., and Van Wagoner, J.C., eds., Sea-Level Changes: An Integrated Approach: Society of Economic Paleontologists and Mineralogists Special Publication No. 42, p.125-153.

Quinlan, G.M., and Beaumont, C., 1984, Appalachian thrusting, lithospheric flexure, and the Paleozoic stratigraphy of the eastern interior of North America: Canadian Journal of Earth Science, v. 21, p. 973-996.

Reineck, H.E., and Singh, I.B., 1986, Depositional Sedimentary Environments: Springer-Verlag, Berlin, Heidelberg, New York, 551p.

Rodgers, J., 1953, Geologic map of east Tennessee with explanatory text: Tennessee Division of Geology Bulletin, v. 58, 168p.

Rodgers, J., 1971, The Taconic Orogeny: Geological Society of America Bulletin, v. 82, p. 1141-1178.

Roeder, D. and Witherspoon, W.D., 1978, Palinspastic map of East Tennessee: American Journal of Science, v. 278, p. 543-550.

Ryer, T.A., 1977, Patterns of Cretaceous shallow-marine sedimentation, Coalville and Rockport areas, Utah: Geological Society of America Bulletin, v. 88, p. 177-188.

Saito, Y., Nishimura, A., and Matsumoto, E., 1989, Transgressive sand sheet covering the shelf and upper slope off Sendai, northeast Japan: Marine Geology, v. 89, p. 245-258.

Schoner, A. E., 1985a, The sedimentology and sedimentary petrology of the Lower Silurian Clinch Sandstone at Beans Gap, Grainger County, Tennessee: University of Tennessee, unpub. M.S. Thesis, 227p.

Schoner, A. E., 1985b, The Clinch Sandstone (Lower Silurian) along Highway 25E at Beans Gap, *in* Walker, K. R., (ed.), The Geologic History of the Thorn Hill Paleozoic Section (Cambrian-Mississippian), Eastern Tennessee: University of Tennessee, Dept. of Geological Sciences, Studies in Geology 10, p. 100-110.

Seilacher, A., 1967, Bathymetry of trace fossils: Marine Geology, v.5, p. 413-425.

Shanmugam, G., and Walker, K. R., 1980, Anatomy of the Middle Ordovician Sevier Shale basin, eastern Tennessee: Sedimentary Geology, v. 34, p. 315-337.

Shanmugam, G., and Moiola, R.J., 1982, Eustatic control of turbidites and winnowed turbidites: Geology, v. 10, p. 231-235.

Sheldon, R. P., 1980, Episodicity of phosphate deposition and deep ocean circulation- a hypothesis: Society of Economic Paleontologists and Mineralogists Special Publication No. 29, p. 239-247.

Smith, R. W., and Whitlatch, G. I., 1940, The phosphate resources of Tennessee: Tennessee Division of Geology Bulletin 48, 444p.

Soil Survey Staff, 1975, Soil Taxonomy: U.S. Department of Agriculture Handbook 436, Washington, D.C., Government Printing Office, 754p.

Swift, D. J. P., 1968, Coastal erosion and transgressive stratigraphy: Journal of Geology, v. 76, p. 444-456.

Swift, D. J. P., Stanley, K. J., and Curray, J. R., 1971, Relict sediments on continental shelves: a reconsideration: Journal of Geology, v. 79, p. 322-346.

Thomas, W.A., 1977, Evolution of Appalachian-Ouachita salients and recesses from reentrants and promontories in the continental margin: American Journal of Science, v. 277, p. 1233-1278.

Thompson, A.M., 1970a, Lithofacies and formation nomenclature in Upper Ordovician stratigraphy, central Appalachians: Geological Society of America Bulletin, v. 81, p. 1255-1260.

Thompson, A.M., 1970b, Tidal-flat deposition and early dolomitization in Upper Ordovician rocks of southern Appalachian Valley and Ridge: Journal of Sedimentary Petrology, v. 40, p. 1271-1286.

Towe, K. M., 1962, Diagenesis of clay minerals as a possible source of silica cement in sedimentary rocks: Journal of Sedimentary Petrology, v. 32, p. 26-28.

Vail, P. R., 1987, Seismic stratigraphy interpretation using sequence stratigraphy, part 1, seismic stratigraphy interpretation procedure, *in* A. W. Bally, ed., Atlas of seismic stratigraphy, v. 1: American Association of Petroleum Geologists Studies in Geology 27, p. 1-10.

Van der Plas, L., and Tobi, A.C., 1965, A chart for judging the reliability of point counting results: American Journal of Science, v. 263, p. 87-90.

Walker, K. R., Shanmugam, G., and Ruppel, S. C., 1983, A model for carbonate to terrigenous clastic sequences: Geological Society of America Bulletin, v. 94, p. 700-712.

Walker, R.G., Duke, W.L., and Leckie, D.A., 1983, Hummocky stratification: significance of its variable bedding sequences: discussion: Geological Society of America Bulletin, v. 94, p. 1245-1249.

Weimer, R.J., Howard, J.D., and Lindsay, D.R., 1982, Tidal Flats: *in* Scholle, P.A., and Spearing, D.R., eds., Sandstone Depositional Environments: American Association of Petroleum Geologist Memoir # 31, p. 191-245.

Wilson, M.D., and Pittman, E.D., 1977, Authigenic clays in sandstones: recognition and influence on reservoir properties and paleoenvironmental analysis: Journal of Sedimentary Petrology, v. 47, p. 3-31.

Zuffa, G.G., 1980, Hybrid arenites: Their composition and classification: Journal of Sedimentary Petrology, v. 50, p. 21-29.

APPENDICES

APPENDIX A:

MEASURED SECTION DESCRIPTIONS

Unit Thickness	Cumulative Thickness	Beans Gap, TN
20	20	Tan-yellow silty sandstone containing iron-oxide vugs near the top and 2-5cm peds throughout. Displays a hockly fracture pattern. Massive-bedding grades downward into purple strata.
7	27	Transgressive surface consisting of siltstone with abundant phosphate nodules and concretions. Sample 8.7-BG-88 taken at 27 cm.
98	125	Thin-bedded, tan-yellow, very fine-grained sandstone containing climbing wave ripple cross-laminations. Local gray clayshale occurs at base (27-32 cm). Beds grade upwards into sandstone which is predominantly parallel laminated and tan-yellow in color. Some gentle undulations occur which do not appear to be hummocky or swaly. No evidence for bioturbation. Sandstone grades upward into massive silty sandstone containing rare wave ripples. Samples 8.75-BG-88 and 9.2-BG-88 taken at 75 and 121 cm, respectively.
82	207	Color change in shale from red(?) to gray (e.g., Hagan Shale). Mostly semi-fissile gray clay shale with scattered cm-thick lenses and layers of fine- to very fine tan-yellow sandstone. Horizon of ellipsoidal carbonate-cemented concretions occurs at 167 cm.
3	210	Tan-yellow, medium- to coarse-grained sandstone. Begin Poor Valley Ridge member of Clinch Sandstone.

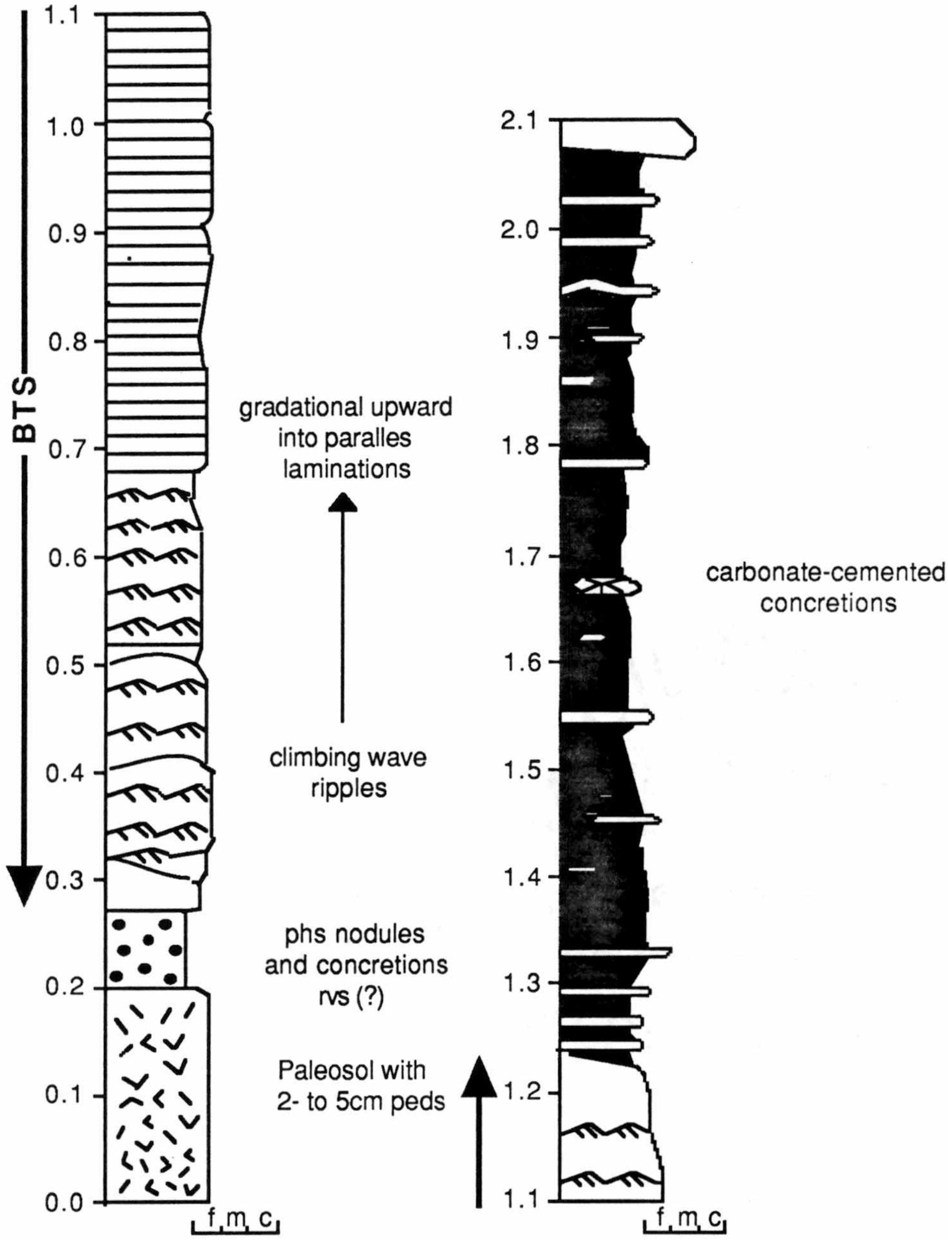

Figure A.1. Measured stratigraphic section at Beans Gap, TN.

Unit Thickness (cm)	Cumulative Thicknes (cm)	Flat Gap, TN
21	21	Gray siltstone to fine-grained sandstone which appears to be bioturbated.
92	113	Red, semi- to non-fissile clay shale. Color change occurs at 112 cm.
5	118	5 cm of semi-fissile silty clay shale.
38	156	Medium-bedded fine-grained sandstone which has been extensively mineralized by manganese (?). Possible trilobite traces occur at the base of this unit which otherwise appears to be structureless. Thin unit is more resistant than overlying beds.
204	360	Brown, thin-bedded fine-grained sandstone which is extremely weathered and mineralized such that no sedimentary structures are visible. One bed which occurs from 305 to 314 cm contains burrows which are stained with iron-oxide.
20	380	Gray-green semi-fissile clay shale. Overlying stratigraphy is covered.

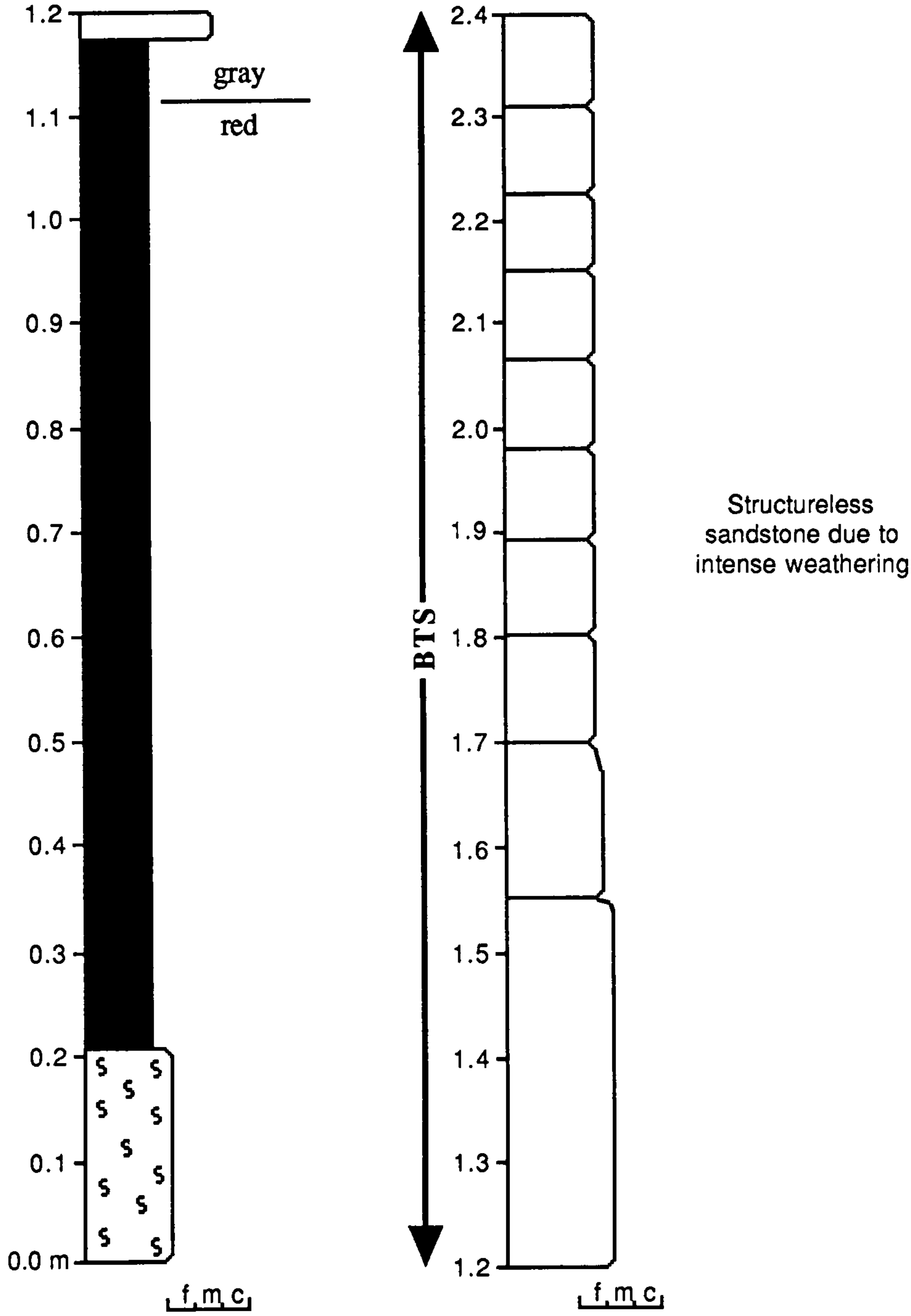

Figure A.2. Measured stratigraphic section at Flat Gap, TN.

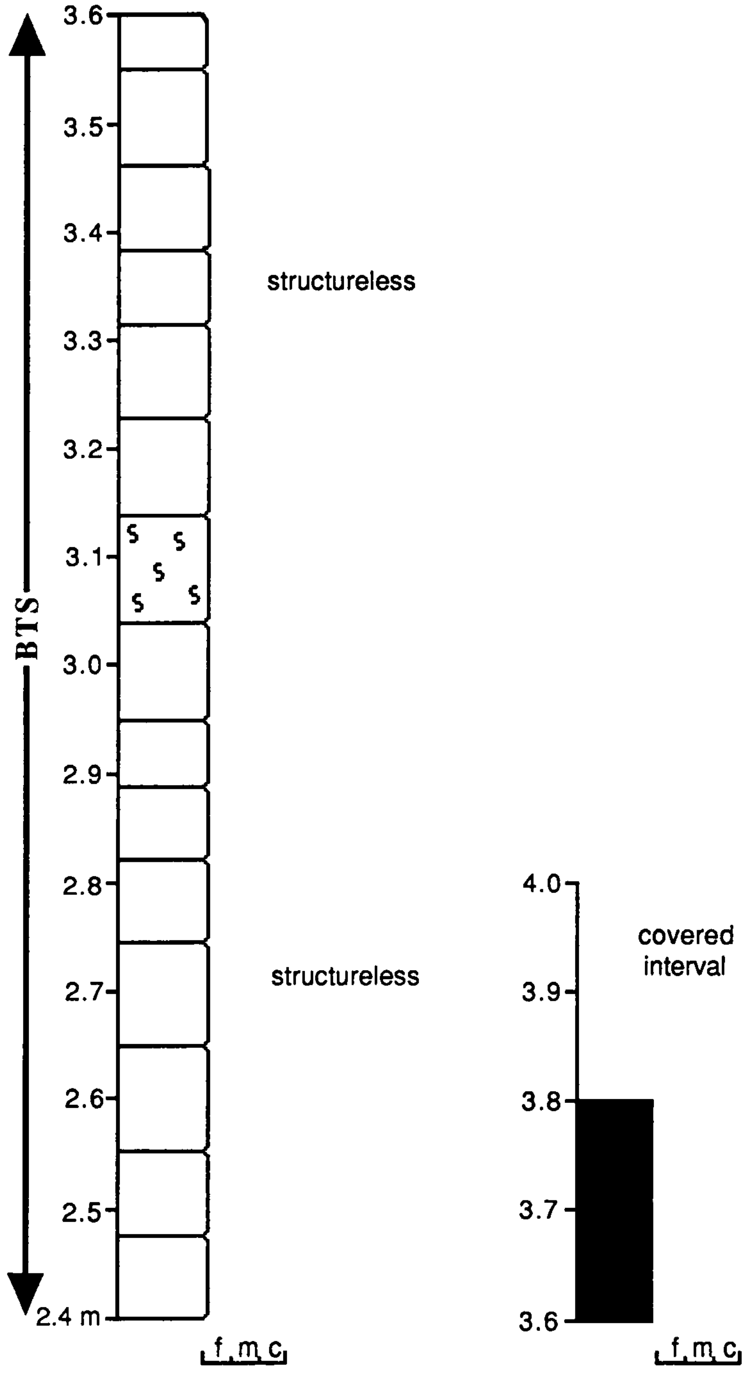

Figure A.2 continued.

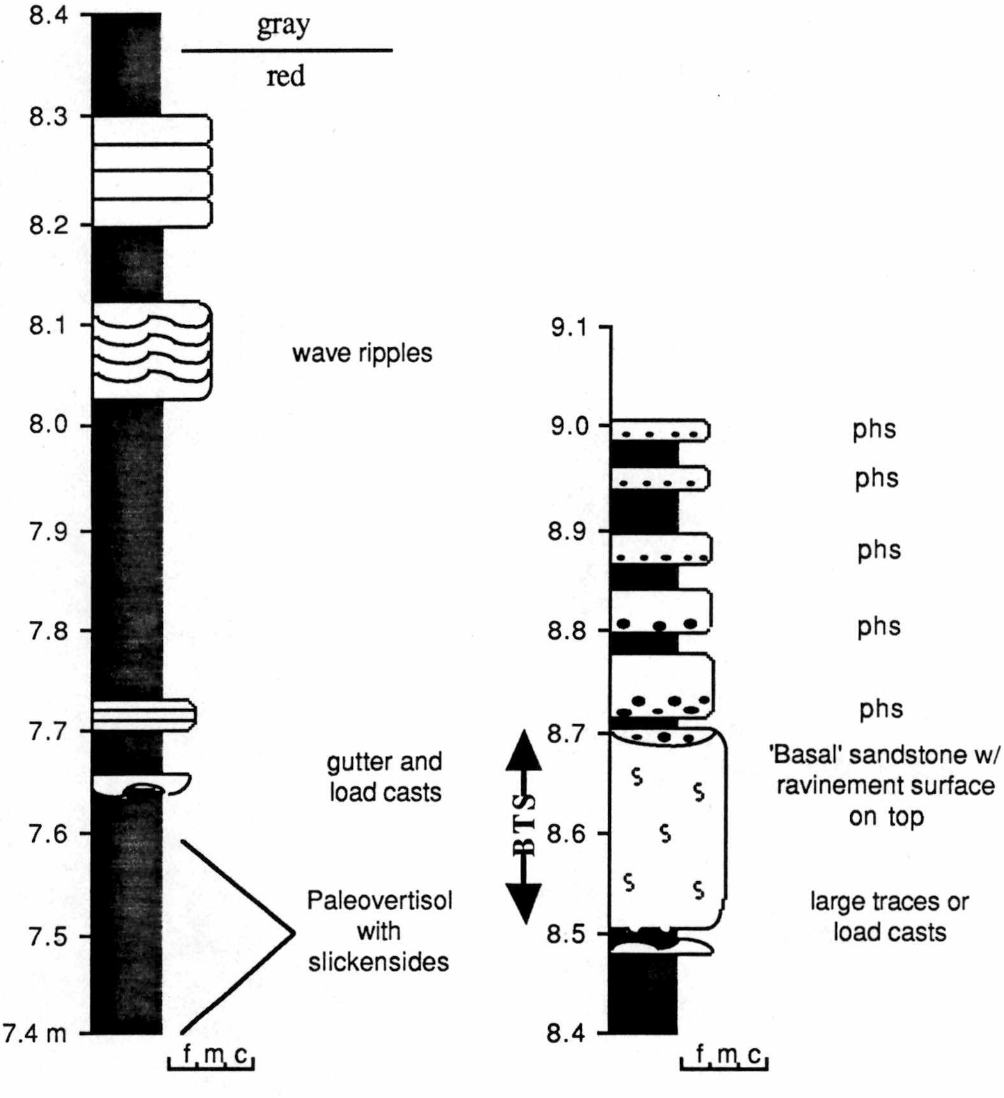

Figure A.3. Measured stratigraphic section at Powell Mountain, VA. Section was measured by Steve Driese.

Unit Thickness (cm)	Cumulative Thickness (cm)	Melton Lake, TN
80	80	Lenticular sandstone which is incised into the underlying silty shale. The lowermost 30cm of the unit contains ripple structures with mud drapes. Dessication cracks occur at 34cm cumulative thickness. These structures are overlain by a channel-like feature displaying accreting bedding. Overlying sedimentary structures consist of horizontal laminations. A coarse phosphate pebble lag occurs at 70cm thickness which contains mud drapes and is 4cm thick. The uppermost part of the unit is horizontally laminated and contains scattered phosphate granules. Samples 0.0-ML, 0.2-ML, and 0.7-ML were taken at 0cm, 20cm, 70cm, respectively.
10	90	Base of basal transgressive sandstone with the exception of the underlying lenticular unit. This unit consists of lenticular, coarse, phosphatic lag deposits which are cross-stratified in the upper 5cm of the unit. Sample 0.85-ML was taken at 85cm.
7	97	Fining upwards sandstone unit which occurs in sharp contact with the underlying and overlying units.
53	150	Medium- to thick-bedded sandstone containing medium- to small-scale trough cross-stratification. The base of the unit is marked by a 3cm thick phosphate horizon. Skolitos tubes occur at 110cm cumulative thickness. Sample 1.2-ML was taken at 120cm.
138	288	Structureless fine-grained sandstone occurring in medium to thick beds. The contact with the underlying sand is gradational whereas it is very sharp with the overlying unit. Samples 1.65-ML, 1.9-ML, 2.1-ML, and 2.8-ML were taken at 165cm, 190cm, 210cm, and 280cm, respectively.
12	300	Bioturbated siltstone/sandstone marking the top of the basal transgressive sequence.

Unit Thickness (cm)	Cumulative Thickness (cm)	Melton Lake, TN (contiued)
140	440	Sharp contact with the underlying sands. Thin rippled sandstone interbedded with gray, silty clay shale. Occasionally see thin bioturbated beds interspersed througout the sequence. Capped by a large gutter cast with tool marks. Sequence is interpreted to represent the distal Rockwood tempestites.

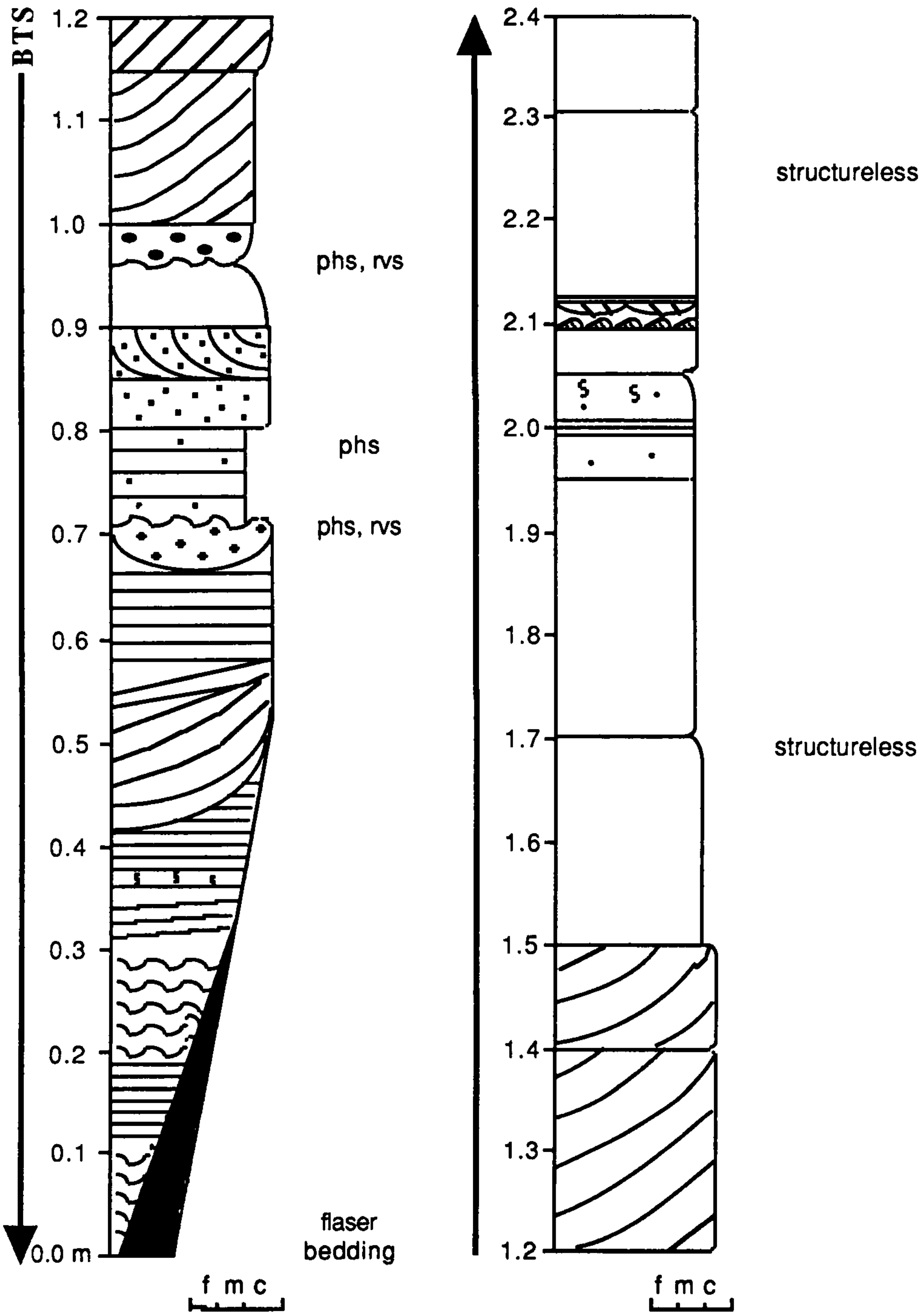

Figure A.4. Measured stratigraphic section at Melton Lake, TN.

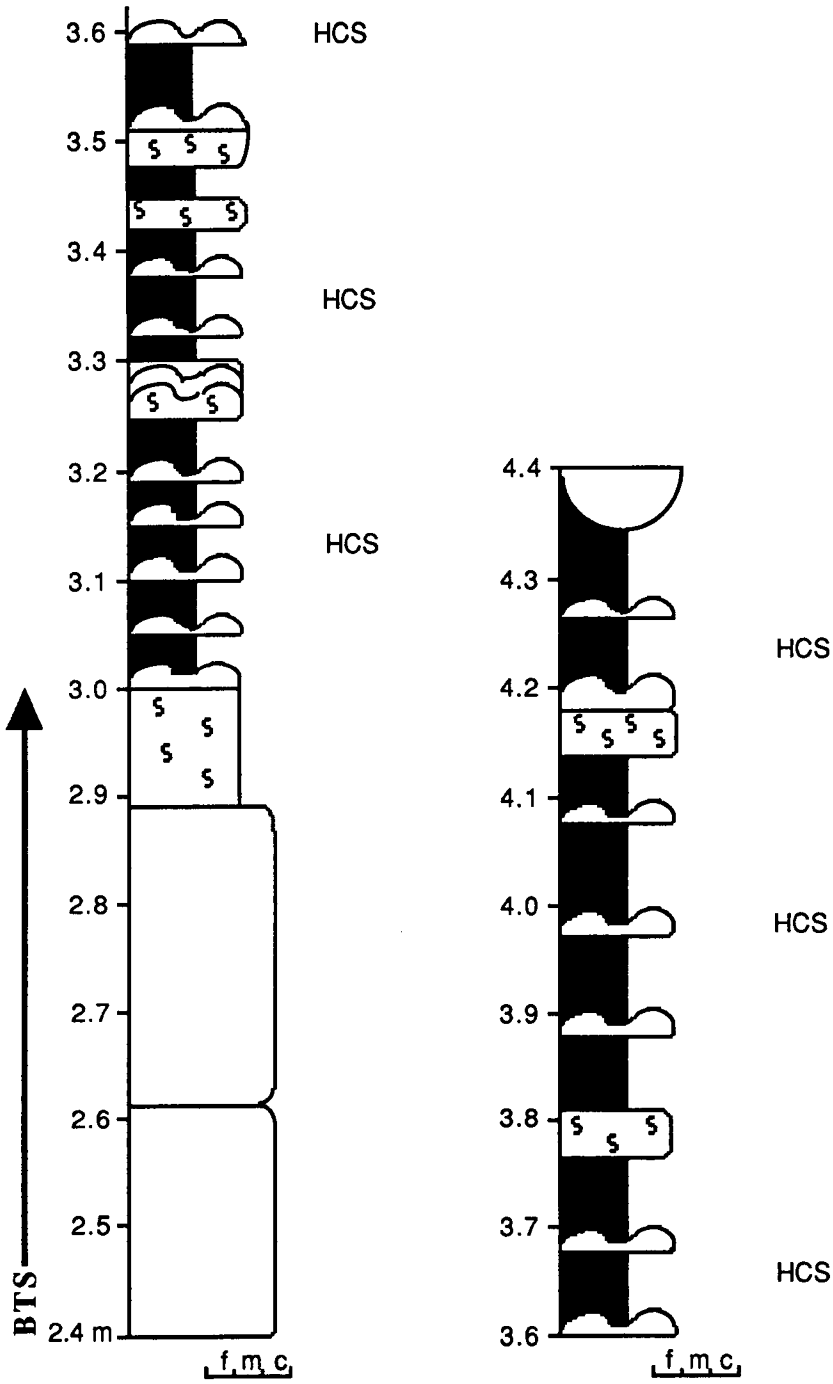

Figure A.4 continued.

Unit Thickness (cm)	Cumulative Thickness (cm)	Lone Mountain, TN
120	120	Thrust faulted Ordovician and Silurian strata
70	190	Red- to maroon-colored calcareous siltstone. Very thin beds tend to be parallel laminated whereas thin beds are mostley bioturbated. Contact with overlying strata is gradational.
68	258	Gradational contact with underlying unit. Gray to tan-brown calcareous siltston which is thin-bedded towards the base and becomes medium-bedded (up to 20cm thick) towards the top. Mostly bioturbated.
42	300	Green-gray, massive, bioturbated calcareous siltstone which has a gradational contact with the underlying unit.
25	325	Tan-gray, thin- to medium-bedded calcareous siltstone which is essentially structureless.
15	340	Sharp contact with the underlying siltstones. Silty lime wackestone which becomes more fossiliferous toward the top.
10	350	Gray clayshale displaying sharp contacts with both the underlying and overlying units.
3	353	Silty lime mudstone
3	356	Gray clayshale displaying sharp contacts with both the underlying and overlying units.
9	365	Fossiliferous, silty lime packstone. Sample 3.65-LM at 365cm.
35	400	Sharp contact. Ultrafissile red-brown clay shale.

Unit Thickness (cm)	Cumulative Thickness (cm)	Lone Mountain, TN (continued)
5	405	Nodular, impure (clayey) wackestone/mudstone in gradational contact with the clay shale.
25	430	Thin-bedded, silty, lime wackestone which contains whole-fossil brachiopods. Sample 4.3-LM at 430cm.
20	450	Grayish-green semi-fissile clay shale.
10	460	Somewhat gradational contact with grayish-green clay shale. Ultra-fissile red-brown clay shale.
3	463	Dolostone containing phosphatic allochems and minor amounts of silt occurs in sharp, but irregular contact with the underlying and overlying units. Bioturbated. Sample 4.6-LM at 460cm.
27	490	Gray semi-fissile clay shale.
2	492	Burrowed siltstone in sharp contact with underlying and overlying shales.
10	502	Gray fissile clay shale.
2	504	Burrowed siltstone in sharp contact with underlying and overlying shales.
81	585	Red-gray fissile clay shale.
35	620	Olive-gray-green burrowed clay shale in gradational contact with the underlying red-gray clay shale.
40	660	Base of basal transgressive sandstonesequence in sharp (scoured?) contact with the underlying clay shale. The unit contains horizontal stratification and pinches out laterally.Sands are fine- to medium-grained. Samples 6.25-LM and 6.55-LM at 625cm and 655cm, respectively.

Unit Thickness (cm)	Cumulative Thickness (cm)	Lone Mountain, TN (continued)
25	685	Fine- to medium-grained sandstone marked by low-angle cross-stratification and capped by a 5cm-thick erosional lag containing coarse sand and phosphate pebbles. The unit displays a sharp, but irregular, contact with the underlying sandstone Thin layers contain some mud drapes. Sample 6.65-LM at 665cm.
65	750	Sharp contact with underlying erosional lag. Medium-bedded, bioturbated, calcareous sandstone containing dewatering structures at 740cm. Top of basal sandstone at 750cm. Samples 6.9-LM, 7.1-LM, and 7.45-LM at 690cm, 710cm, 720cm, and 745cm, respectively.
30	780	Interbedded thin sandstone and shale in sharp contact with the top of the basal transgressive sandstone sequence. Sandstones contain micro-hummocky cross-stratification.
30	810	Interbedded thin, bioturbated sandstones and and clayshale.
10	820	Medium-thick bioturbated sandstone.
48	868	Interbedded siltstone and semi-fissile gray clay shale. Siltstones are bioturbated.
5	875	Interbedded gray semi-fissile clay shale and thin sandstone/siltstone beds which contain combined flow ripples and micro hummocky cross-stratification.

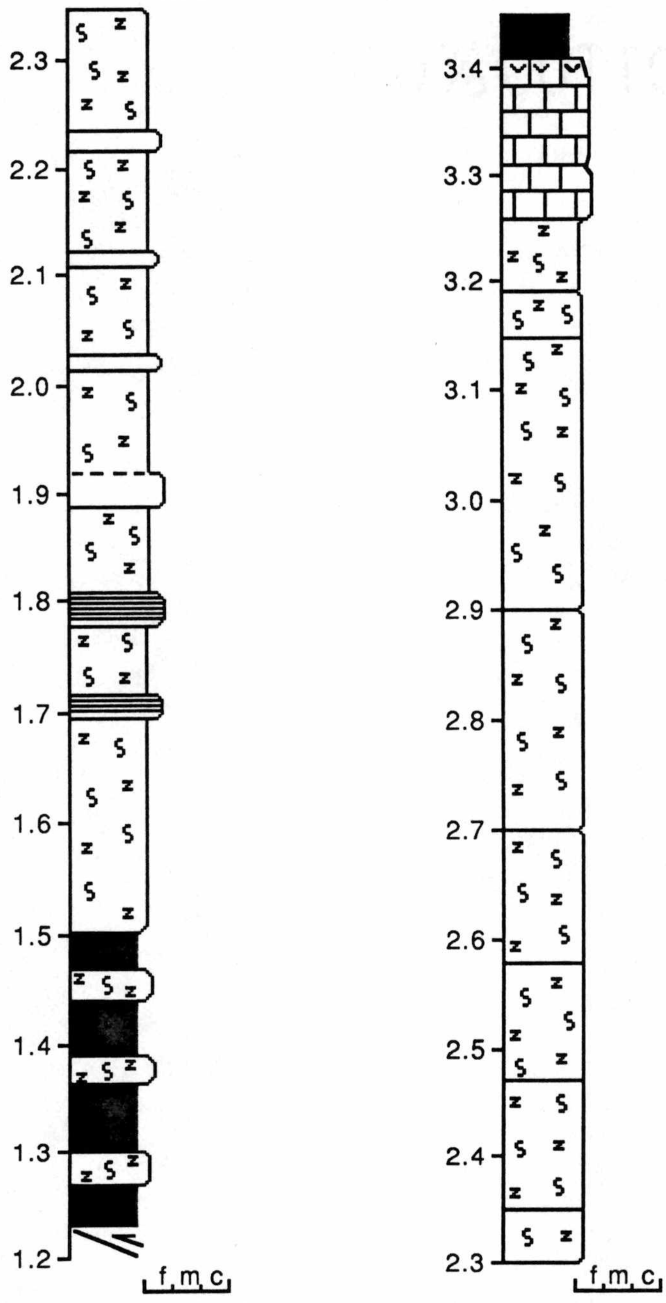

Figure A.5. Measured stratigraphic section at Lone Mountain, TN.

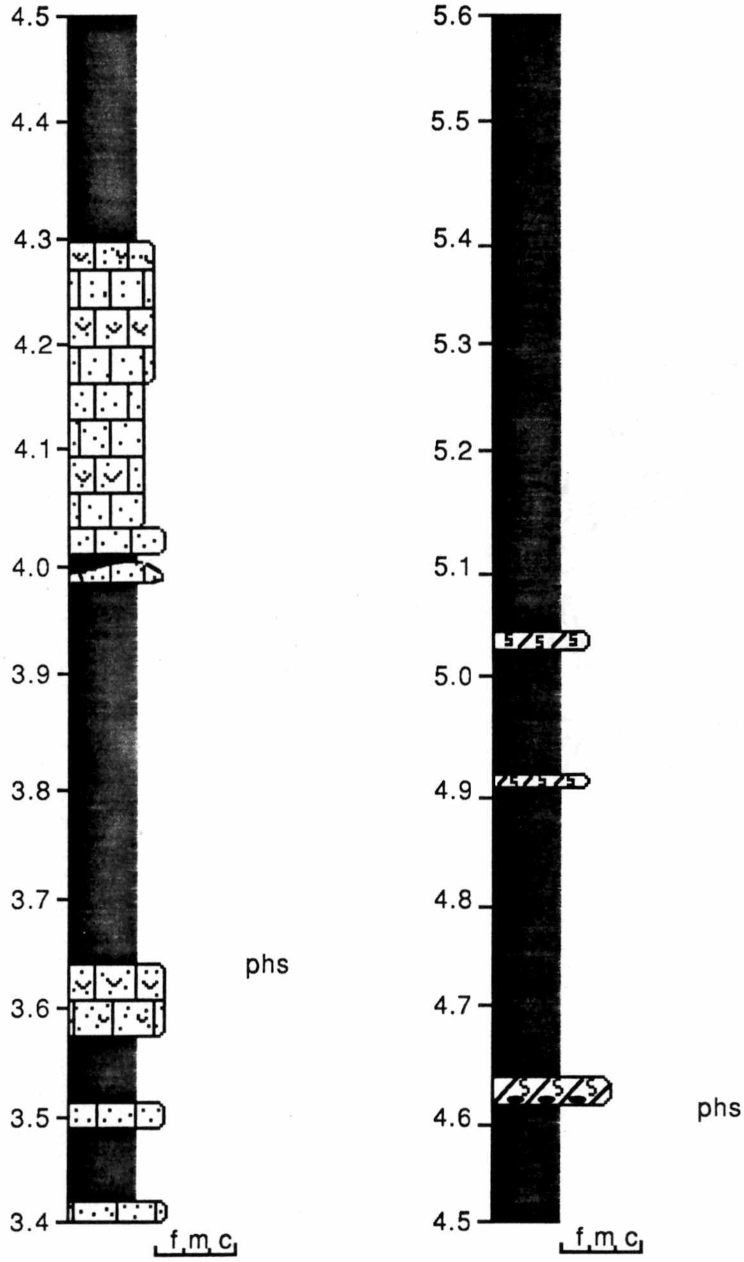

Figure A.5 continued.

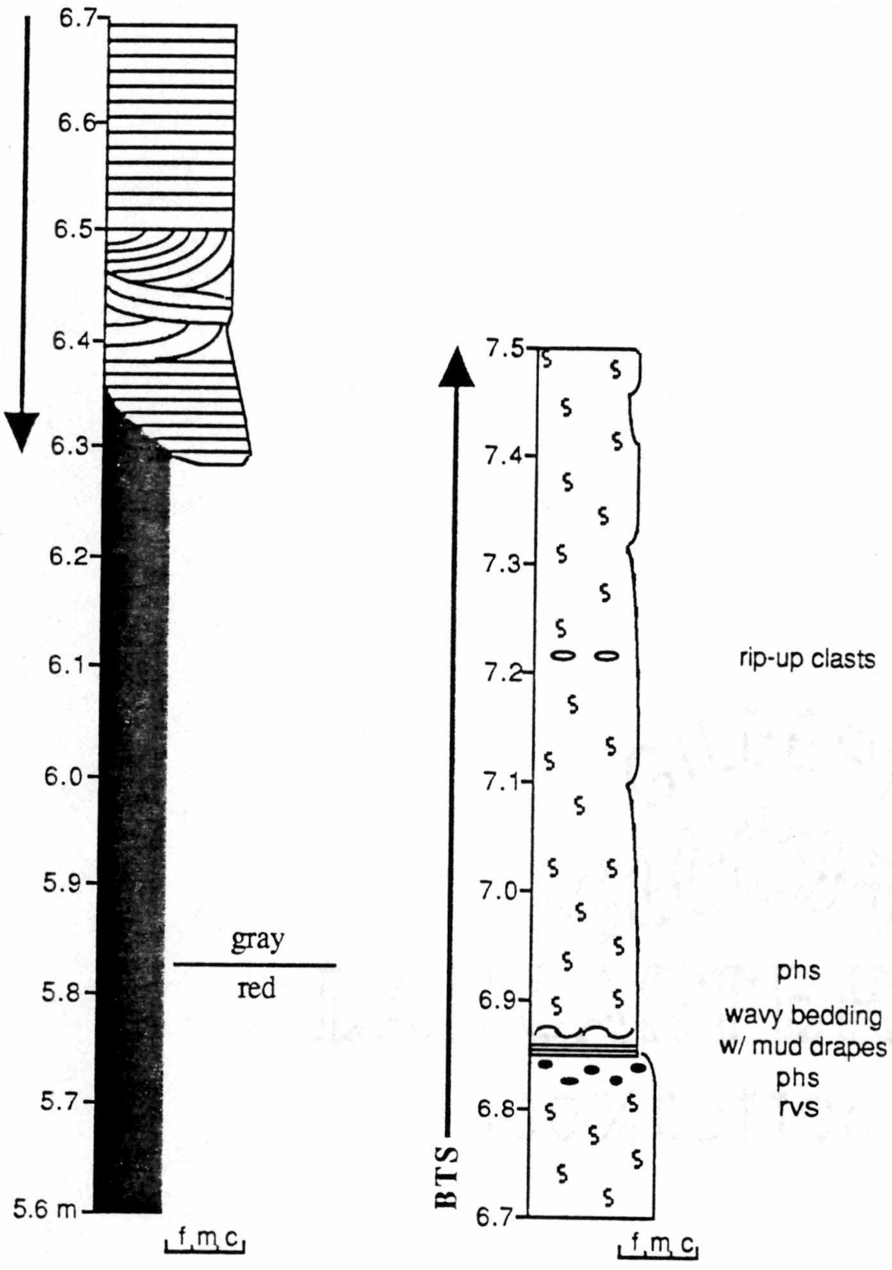

Figure A.5 continued

Unit Thickness (cm)	Cumulative Thickness (cm)	Cumberland Gap, TN
170	170	Covered.
54	224	Red-yellow, mottled, calcareous siltstone. Densely bioturbated. Red micritic nodule occurs at 180 cm. Possible mudcracks just above this nodule within the siltstone.
56	280	Red, fissile, calcareous siltstone which become slightly coarser and more resistent at 252cm. The unit has gradational contacts with the underlying and siltstone units.
21	301	Sharp color change at 280cm from maroon to reddish-gray marking the base of the basal transgressive sandstone. Faintly laminated calcareous siltstone/fine-grained sandstone. Sample 2.9-CG at 290cm.
9	310	Gray, semi-fissile, silty shale which is in gradational contact with both the underlying and overlying units. Sample 3.05-CG at 305cm.
10	320	Densely bioturbated, gray, calcareous sandstone capped by phosphatic hardground at 320cm which forms a sharp but irregular contact with the overlying unit. Sample 3.2-CG at 320cm.
10	330	Calcareous, gray, fine-grained sandstone which contains disseminated phosphate granules. Rip-up clasts of shale and siltstone occur at 325cm. This unit marks the top of the basal transgressive sandstone. Sample 3.25-CG at 325cm.
67	397	Gradational contact with underlying transgressive sandstone. Sequence of interbedded siltstone and gray-green shale.
4	401	Fine-grained, micro-hummocky cross-stratified sandstone in sharp contact with the interbedded siltstone and shale.

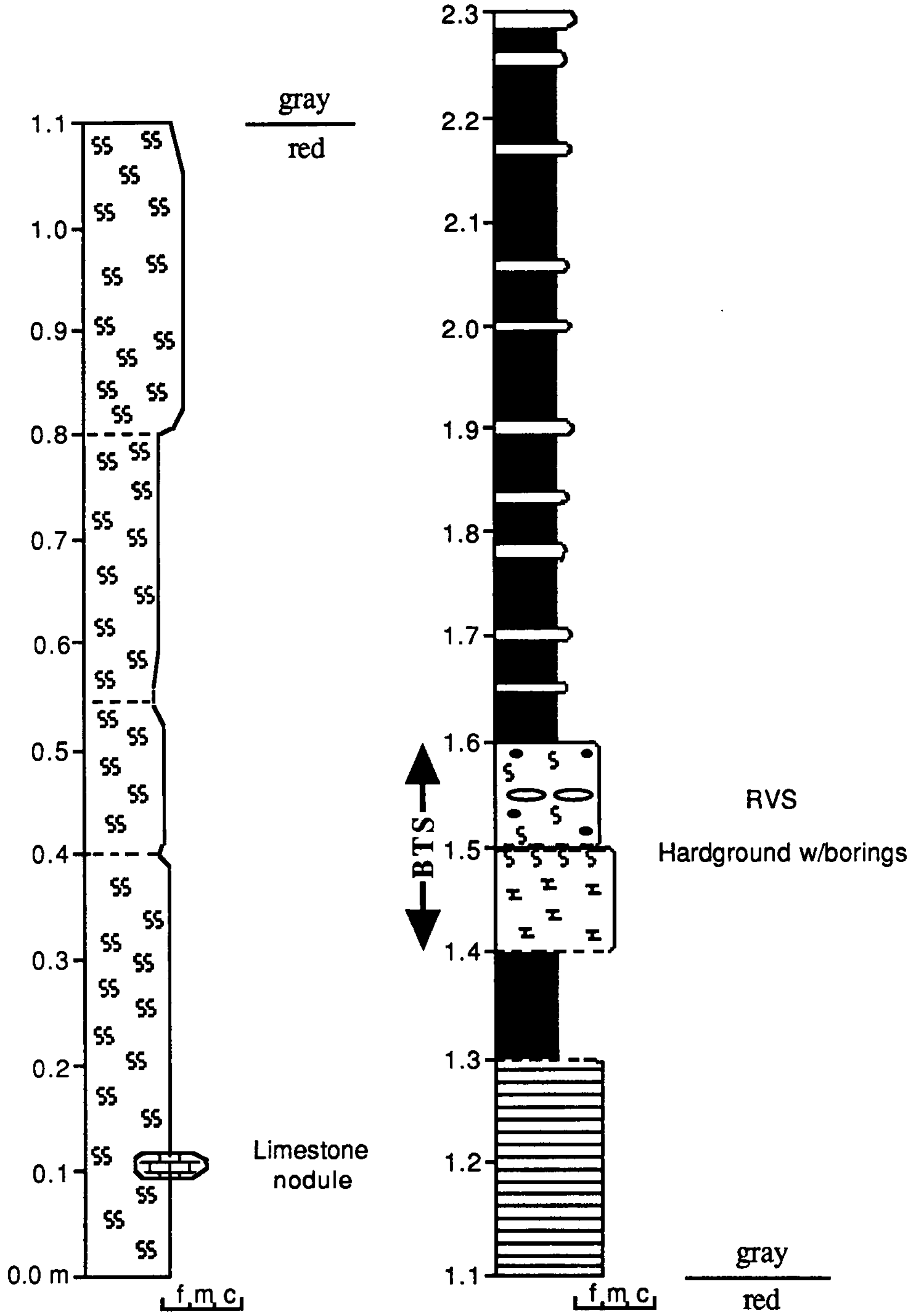

Figure A.6. Measured stratigraphic section at Cumberland Gap, TN.

Unit Thickness (cm)	Cumulative Thickness (cm)	Lithologic Description at Whiteoak Mtn., TN.
7	7	Gray calcareous semi-fissile shale which is in sharp contact with the underlying massive, fossiliferous grainstone/packstone.
12	19	Structueless, brown siltstone displaying sharp contacts with both the underlying and overlying shales.
11	30	Gray, non-fissile shale.
4	34	Brown, fine-grained sandstone/siltstone which has a gradational contact with the underlying shale and a sharp contact with the overlying shale.
116	150	Red-gray non-fissile shale which becomes semi-fissile going upwards. Color gradually changes upwards from red-gray to red and finally, to dark red. Small, discontinuous, 1-5cm thick lenses of fine-grained sandstone/siltstone occur at 20-30cm intervals. These lenses are essentially structureless.
10	160	Sharp color change at 150cm which goes from dark red semi-fissile shale to gray fissile shale. Contacts are sharp with the underlying and overlying units.
630	790	Gray-green semi-fissile shale containing widely spaced thin lenses of sand. These lenses are usually bioturbated. One lense at 270cm contains some phosphatic pebbles at its base however, it has a gradational contact with the underlying shale. Another lense, at 420cm, contains some horizontal laminations at its top. Overlying lenses also tend to be horizontally laminated.
65	855	Interbedded gray, semi-fissile shale and thin (1-2cm thick) sandstone/siltstone stringers which occur at 10cm intervals.Gradational contact with the underlying unit and a sharp contact with the overlying unit.

Unit Thickness (cm)	Cumulative Thickness (cm)	Whiteoak Mountain, TN (continued)
90	945	Basal transgressive sandstone sequence consisting of fine-grained bioturbated sandstone capped by a phosphatic pebble lag. Herbetella brachiopods were noted at 884cm. Samples 8.6-WO, 8.85-WO, 8.9-WO, 8.95-WO, 9.1-WO, 9.35-WO, and 9.4-WO were taken at 860cm, 885cm, 890cm, 895cm, 910cm, 935cm, and 940cm, respectively.
125	1075	Sharp contact with the basal transgressive sandstone. Fissile to semi-fissile gray shale with occasional 1-3cm thick bioturbated fine-grained sandstone/siltstone beds.
15	1090	Brown, fine-grained sandstone which is cross-stratified at its base followed by horizontal laminations and bioturbation. Sharp contacts occur with the overlying and underlying units.
2	1092	Gray, fissile shale.
13	2005	Massive horizontally laminated sandstone which grades upwards into hummocky cross-stratified sandstone/siltstones interbedded with shales.

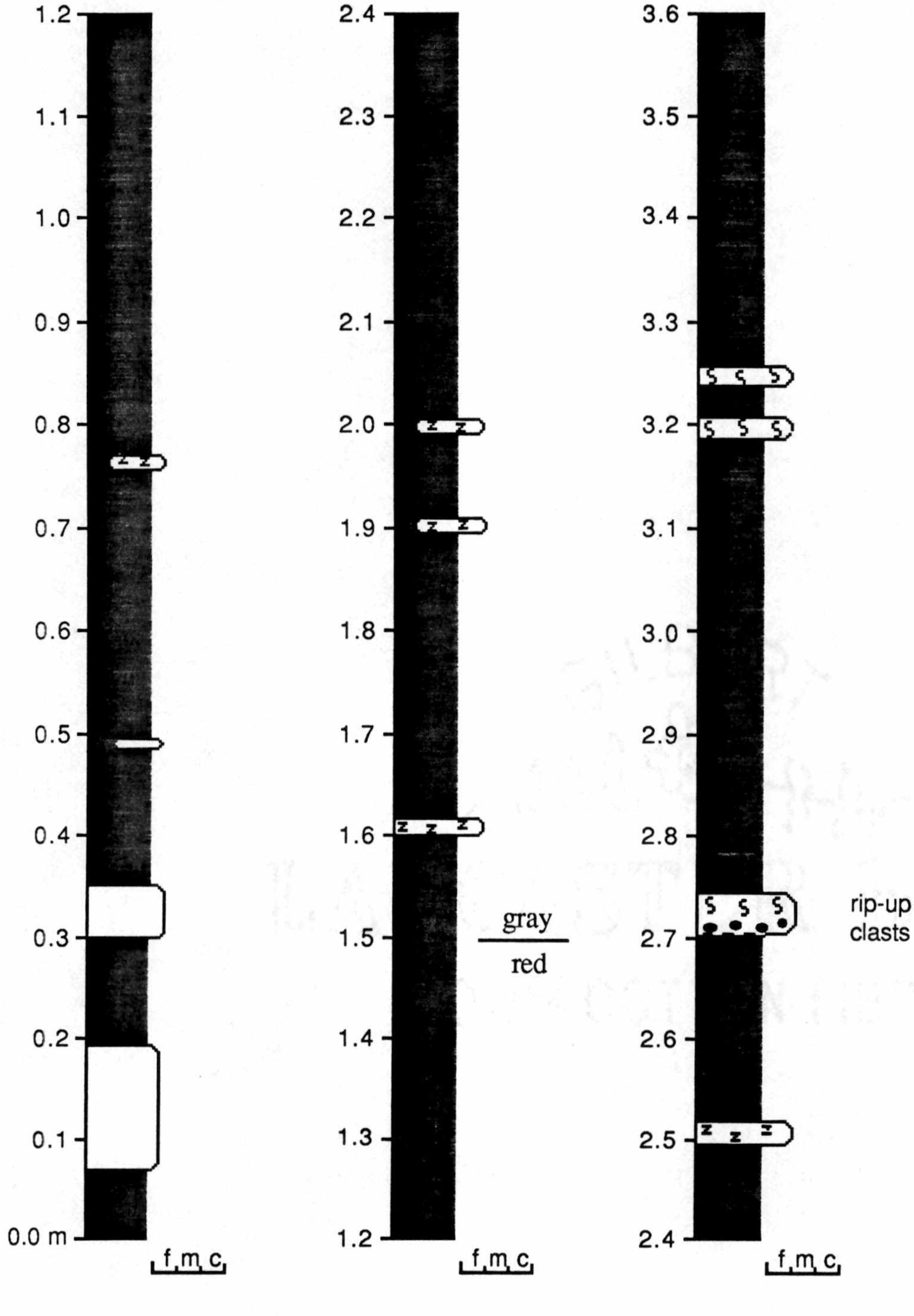

Figure A.7. Measured stratigraphic section at Whiteoak Mountain, TN.

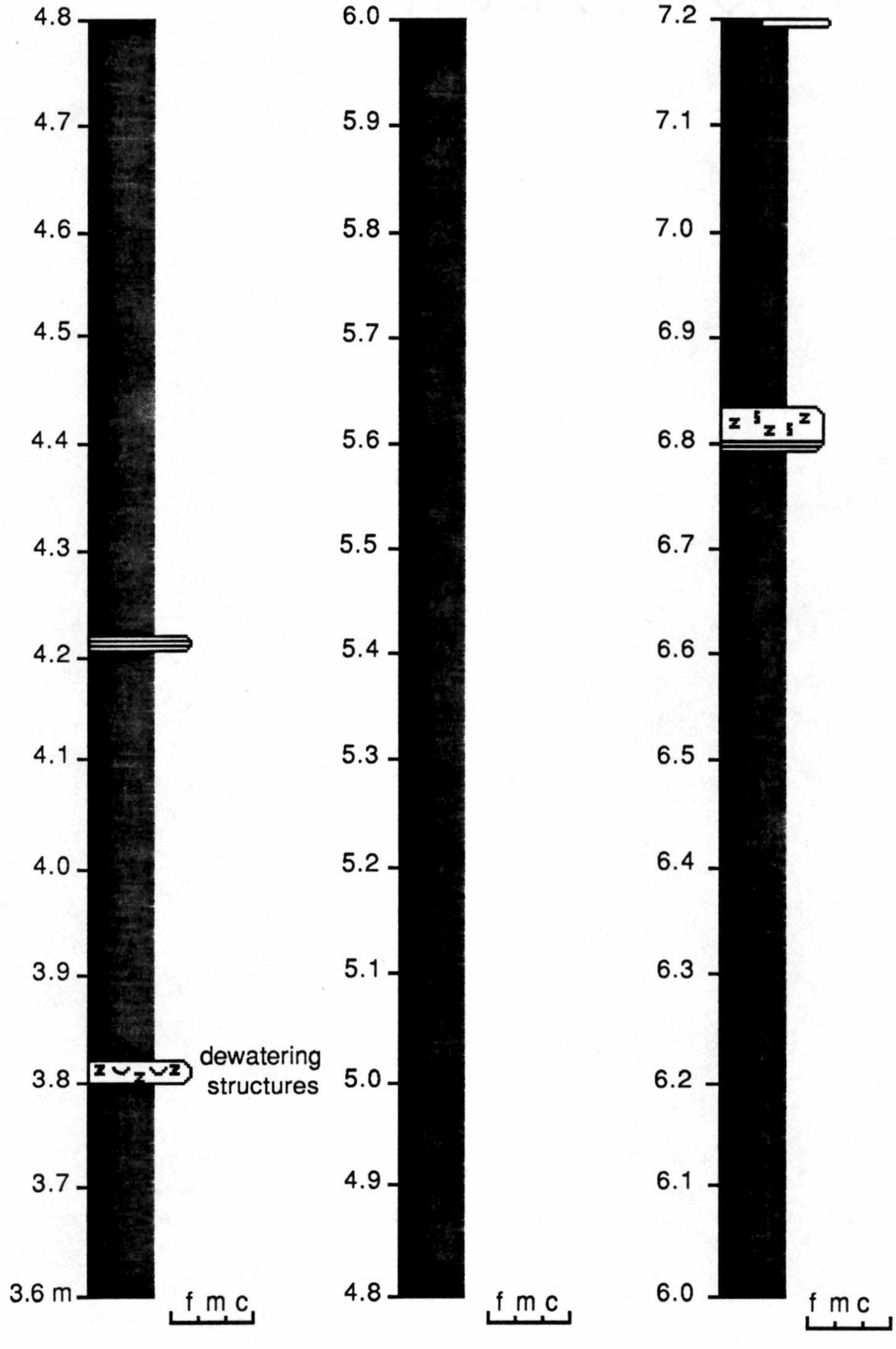

Figure A.7 continued.

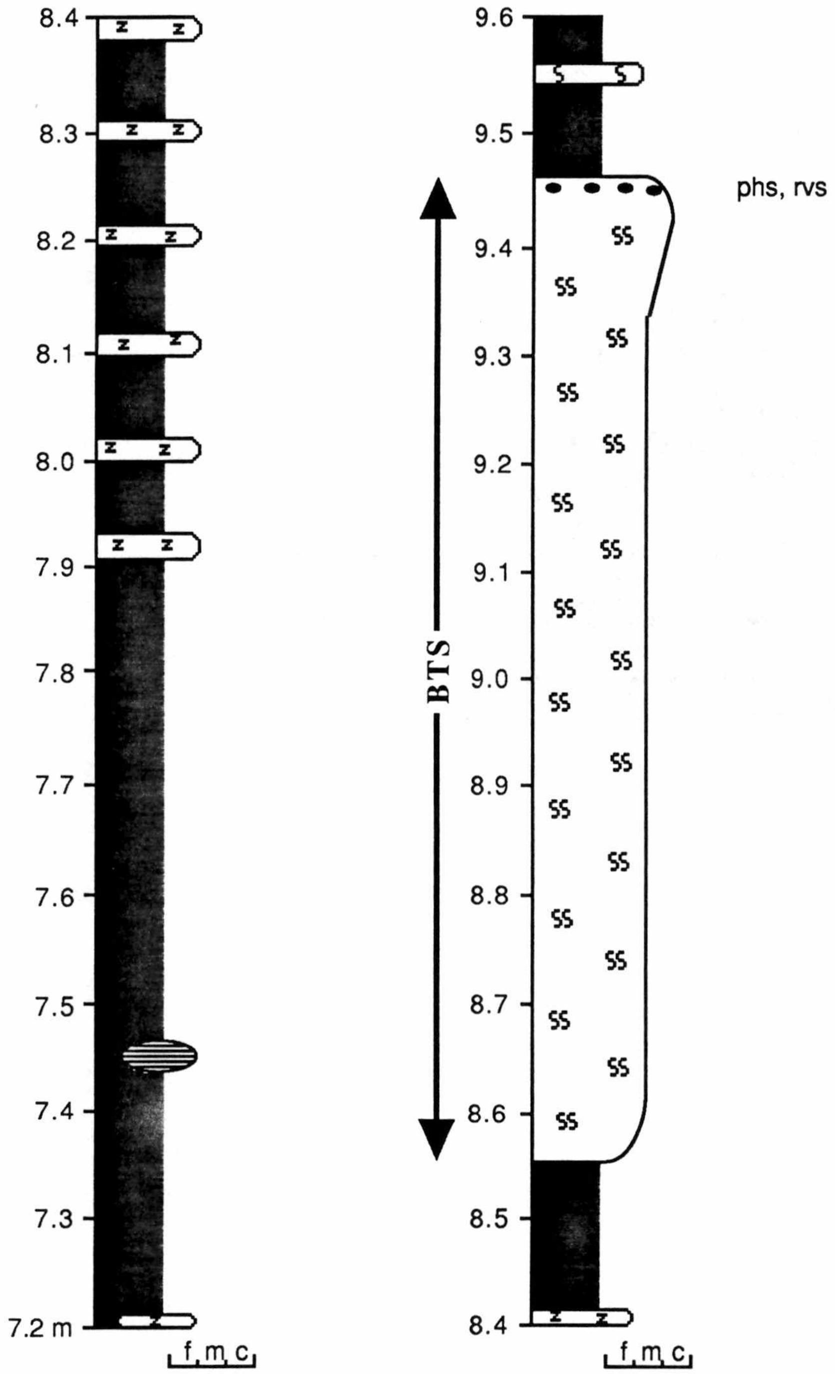

Figure A.7 continued.

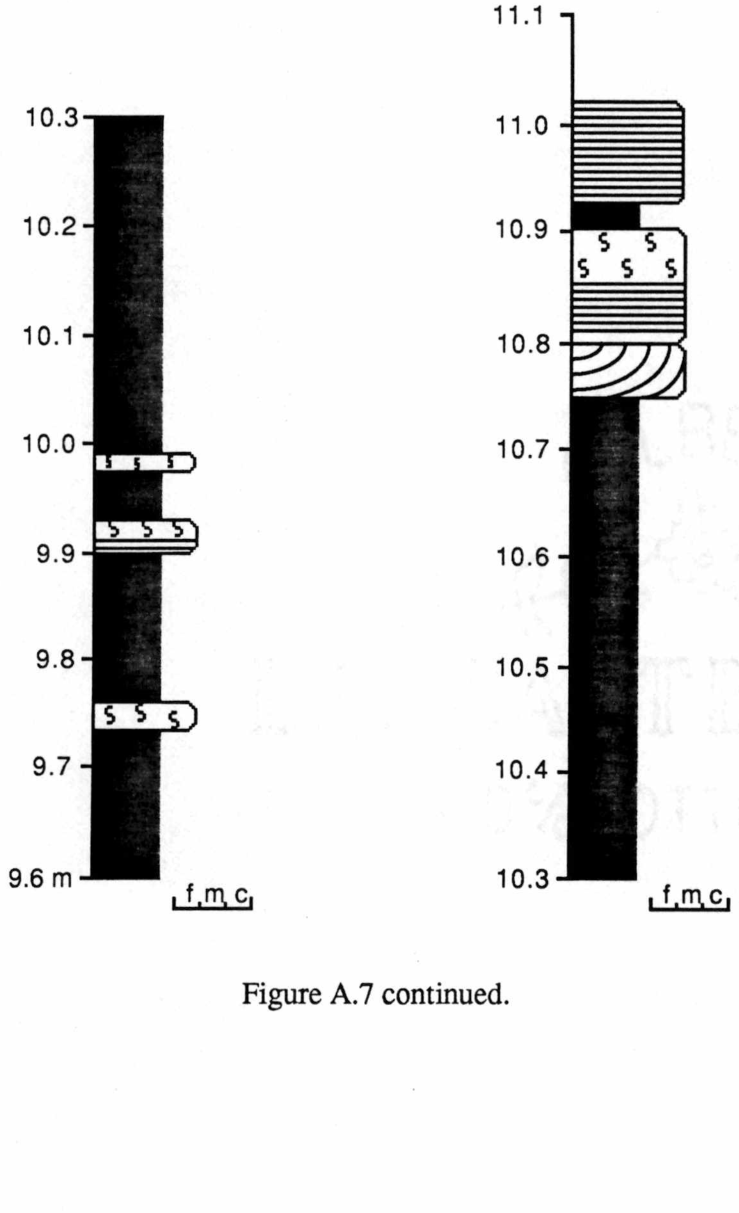

Figure A.7 continued.

Unit Thickness (cm)	Cumulative Thickness (cm)	Lithologic description at Ringgold, GA
10	10	Gray-green, calcareous siltstone which is extremely bioturbated. Continues down section as medium beds interbedded with semi-fissile gray shale.
7	17	Gray fissile shale which is in gradational contact with both the underlying and overlying units.
13	30	Gray-green calcareous siltstone which is highly bioturbated. The upper three centimeters of theunit contain disseminated phosphate granules and brachiopod valves. Samples 0.25-RG and 0.3-RG at 25cm. and 30cm, respectively.
37	67	Gray fissile shale containing thin (1-2cm) stringers of graded sandstone which display sharp contacts with the shale. The bases of these stringers contain phosphate granules as well as medium- to coarse-grained sand. One 5cm-thick unit contains a gutter cast and some small-scale trough cross-beds. It is interpreted to be a small scour channel which occurs at 47cm cumulative thickness. Sample 4.0-RG of graded sand taken at 40cm.
25	92	Gray-tan unit marked by a medium- to coarse-grained phosphatic lag at its base which is in sharp contact with the underlying shale. This is overlain by climbing ripples and mud drapes. These structures are followed by gentle trough cross-stratification which grades into horizontal laminations which are then capped by symmetrical wave ripple laminations. These structures are capped by ~3cm of clay shale. A very small-scale channel or large scale gutter cast containing a coarse phosphatic lag occurs at 75cm within the trough cross-stratified part of the unit. Samples 7.0-RG, 7.5-RG, and 8.0-RG were taken at 70cm, 75cm, and 80cm, respectively.

Unit Thickness (cm)	Cumulative Thickness (cm)	Ringgold, GA (continued)
28	120	Massively bedded, calcareous, fine- to medium-grained sandstone which appears to beslightly hematitic due to weathering. The base of the unit displays a sharp, but irregurlar, contact with the underlying unit and contains scattered phosphate granules and is densely bioturbated. This unit is interpreted to be the lower portion of the basal transgressive sandstone sequence. The intensity of bioturbation decreases upwards. Sample 1.0-RG at 100cm.
33	153	Fine-grained, calcareous, bioturbated sandstone which has a gradational contact with the underlying unit. Very small-scale ripple cross-stratification marks the top of this unit. Samples 1.25-RG and 1.5-RG were taken at 125cm and 150cm, respectively.
57	210	Thin-bedded siltstone to fine-grained sandstone interbedded with gray, semi-fissile shale which displays gradational contacts with both the underlying and overlying units. Siltstone/sandstone beds are moderately bioturbated.

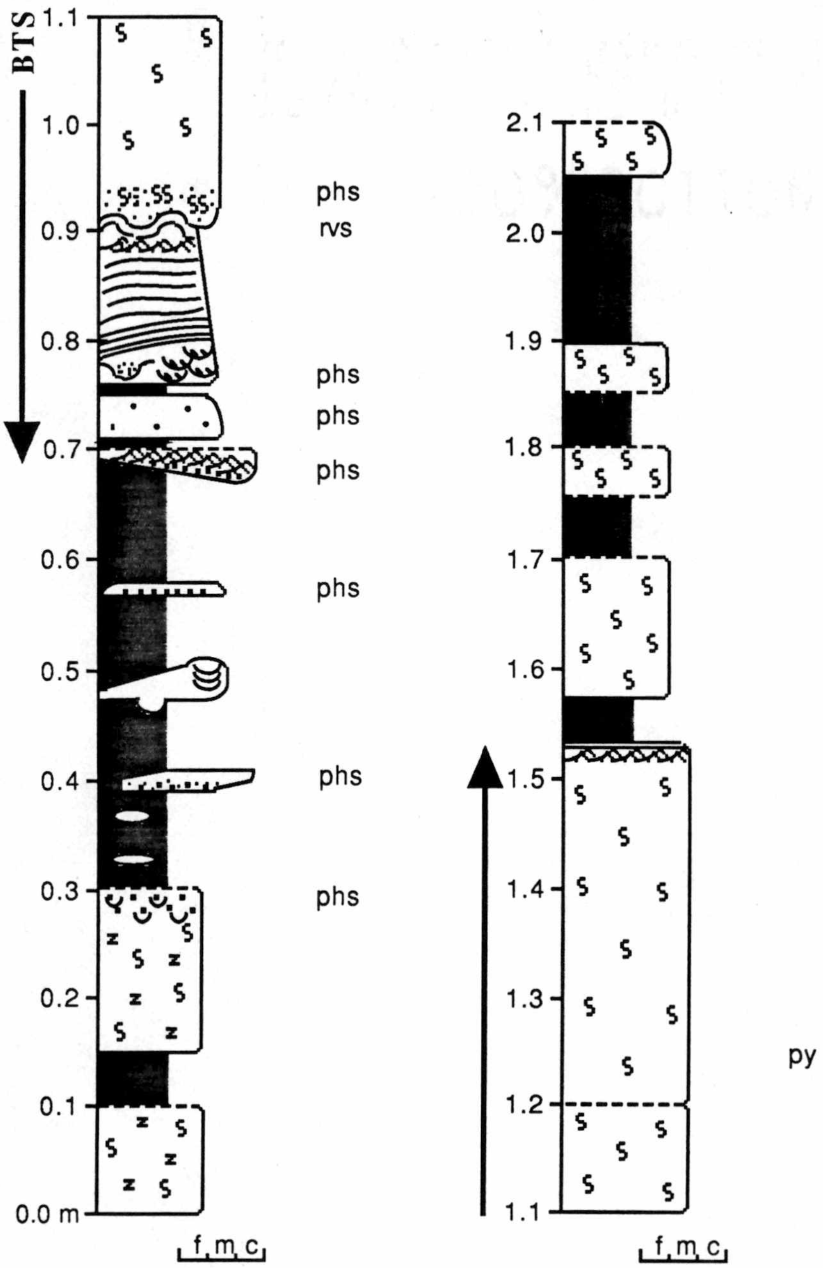

Figure A.8. Measured stratigraphic section at Ringgold, GA.

Unit Thickness (cm)	Cumulative Thickness (cm)	Tiftonia, GA
48	48	Red fossilferous grainstone. Fossils constist of horn corals, brachiopods, bryozoans, trilobite fragments, and ?. Glauconitic horizon occurs at 38 cm. Contains numerous cavities which are lined with coarse calcite crystals.
42	90	Red fossiliferous grainstone containing same fossil groups as the underlying bed. Glauconitic horizon occurs at 70 cm. The bed is capped by a phosphatic hardground with an underlying coarse phosphatic lag. Photograph taken at 80-90 cm of phosphatic horizon. Sample taken at 90 cm.
30	120	Reddish-gray calcareous shale encloses a pod of gray fossiliferous packstone. Sample of limestone taken at 98 cm.
87	207	Closely spaced interbedded silty shale and calcaeous siltstone. Siltstone beds are structureless up to 180 cm. Here the siltstone beds contain symmetrical wave ripples which continue upward to 207 cm. Sample taken at 180 cm.
33	240	Medium-bedded, gray, silty, slightly fossilferous limestone.
8	248	Thin bed of gray limestone (wackestone) contaning a thin, discontinuous, fossiliferous lag at 246 cm.
9	257	Gray-tan, calcarous, slightly fossiliferous, siltstone which appears to coarsen upwards. Sample taken at 255 cm.
9	266	Tan-gray horizontally laminated siltstone/fine sandstone which becomes trough to ripple cross-stratified at the top. Photograph taken of entire bed.
12	278	Gray, semi-fissile, silty clayshale.

Unit Thickness (cm)	Cumulative Thickness (cm)	Tiftonia, GA (continued)
11	299	Tan-colored, horizontally laminated fine-grained sandstone containing thin horizontal stringers of of coarser sand. Sample taken at 290 cm.
4	303	Gray, semi-fissile, silty clayshale.
48	351	Tan-gray, slightly fossiliferous, calcareous siltstone which appears to be horizontally laminated.
4	355	Gray, semi-fissile, silty clayshale.
22	372	Tan-gray, calcareous, slightly fossiliferous calcareous siltstone. Contains a discontinuos lag. Faint horizontal laminations are present near the top and base of the unit. Sample 3.65-TF taken at 365 cm.
10	382	Tan-gray silty clayshale which grades upwards into a fine-grained sandstone. Top of unit displays low-angle cross-stratification. Sample 3.8-TF taken at 380 cm.
8	390	Gray, fissile, silty clayshale.
3	393	Siltstone containing lag of brachiopods.
7	400	Gray, fissile, silty clayshale.
50	450	Interbedded gray, fissile, clay shale and thin, very fine-grained, tan-gray, calcareous sandstone/siltstone beds that tend to be 3 to 6 cm thick.
7	457	Hummocky cross-stratified fine-grained sandstone, tan-gray in color.
3	460	Gray, fissile, silty clayshale.

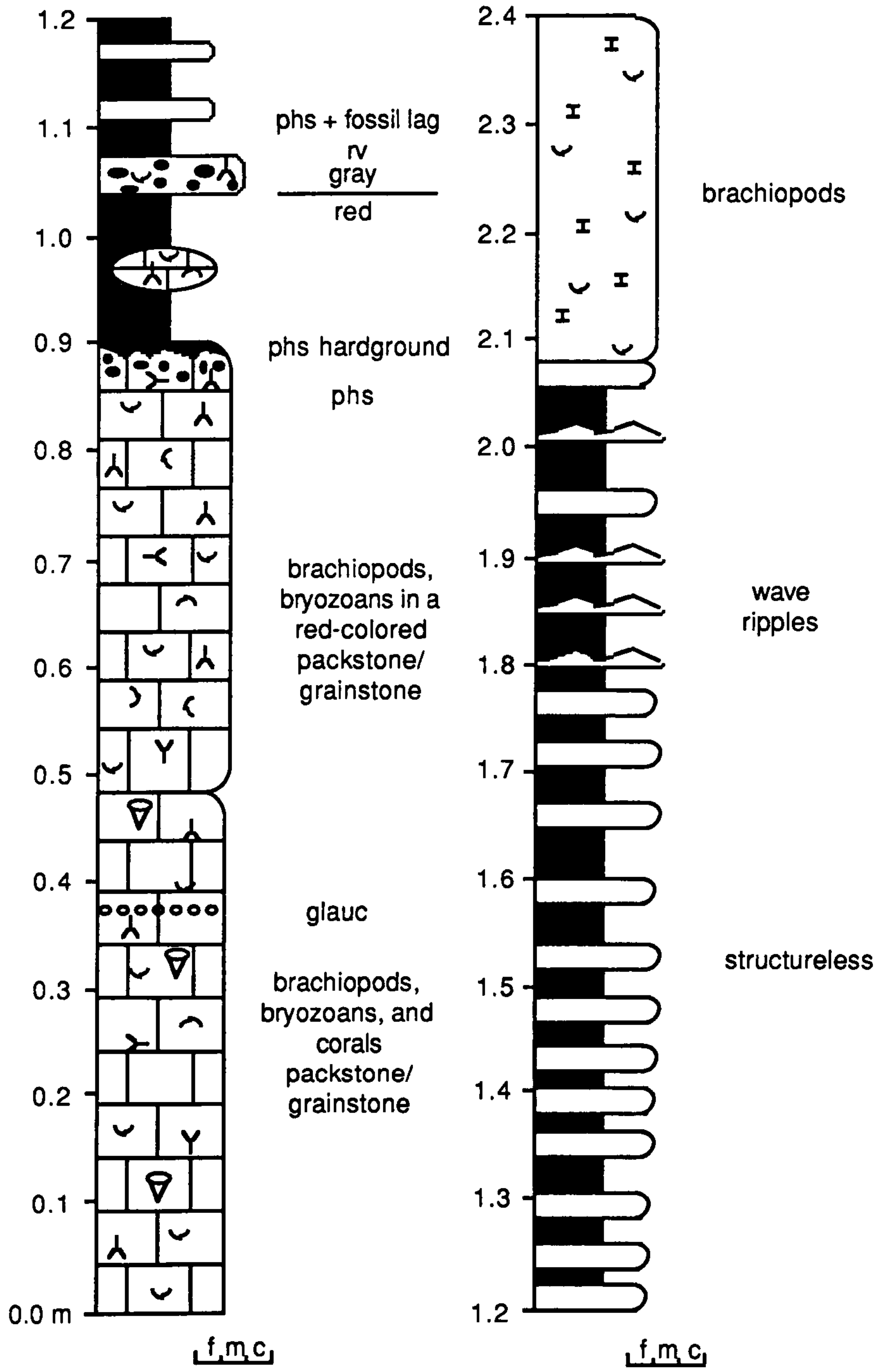

Figure A.9. Measured stratigraphic section at Tiftonia, GA.

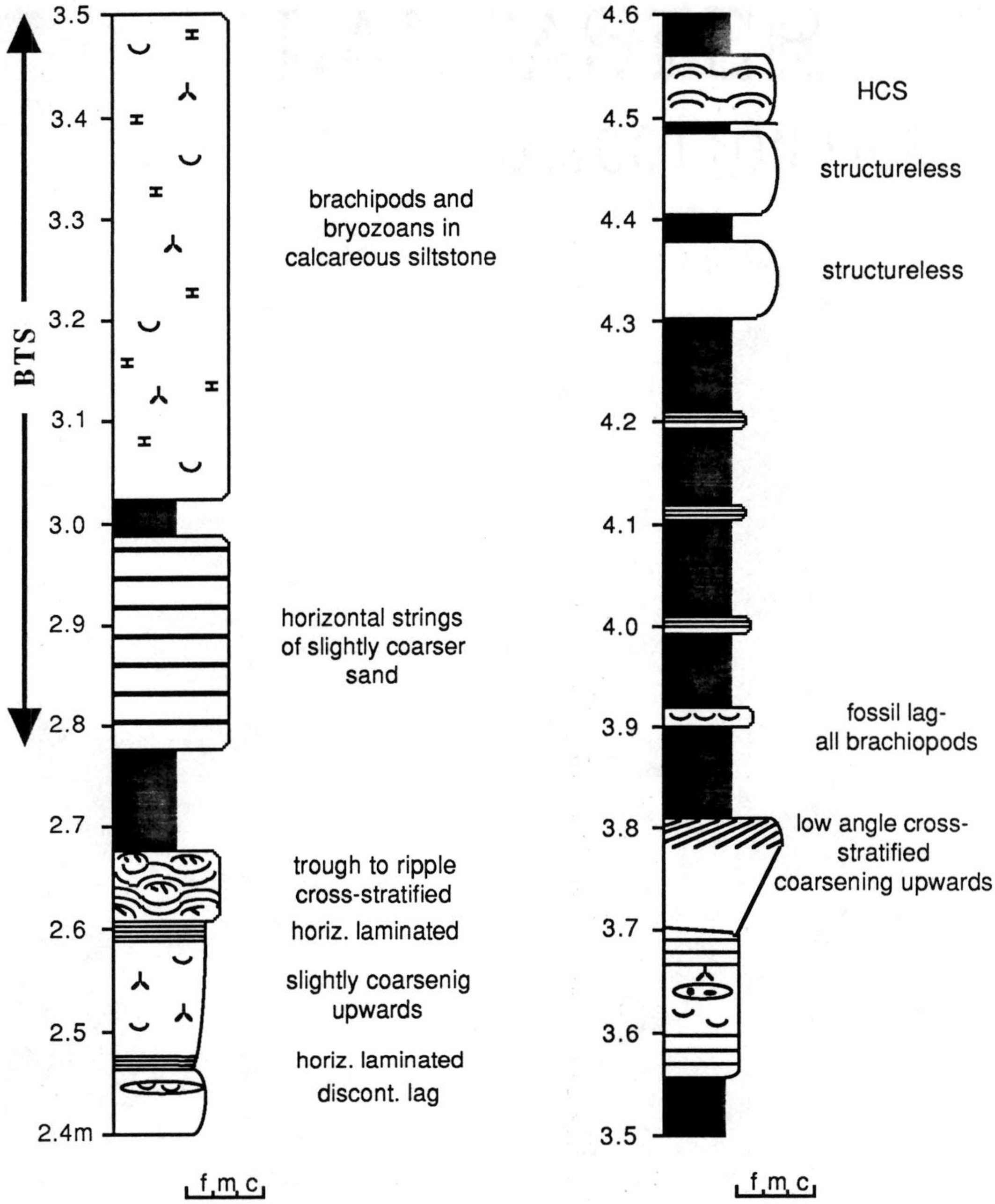

Figure A.9 continued.

APPENDIX B

Given the inconsistent results of the isotopic analyses, the samples that were examined isotopically as well as some others were also X-rayed in order to determine if there was a mineralogical explanation for the scatter of isotopic data. Seven samples were crushed with a shatterbox. Elutriated slides were prepared from a mixture of the crushed samples and distilled water. The following steps were taken with the prepared slides:

The d211 (hkl=104) peaks for calcite and dolomites were analyzed with a Phillips Model X-ray diffractometer (XRD) in order to determine both mineralogy and peak symmetry. The purpose of this was to see if minor carbonate phases were present that might normally be masked by major phases. The method for determining peak symmetry is after Milliman (1971) and Foreman (1986). Before each sample was run, the XRD goniometer was calibrated to the quartz peak (26.64 degrees 2-theta) in order to insure the most accurate readings. The samples were then scanned from 28 degrees 2-theta through 32 degrees 2-theta. This range of 2-theta values covers the spectrum of the carbonate group.

The peaks drawn on the X-Ray diffractograms were then measured for full- and half-peak symmetry in order to see if the major carbonate phases were actually masking the occurrence of minor phases. Peak symmetry can be measured in the following manner. Figure B.1 illustrates all of these steps.

1. Draw a line through the base of the peak to mark out background. Then draw a horizontal line at the point of maximum peak height. The distance between these two horizontal lines is the full peak height. Then draw a vertical line from the base of the

peak through the point of maximum peak height. Record the 2-theta value for the peak maximum.

2. Draw horizontal lines at 10% and 50% of the peak heights. Then determine the 2-theta values at the intersection of the 10% and 50% lines with the peak trace. Do this for both sides of the peak as shown in Figure .

3. The purpose of drawing lines that intersect with the peak trace is to divide the peak trace into equilateral triangles. Then by comparing the areas of the equilateral triangles, peak symmetry will be determined. Comparison of the triangle areas with the 50% lines as bases, half-peak symmetry will be resolved. Full peak symmetry is determined by comparing the areas of the two triangles based by the 10% line.

4. A sample calculation of full and half-peak symmetry is provided in Figure B.1. Full peak symmetry is equal to the sum of the difference between the 2-theta values for the intersection of the 10% line and peak trace and the peak maximum minus the sum of the difference between the peak maximum and the intersection of the 10% line and peak trace on the right side of the peak trace. In the case of Figure B.1, the value for full peak symmetry is equal to 0.06 which indicates that the base of the left-hand triangle is slightly larger than the base of the right-hand triangle. The same procedure is used in calculating half-peak symmetry except that the 2-theta values for the intersections of the 50% line with the trace of the peak are used instead of those of the 10% line. The significance of the peak symmetry values are as follows:

Peak symmetry = 0: Peak is symmetrical with probably only one carbonate phase present.

Peak symmetry < 0: peak is asymmetrical and therefore probably more than one carbonate phase is present. The minor carbonate phase has a 2-theta value that is less than that of the peak maximum.

Peak symmetry > 0: peak is asymmetrical and probably more than one carbonate phase is present. The minor carbonate phase has a 2-theta value that is greater than that of the peak maximum.

Full-peak symmetry:
= (31.25-30.83) - (30.83-30.47)
= 0.06

Half-peak symmetry
= (31.0-30.83) - (30.83-30.67)
= 0.01

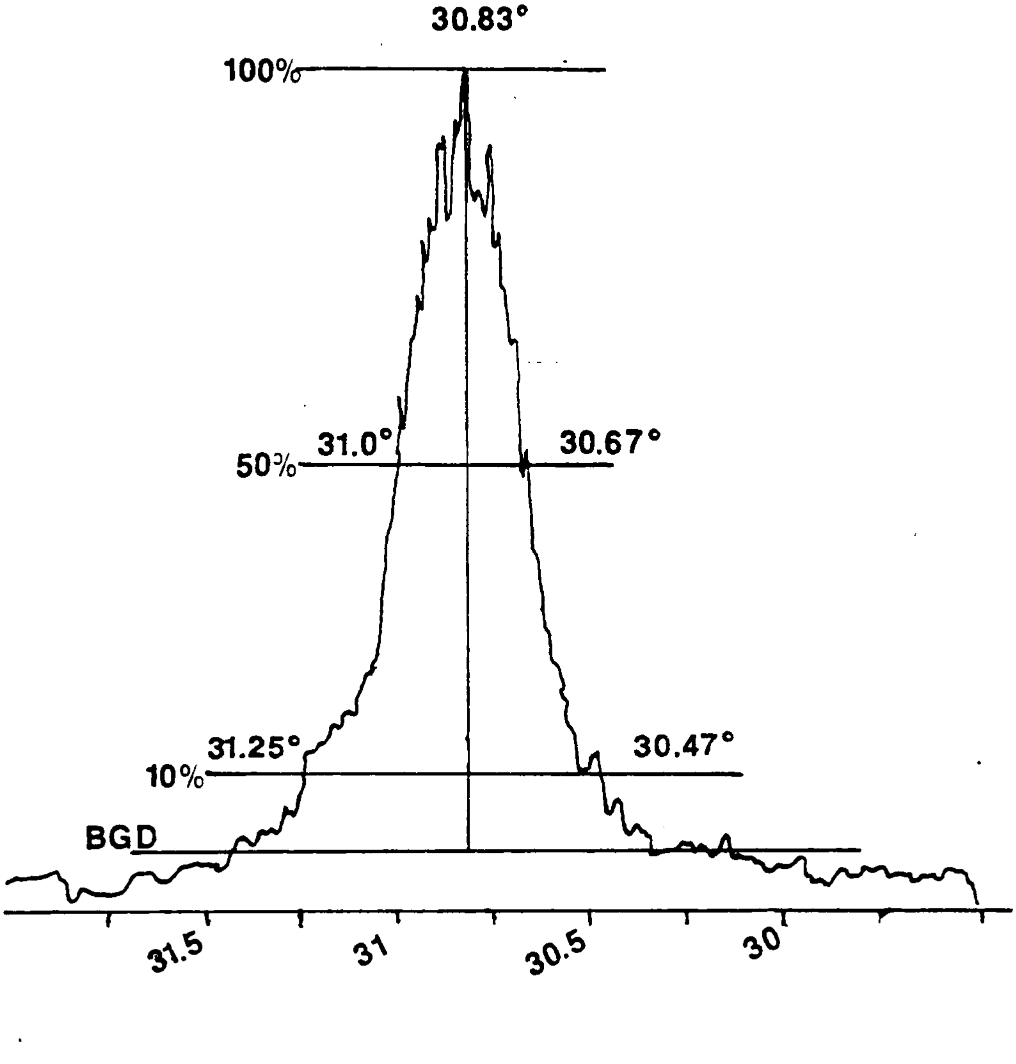

Figure B.1. Actual XRD peak illustrating the method for calculating full- and half-peak symmetry. Peak is from sample number 9.45-LM from Lone Mountain, TN.

APPENDIX C

POINT-COUNT DATA

The following pages contain all point-count data in the form of volume percentages of each phase counted. Column A displays the location that each sample was collected from and column B gives the position, in meters, of the sample within the respective measured sections from which each was derived. Thus a stratigraphic position of 0 indicates that the sample was collected from the very base of the section where measuring began, 0.75 indicates that the sample was collected 0.75 meters above the base of the section where measuring began and so on.

Location Key:

TF..............Tiftonia, GA
CG.............Cumberland Gap, TN
RG.............Ringgold, GA
WO............Whiteoak Mountain, TN
ML.............Melton Lake, TN
LM.............Lone Mountain, TN
AG.............Powell Mountain, VA
BG.............Beans Gap, TN
FG..............Flat Gap, TN

Location	Strat. Positior	Mono Qtz	Poly Qtz	srf's	phsall	phssrf	phs
TF	2.6	297	4	0	1	0	0
TF	2.9	315	0	0	0	0	0
CG	3.05	191	1	72	0	1	0
CG	2.95	219	2	0	0	1	0
RG	1	26	10	0	0	0	0
RG	0.75	627	102	18	10	6	7
WO	9.4	274	54	0	1	0	0
WO	9.35	313	48	0	0	0	1
WO	8.9	669	103	1	1	0	2
ML	3	205	23	1	6	0	3
ML	1.5	523	56	1	4	1	12
ML	0.7	155	59	3	4	89	1
ML	0	355	50	6	5	0	19
LM	7.45	352	29	3	2	0	6
LM	7.2	204	33	0	6	0	8
LM	7.1	210	18	2	6	0	16
LM	6.9	377	68	4	7	3	6
AG	6	381	119	1	9	1	4
AG	2	390	51	6	7	0	6
AG	1	444	81	2	17	99	13
BG	8.5	58	46	1	1	0	0
BG	8.3	147	38	0	1	0	2
FG	2	335	135	0	0	0	0
FG	1	390	135	0	0	0	0

rpdol	eufedol	fecc	ansufedo	qtz cement	det clays	glauconite	chlorite
3	452	15	0	14	65	2	0
3	710	237	1	0	40	5	0
0	0	0	0	0	331	0	0
1	0	0	0	0	451	0	0
31	0	0	0	0	2	0	0
258	3	1	0	23	198	3	2
341	0	2	0	21	0	1	0
298	0	21	2	19	3	6	1
480	1	1	0	5	105	12	1
140	19	2	76	3	82	15	0
328	0	6	0	93	2	0	1
141	0	51	0	0	2	0	0
427	0	27	1	0	75	7	1
514	1	24	0	0	65	8	0
822	0	23	1	0	264	5	3
555	0	7	0	1	195	4	0
502	7	0	0	2	33	0	0
361	23	1	0	53	44	16	0
418	42	0	0	56	38	26	0
183	25	28	0	17	25	23	0
0	0	0	0	0	10	0	4
1	0	0	0	6	2	2	0
0	0	0	0	61	13	1	2
0	0	0	0	116	33	0	1

opaques	heavies	nonfedol	plag	microcline	kspar	pyrite	muscovite
43	1	570	0	0	0	0	0
30	0	144	0	0	0	0	0
28	0	737	6	0	0	0	0
24	0	669	0	0	1	0	0
6	1	0	0	0	0	0	0
68	4	0	22	8	11	0	0
1	0	0	8	0	37	0	0
1	0	0	3	0	23	0	0
2	1	0	16	3	75	0	0
31	4	18	8	2	3	0	0
16	5	0	11	1	4	0	0
0	0	0	1	0	1	0	0
7	0	0	3	2	3	0	0
24	1	0	4	0	2	5	0
61	4	0	2	0	1	0	0
41	2	0	1	0	0	0	0
36	0	0	5	3	7	0	0
12	3	0	29	0	9	0	0
23	2	0	23	0	36	0	0
10	1	0	3	0	7	0	0
2	0	49	4	0	2	0	1
1	0	0	1	2	10	0	0
147	3	0	3	1	4	0	0
28	0	0	2	3	4	0	0

biotite	iron oxide	stage only	Total
0	0	13	1467
0	0	0	1485
0	0	0	1367
0	0	0	1368
0	0	0	76
0	0	0	1371
0	0	0	740
0	0	1	739
0	0	2	1478
0	0	0	641
0	0	0	1064
0	0	11	507
0	0	0	988
0	0	24	1040
0	0	0	1437
0	0	3	1058
0	0	0	1060
0	0	0	1066
0	0	0	1124
0	0	0	978
1	29	14	208
0	0	46	213
0	0	35	705
0	0	37	712

VITA

Anne Ruth Gogola was born in Vanersborg, Sweden on May 21, 1965. She was barely a year old when she and her family moved to Marburg, West Germany. There, she spoke her first sentences in German. When she was three, the family moved to Detroit, Michigan where she attended primary and secondary school all the while forgetting most of the German language she had originally spoken. Tired of urban blight, the family took flight to the small, Detroit suburb of Berkley where the author attended Berkley High School and graduated in 1982. Following High School, the author accepted a Merit Scholarship from Wayne State University in Detroit. She graduated with a B.S. in Geology in 1986. Following graduation, the author spent a meaningless year working at a meaningless restaurant before the call of geology brought meaning back into her life. In the fall of 1987, she accepted the offer of a teaching assistantship from the Department of Geological Sciences at the University of Tennessee and began her studies toward a Master of Science degree. She was awarded that degree in the Spring of 1990. Anne is now in the grease business working as a petroleum geologist for Exxon U.S.A.